INVESTIGATION OF MULTISCALE BIODEGRADATION PROCESSES: A MODELLING APPROACH

by

MARIO SCHIRMER

A thesis

presented to the University of Waterloo

in fulfillment of the

thesis requirement for the degree of

Doctor of Philosophy

in

Earth Sciences

Waterloo, Ontario, Canada, 1998

The University of Waterloo requires the signatures of all persons using or photocopying this thesis. Please sign below, and give address and date.

ABSTRACT

This thesis attempts to link processes involved in biodegradation of BTEX (benzene, toluene, ethylbenzene and the xylenes) compounds in groundwater environments at three different observation scales, the micro-, meso- and macroscale, by means of numerical modelling. Different processes, phenomena and characteristics are predominant at each scale. The link between the micro- and mesoscale is performed by using the zero-dimensional model BIOBATCH, whereas the three-dimensional transport model BIO3D is used to link the meso- and macroscale. The assumption is made that small-scale phenomena fully apply at the larger scale where additional processes play a role as well.

A new method was developed to calculate Monod degradation parameters for BTEX compounds using laboratory batch experiments. The problem of non-uniqueness of the calculated parameters was overcome by using several different initial substrate concentrations. With a relative-least-squares technique, unique kinetic degradation parameters were obtained. Calculation of the microbial yield, based on microbial counts at the beginning and the end of the experiments, was crucial for reducing the number of unknowns in the system and therefore for the accurate determination of the kinetic degradation parameters. The new method worked for a constant microbial yield (Chapter 1) and for a case of decreasing microbial yield with an increase in initial substrate concentration (Appendix A).

In order to assess all relevant processes contributing to the transport and degradation of contaminants in the field, a procedure was developed to define an optimal sampling grid to perform a reliable field mass balance by applying numerical modelling and geostatistical methods (Chapter 2). The procedure was used to assess the field behaviour of the slowly degrading compound methyl tertiary butyl ether (MTBE) within the Borden aquifer. By exclusion of other processes such as sorption, volatilization, abiotic degradation and plant uptake, it is suggested that MTBE biodegradation played a major role in the attenuation of MTBE at Borden.

Furthermore, the phenomenon of changing flow directions on the behaviour of conservative and biodegradable compounds was investigated (Chapter 3). The transient nature of the flow field contributed to the transverse spreading of the plume and therefore enhanced the mixing between the substrate and the electron acceptor which in turn enhances biodegradation. However, the results suggest that in the case of moderate changes of flow direction, a steady-state flow field is justified for many practical applications, thereby avoiding the higher computational costs of a fully transient simulation. Under these conditions, the use of a higher transverse horizontal dispersivity in a steady flow field can adequately forecast plume development.

Finally, linkage of the laboratory and field scale was attempted using a numerical modelling approach with small elements (Chapter 4). Laboratory-derived kinetic degradation and sorption parameters were applied, along with additional physical, chemical and microbiological information, to a dissolved gasoline field experiment at the Borden aquifer (Chapter 4). All additional input parameters were derived from laboratory and field measurements or taken from the literature. The simulated results match the experimental results reasonably well without model calibration.

Based on these results, an extensive sensitivity analysis was performed to estimate the influence of the key controlling factors at the field scale. It is shown that the flow field, in particular, significantly influences the simulated results. Under the field conditions modelled and the assumptions made for the simulation, it could be concluded that laboratory-derived Monod kinetic parameters can adequately describe field-scale degradation processes. By choosing small elements for the simulations, lab-scale processes could be resolved at the field scale, yielding field-scale degradation behaviour without the need for scale relationships to link the laboratory and the field scale. Accurately incorporating the additional processes, phenomena and characteristics such as a) advective and dispersive transport of the contaminants, b) advective and dispersive transport and availability of the electron acceptor, c) mass transfer limitations and d) spatial heterogeneities, at the larger scale and applying well defined lab-scale parameters should accurately describe field-scale processes.

ACKNOWLEDGEMENTS

Going through the years of doing a Ph.D. is similar to growing up from a child to an adult. The difference is that it takes less time, although it sometimes doesn't seem that way. Still, as in childhood you go through various stages. First, you need support to be able to survive but later you can even offer your own hand to help others.

It's the journey that matters not just the arrival.

I'd like to thank all those who helped me to get to this point in my life and I want to apologize to all those I can't include by name into these acknowledgements because there are too many of you.

I had a truly great Ph.D. committee. With each single member of the committee, I had an open and productive working relationship. I'd like to thank Emil Frind, my supervisor, for giving me the opportunity to work on this project and for his guidance in the world of modelling. His never-ending drive for perfection pushed me over hurdles I was never thinking to be able to take. I'd like to thank Jim Barker for letting me see the big picture from time to time and for all the freedom I had in handling the project. I'd like to thank Barb Butler for introducing me to the wonders of microbiology and her incredible patience during the lab work. I've lost count of the number of nights Barb spent to read my papers because I "needed" them back right the next day. And I'd like to thank Ed Sudicky for his guidance in evaluating the field results and many helpful suggestions in finding the right modelling approaches.

I also want to thank the other faculty members at Waterloo for their support and help during my five-year journey in form of supporting letters, sharing research ideas, discussing research approaches, finding the right contact persons and their great teaching skills. Particularly valuable for me was the opportunity to organize our Field School for two years. I'd like to thank especially Dave Rudolph, Bob Gillham, John Cherry, Doug Mackay, John Greenhouse, Eric Reardon and Rick Devlin.

Furthermore, I'd like to thank our technicians Paul Johnson, Bob Ingleton, Rick Gibson and Jesse Ingleton for their invaluable help during my field research and during Field School. Any Earth Science Department would be happy to have you guys.

Before I'll talk about the many students who helped me to achieve my goals, I want to thank two of them who helped me the most. There is no doubt that I wouldn't be there where I am right now without those two. Ty Ferré taught me how to teach and I'm grateful that I had the chance to learn from him as a TA and Field School organizer. I'll always remember his thoroughness and enthusiasm when he's teaching. John Molson is the second student I'd like to thank. Without John, my modelling would be far from where it is today. He spent countless hours in addition to his busy working days to help me with my modelling adventures. No words can say how grateful I am for his help and I'd like to apologize at the same time to Jenny, John's wife, for stealing some of John's limited family time.

As always, a journey wouldn't be as much fun without the many others sitting in the same boat. Many students were at my side during these years and many are now professors themselves or have other challenging positions. Beside many others, I'd like to thank Ian Callow, Raymond Henry, Mike Janzen, Scott Fidler, Tina Hubbard, Murray Einarson and Masaki Hayashi. I also received big help from the "Modelling Group". There was always time to discuss and it was never too late at night. There's still lots of beer to come. I especially want to thank Uli Mayer, Jos Beckers, Graham Durrant, Kerry MacQuarrie, Rob McLaren and Paul Chin.

There were of course also many people who helped me to get to Waterloo. I'd like to thank my teacher and friend Georg Teutsch (University of Tübingen, Germany) for his continuous and encouraging support while I was applying for Waterloo and all the time thereafter. I also would like to thank Ludwig Luckner (Dresden Centre for Groundwater Research, Germany) for his personal and professional support to obtain the much needed scholarship in the very beginning of my stay at Waterloo that enabled me to transfer into the graduate program.

Because research and graduation are two expensive adventures, funding is often a crucial necessity on the way. I'm grateful to the following funding agencies: the Gottlieb

Daimler- and Karl-Benz Foundation (Germany), the Dresden Centre for Groundwater Research (Germany), the University of Waterloo and the Government of Canada for their scholarships, as well as the Natural Science and Engineering Research Council of Canada and the American Petroleum Institute for their research grants.

I, finally, would also like to thank my family for all their support. I thank my wife, Kristin, for all the encouraging words and her understanding and I forgive her that she started her Ph.D. one year after I did and finished one year earlier. I thank my son for his early smiles that mean so much to me. And finally I'd like to thank my parents and my parents-in-law:

Liebe Eltern und liebe Schwiegereltern, ich möchte Euch von ganzem Herzem danken für alle Eure Unterstützung während der Zeit meiner Doktorarbeit und natürlich auch davor. Ich hoffe, daß ich Euch das alles einmal zurückgeben kann.

DEDICATION

For Isobel and Barry Fox,
our Kitchener host parents for all their love and
for showing us the Canadian way of life.

TABLE OF CONTENTS

LIST OF TABLES

LIST OF FIGURES

CHAPTER 1:

CHAPTER 2:

CHAPTER 3:

CHAPTER 4:

APPENDIX A:

ABBREVIATIONS

aq - subscript refers to aqueous phase

A - electron acceptor concentration [M/L^3]; subscript electron acceptor

α_L - longitudinal dispersivity [L]

α_{TH} - transverse horizontal dispersivity [L]

α_{TV} - transverse vertical dispersivity [L]

b - first-order microbial decay coefficient [T^{-1}]

BTEX - benzene, toluene, ethylbenzene and the xylenes

c - concentration [M/L^3]

C_{integr} - depth integrated concentration [M/L^2]

CFB - Canadian Forces Base

Cl^- - chloride

d - derivative

D - mass distribution coefficient

D* - effective diffusion coefficient [L^2/T]

D_{ij} - dispersion tensor [L^2/T]

DAI - direct aqueous injection

DO - dissolved oxygen

DAPI - 4',6-diamidino-2-phenylindole

ΔM - total mass of microbes gained [M]

ΔS - total mass of substrate utilized [M]

Δz - vertical spacing [L]

f_{OC} - organic carbon content of aquifer material [%]

θ - porosity

g - subscript refers to gaseous phase

H - dimensionless Henry's law constant as ratio of the gaseous to the aqueous concentrations

K - hydraulic conductivity [L/T]

K_d - distribution coefficient [L^3/M]

K_I - Haldane inhibition concentration [M/L^3]

k_{max} - maximum-utilization rate of the organic substrate [T^{-1}]

K_S - half-utilization constant of the organic substrate [M/L^3]

λ_H - horizontal correlation length [L]

λ_V - vertical correlation length [L]

m - substrate mass [M]

M - microbial concentration [M/L^3]

M_{max} - maximum microbial concentration [M/L^3]

MPN - most probable number

MTBE - methyl tertiary butyl ether

NAPL - non-aqueous phase liquid

P - product concentration [M/L^3]

R - retardation factor

REV - representative elementary volume

RSE - relative squared error between the measured and calculated degradation curve

RLS - relative least squares between the measured and best-fit calculated degradation curve

ρ_b - bulk density of the porous media [M/L^3]

S - substrate concentration [M/L^3]; subscript substrate

S_c - calculated substrate concentration using BIOBATCH [M/L^3]

S_m - measured substrate concentration in the lab [M/L^3]

sorb - subscript refers to sorbed phase

σ_Y^2 - variance of ln (K)

t - time [T]

TBA - tertiary butyl alcohol

TBF - tertiary butyl ether

v - velocity [L/T]

V - volume [L^3]

x - spatial coordinate [L]

X - ratio of oxygen to organic substrate consumed

y - spatial coordinate [L]

Y - microbial yield (mass increase of microbial population/mass loss of organic substrate)

$\hat{Y}$ - ln (hydraulic conductivity [K] in cm/s)

z - number of measuring points and spatial coordinate

GENERAL INTRODUCTION

Natural attenuation is now widely recognized as a cost-effective remediation technology, but it often relies to a large extent on microbial processes to degrade the contaminants in the subsurface. Extensive research over the last two decades has brought many new insights into these processes in terms of substrate utilization, electron acceptor involvement, microbial kinetics and population dynamics (e.g., Chapelle, 1992). Understanding the complex interactions involved is crucial for forecasting plume development and for verifying natural attenuation as a possible remedial option for groundwater protection.

The largest uncertainty in assessing field degradation processes typically lies in the determination of the kinetic degradation parameters. Researchers and practitioners have used simplified zero- or first-order degradation rates to forecast contaminant behaviour. However, because this approach does not take microbial kinetics and electron acceptor levels into account, it often fails to predict the long-term behaviour of plumes. On the other hand, Monod-type degradation kinetics include substrate and electron acceptor concentrations, as well as microbial growth to assess the degradation process. Therefore, this approach should provide more reliable results in the attempt to forecast long-term plume behaviour in the environment. But the only way to calculate reliable Monod parameters is by means of lab experiments, and it has to be shown that those lab parameters can be applied to the field scale. In this way, numerical modelling can help to link different observation scales, as is attempted in this thesis.

The work presented here introduces a new method to calculate Monod degradation parameters for BTEX (benzene, toluene, ethylbenzene and the xylenes) compounds using laboratory batch experiments. The proposed method allows for substrate degradation under microbial growth conditions. The problem of non-uniqueness of the calculated parameters is overcome by using several different initial substrate concentrations. With a relative-least-squares technique, unique kinetic degradation parameters are obtained. Calculation of the microbial yield based on microbial counts at the beginning and the end of the experiments is crucial for reducing

the number of unknowns in the system and therefore for the accurate determination of the kinetic degradation parameters. The new method works for a constant microbial yield (Chapter 1) and for a case of decreasing microbial yield with increasing initial substrate concentration (Appendix A).

It is often difficult to assess all relevant processes contributing to the transport and degradation of contaminants in the field. Chapter 2 introduces a procedure involving the application of a numerical model and geostatistical methods to define an optimal sampling grid in an attempt to perform a reliable mass balance for the slowly degrading compound methyl tertiary butyl ether (MTBE) within the Borden aquifer. By exclusion of other processes such as sorption, volatilization, abiotic degradation and plant uptake, it is suggested that MTBE biodegradation played a major role in the attenuation of MTBE within the Borden aquifer.

Chapter 3 deals with the phenomenon of changing groundwater flow directions and its effect on the behaviour of conservative and biodegradable compounds in groundwater. The transient nature of the flow field contributes to the transverse spreading of the plume and therefore enhances mixing between the biodegradable compounds serving as microbial substrates and the electron acceptor (e.g., oxygen) which in turn enhances biodegradation. However, the results suggest that in the case of moderate changes in flow direction, a steady-state flow field is justified for many practical applications, thereby avoiding the higher computational costs of a fully transient simulation. Under these conditions, the use of a higher transverse horizontal dispersivity in a steady flow field can adequately forecast plume development.

Finally, Chapter 4 attempts to link the different observation scales with which hydrogeologists concerned with biodegradation of contaminants must contend. On one hand, we have to contend with microscale phenomena such as microbial growth, diffusion layers, and groundwater flow around soil grains. On the other hand, we have mesoscale (batch or column) experiments conducted to assess, for example, degradation kinetics, sorption characteristics and mass transfer phenomena. At the field scale, additional phenomena such as advection, dispersion, spatial and temporal substrate and

electron acceptor distributions and spatial heterogeneities play a role in controlling contaminant plume behaviour.

The scaling between the three scales is performed on two levels. First, the microscale biodegradation parameters, in terms of microbial counts and percentage of degrader population, are applied to the larger scale (mesoscale) representative elementary volume (REV) of the batch experiment. This has been done by microbiologists for decades. The analogy in hydrogeology is the application of concepts of water movement at the pore scale to derive conceptual models of water movement at the column (meso-) scale.

The second step is the scaling from the lab (meso-) to the field (macro-) scale. The hypothesis of this thesis is that laboratory derived kinetic biodegradation and sorption data can be applied to simulate field degradation processes. Therefore, lab derived degradation parameters (Chapter 1 and Appendix A) are applied to the BTEX field experiment by Hubbard et al. (1994). This approach is similar to the approach Schellenberg (1987) took to investigate the phenomenon of macrodispersion. She applied local-scale dispersivity values at local-scale REVs (cm scale) within an aquifer setting of tens of metres that incorporated heterogeneities. By theory, the local-scale dispersivity values applied at local-scale REVs in a heterogeneous aquifer should, over sufficient travel distance, yield macroscale dispersivity values. As theory predicted, macroscale dispersivity values developed although only local-scale dispersivity values were used in the simulations (Schellenberg, 1987; Frind et al., 1987).

Unlike for the case of macrodispersivity, no rigorous scaling theory exists in the case of field scale biodegradation processes. The difficulty in the biodegradation case is that several different processes, phenomena and characteristics, such as advective and dispersive transport of one or more contaminants and the electron acceptors, mixing, mass transfer limitations and spatial heterogeneities, interact to yield the overall field degradation rate. Therefore, a field experiment was considered to determine if lab-derived degradation and sorption data can help to reproduce field scale degradation processes when applying a sufficiently small REV to resolve field phenomena.

The laboratory batch experiments evaluated in Chapter 1 and Appendix A were conducted by James W. Roy. Barbara J. Butler performed the microbial plate counts and derived the initial microbial concentrations (Chapter 1). John Molson developed the numerical model BIO3D that was used throughout this thesis and Graham Durrant performed a large proportion of the simulations used in Chapter 3.

REFERENCES

Chapelle, F. H. 1992. Ground-water microbiology and geochemistry. New York, John Wiley and Sons Inc.

Frind, E. O., Sudicky, E. A. and Schellenberg, S. L. 1987. Micro-scale modelling in the study of plume evolution in heterogeneous media. Stochastic Hydrol. Hydraul. 1, p. 263-279.

Hubbard, C. E., Barker, J. F., O'Hannesin, S. F., Vandegriendt, M. and Gillham, R. W. 1994. Transport and fate of dissolved methanol, methyl-tertiary-butyl-ether, and monoaromatic hydrocarbons in a shallow sand aquifer. Health and Environmental Science Department, API Publication Number 4601, American Petroleum Institute, Washington, DC, 1994.

Schellenberg, S. L. 1987. Groundwater flow and non-reactive tracer motion in heterogeneous statistically anisotropic porous media. M.Sc. Thesis, Department of Earth Sciences, University of Waterloo, Waterloo, Ontario, Canada.

CHAPTER 1

A RELATIVE-LEAST-SQUARES TECHNIQUE TO DETERMINE UNIQUE MONOD KINETIC PARAMETERS OF BTEX COMPOUNDS USING BATCH EXPERIMENTS[1]

1.1. ABSTRACT

An analysis of aerobic m-xylene biodegradation kinetics was performed on the results of laboratory batch microcosms. A modified version of the computer model BIO3D was used to determine the Monod kinetic parameters, k_{max} (maximum utilization rate) and K_S (half-utilization constant), as well as the Haldane inhibition concentration, K_I, for pristine Borden aquifer material. The proposed method allows for substrate degradation under microbial growth conditions. The problem of non-uniqueness of the calculated parameters was overcome by using several different initial substrate concentrations. With a relative-least-squares technique, unique kinetic degradation parameters were obtained. Calculation of the microbial yield, Y, based on microbial counts from the beginning and the end of the experiments was crucial for reducing the number of unknowns in the system and therefore for the accurate determination of the kinetic degradation parameters. The kinetic parameters obtained in the present study were found to agree well with values reported in the literature.

1.2. INTRODUCTION

Many aquifers are contaminated with petroleum hydrocarbons, originating from human activity associated with the recovery, refining, storage, use and disposal of petroleum products. The compounds of greatest concern are the monocyclic aromatic

---

[1] This paper has been accepted by the Journal of Contaminant Hydrology. Authors are M. Schirmer, B. J. Butler, J. W. Roy, E. O. Frind and J. F. Barker.

hydrocarbons collectively known as BTEX (benzene, toluene, ethylbenzene and the xylenes). Benzene is a known carcinogen, and all BTEX compounds are hazardous substances subject to regulation in drinking water (Sittig, 1985). Although BTEX may comprise only a small percentage of hydrocarbon fuels, they often have the greatest environmental impact due to their high water solubilities and mobilities allowing them to migrate through groundwater systems and contaminate drinking water supplies far from their source.

The microbial degradation of BTEX is an important in situ remediation pathway for subsurface sites contaminated with gasoline or other petroleum products (Rice et al., 1995). Increasingly, the value of such intrinsic or passive remediation for at least some contaminated sites is being recognized, given the large expense of designing, engineering, and implementing active remediation technologies (Norris et al., 1993). However, given that aquifer properties vary widely, intrinsic bioremediation must be demonstrated for each contaminated site individually. Modelling of potential contaminant attenuation is a required part of the investigation to determine whether natural contaminant depletion is sufficient under site conditions to meet remedial goals.

The largest problem in modelling in situ biodegradation is obtaining reliable kinetic parameters. Typically, contaminant biodegradation is treated as first-order decay, using best-fit coefficients that are matched to field data (e.g., Wiedemeier et al., 1996; Borden et al., 1997). Clearly this simplified representation does not reflect the effects of complex biological processes such as adaptation, inhibition, preferential substrate utilization and growth of the population of degrader microorganisms. Such effects can be incorporated into derivatives of the Monod equation (Monod, 1949), and resultant kinetic equations may consider both substrate and biomass levels, as interactions between these levels greatly affect the pattern of contaminant degradation (Simkins and Alexander, 1984). Although groundwater contaminant data at a given site can be used to derive these Monod kinetic parameters, nonuniqueness of the fitted biodegradation rate parameters is a common difficulty due to the concurrent effects of other field-related processes affecting the measured contaminant concentrations.

Previous studies have found that it is extremely difficult or even impossible to obtain the kinetic Monod parameters from a single substrate depletion curve if the microbial yield is not measured independently (Kelly et al., 1996). Guha and Jaffé (1996) overcame this problem by applying a statistical approach to parameter estimation using a maximum likelihood equation. However, since only one initial substrate concentration was used, the maximum utilization rate (k_{max}) and the half-utilization constant (K_S) of the substrate could not be determined uniquely, with widely varying pairs of values describing the system equally well. Since Guha and Jaffé (1996) evaluated only one initial substrate concentration, the microbial yield calculated applied to this particular initial substrate concentration only but may not apply for different initial concentrations (Connolly et al., 1992; Gaudy, 1992). Alvarez et al. (1991) presented a method to derive Monod kinetic parameters using several initial substrate concentrations. However, their approach can be applied only to a substrate utilization phase where the microbial population does not increase significantly.

To account for the influence of microbial growth, the present study evaluated the kinetic Monod parameters for different initial substrate concentrations. We present a method that combines simple batch experiments using site materials with computer modelling to estimate unique Monod kinetic parameters, using m-xylene as an example compound. Contaminant fate and transport models which incorporate these parameters, rather than a blanket first-order decay term to describe biodegradation, should forecast the intrinsic bioremediation capabilities of a given aquifer more accurately.

The work focused on the aerobic biodegradation kinetics of m-xylene in pristine material and groundwater from the well-documented aquifer at the Canadian Forces Base (CFB) Borden (e.g., Nicholson et al., 1983; Mackay et al., 1986). Batch microcosms provided data for use in a modified version of the numerical computer model BIO3D (Frind et al., 1989; Schirmer et al., 1995), referred to here as BIOBATCH. The calculated kinetic parameters are compared to literature values obtained in previous studies.

1.3. MATERIALS AND METHODS - BATCH EXPERIMENTS

1.3.1. Microcosms

Microcosms consisted of 20 g (wet weight) of pristine aquifer material saturated with 50 mL of groundwater obtained from the CFB Borden aquifer, in 160-mL hypovials sealed with Mininert™ valves (Dynatech Precision Sampling). Filter-sterilized m-xylene was added to the microcosms by syringe. To ensure carbon-limited conditions, excess inorganic nutrients were added to the groundwater in quantities equivalent to a modified Bushnell-Haas medium (Mueller et al., 1991). The hypovial headspace provided oxygen in excess. The microcosms were maintained at 10 ^{0}C, the average temperature of Borden groundwater, and were shaken to enhance oxygen transfer into the liquid. Sterile controls verified that changes in hydrocarbon concentration were due to biodegradation and not abiotic effects such as adsorption or chemical degradation. Control microcosms were sterilized by autoclaving for 1 hour on 3 successive days, and were also poisoned with 0.1% sodium azide. Microcosms were prepared in triplicate for each experimental condition.

1.3.2. Measuring hydrocarbon loss

By headspace gas chromatography, m-xylene was monitored using a Shimadzu GC-9A gas chromatograph equipped with flame ionization detection, and a 60 m Supelcowax 10 capillary column (Supelco). A 400 μL sample of microcosm headspace gas was introduced on-column via a gas sampling valve (Valco Instruments) and a split injection port. The chromatographic conditions were: injector/detector temperature, 200 ^{0}C; oven temperature, 105 ^{0}C; helium carrier gas (column flow 5 mL/min; make-up flow 50 mL/min), with calibration by an external standard method. Gaseous concentrations were converted to aqueous concentrations using a dimensionless Henry's constant of 0.125, determined by the method of Gossett (1987). The detection limit (as aqueous concentration) was approximately 10 μg/L.

1.3.3. Cell Counts

Given that much of an aquifer microbial population is attached, not free-swimming (Holm et al., 1992; Godsy et al., 1992), cell counts were determined for the total sand matrix (i.e., solids plus pore water). Total cell counts were conducted using 4',6-diamidino-2-phenylindole (DAPI)-stained preparations and epifluorescence microscopy. Both an initial count and counts after complete degradation were obtained. Once the hydrocarbon concentration in a given microcosm was below detection, microcosm contents were fixed by addition of 1.5 mL of 10% phosphate-buffered glutaraldehyde, and stored in the dark at 4 ^{0}C for two weeks or less before counting (Clarke and Joint, 1986; Kepner and Pratt, 1994).

To perform the total counts, 0.5 mL sand slurry (equivalent to 0.76 g dry weight) was treated with two mL of MilliQ water, plus 20 µL Tween 80 to desorb bacteria from the sediments and 40 µL of a 10 mg/L DAPI staining solution (Yu et al., 1995). All solutions were filter-sterilized before use with a 0.2 µm pore size filter. The sand suspension was vortex-mixed for 30 seconds, then left for 40 min. After mixing again, a drop of suspension was placed on a microscope slide, overlain with a coverslip and viewed at 1000x magnification by epifluorescence microscopy (Nikon Labophot-2). Two slides were prepared for each microcosm sample, and ten or more fields were counted per slide. To correct for any autofluorescing debris shaped similarly to bacterial cells, the sterile controls were also "counted" and these values subtracted from each corresponding replicate. The average cell number for a sample was then calculated.

To obtain an estimate of the proportion of the Borden microbial population initially capable of aromatic hydrocarbon degradation, monoaromatic hydrocarbon degrader and aerobic heterotroph counts were conducted on pristine Borden material. A suspension of 10 g (wet wt) of aquifer material in 90 mL 0.1% Na pyrophosphate solution was shaken for 10 min at 400 rpm on a rotary shaker, then further diluted in phosphate-buffered saline. Aliquots (0.1 mL) of suitable dilutions were spread on triplicate plates of R2A agar, a general-purpose, low-nutrient medium which supports growth of a wide range of microorganisms (Reasoner and Geldreich, 1985). Aromatic hydrocarbon

degraders were assessed by a three-tube most-probable-number (MPN) determination. Screw-capped test tubes containing 10 mL of a mineral medium (Furukawa et al., 1983) were inoculated with 1 mL of suitably diluted aquifer material suspension, then amended with 1 μL of a neat, filter-sterilized benzene/toluene (1:1) mixture using a micropipettor. Resulting maximum aqueous concentrations were about 50 mg/L for each hydrocarbon, although actual concentrations were lower due to partitioning into the tube headspace, and to losses to the atmosphere during the amendment procedure. After 30 days of incubation at 22-25 ^{0}C, R2A plates were enumerated to obtain an aerobic heterotroph count and MPN tubes were scored for growth (visible turbidity) and the MPN determined from an appropriate table (Mayou, 1976). In the aromatic hydrocarbon degrader assay use of xylenes is avoided because of their relatively greater toxicity (Peters, 1988; Herman et al., 1990), which could cause growth inhibition at the hydrocarbon levels required to produce visible turbidity. The m- and p- isomers of xylene are often degraded by microorganisms capable of growth on benzene and/or toluene (e.g., bacteria possessing the TOL plasmid metabolize toluene and both xylene isomers via the same pathway), so our aromatic hydrocarbon degrader estimate is likely a reasonable estimate for m-xylene degraders.

1.3.4. Calculation of Biomass and Yield

Microbial cell counts were converted to biomass using a factor of 1.72×10^{-10} mg/bacterial cell, a value derived from analysis of aquifer microorganisms (Balkwill et al., 1988). Biomass is expressed as mg/L of microcosm liquid (i.e., mg/vol groundwater in situ) in the model because the decrease in contaminant concentration depends on the degraders per volume of solution, assuming that only dissolved phase contaminants are metabolized.

Based on the initial DAPI counts, the pristine aquifer material contained an average biomass concentration of 1.474 mg/L. However, only part of this initial microbial population was capable of aromatic hydrocarbon degradation. This proportion was estimated as 0.2%, from the ratio of monoaromatic hydrocarbon degraders to aerobic

heterotrophs obtained from analysis of three separate samples of pristine, saturated Borden aquifer material. Use of this value resulted in an estimated initial hydrocarbon degrader concentration of 0.003 mg/L in the microcosms. All the additional cells counted in the "final" microcosm DAPI counts were assumed to have arisen from aromatic hydrocarbon degradation since only m-xylene was provided as substrate in the microcosms. After subtracting the non-degrader biomass from the initial and final values, the yield (Y) was calculated as the difference between the initial and final masses of hydrocarbon degraders divided by the substrate mass utilized.

1.4. THE NUMERICAL MODEL BIOBATCH - GOVERNING EQUATIONS

The numerical model BIOBATCH is a modified version of the advective-dispersive transport model BIO3D (Frind et al., 1989; Schirmer et al., 1995). BIO3D can consider multiple organic substrates in the presence of an electron acceptor and a microbial population by using the dual-Monod formulation for the degradation kinetics. For the present study, oxygen as the electron acceptor is available in excess throughout the duration of the batch experiments. We restricted the solution to one organic substrate while allowing growth of the microbial population.

The assumptions involved are: (1) volatilization of the substrate within the microcosms is instantaneous and reversible, governed by Henry's law; (2) sorption and desorption of the substrate by the aquifer material and the glassware follow linear isotherms and (3) mass transfer is instantaneous between the three phases (solid, liquid, gas).

Three phases are present in the batches: headspace, sediment/glass, and water. Because only the aqueous substrate is available to the microorganisms, not all of the substrate is available for immediate microbial utilization. To account for this, a mass distribution coefficient, D, is introduced. Like a retardation factor in transport models, the mass distribution coefficient represents the ratio of total mass in the system to the bioavailable mass in the aqueous phase with the assumption that partitioning among phases is instantaneous.

The total mass in the system, m_{total}, can be calculated by adding the masses in the aqueous phase, the headspace and sorbed-onto-the-aquifer material and the glassware. The substrate mass in the aqueous phase is calculated as

$$m_{aq} = S_{aq} \; V_{aq} \tag{1.1}$$

where m, S and V refer to the mass, substrate concentration and volume, respectively. The subscript, aq, denotes the aqueous phase.

It is assumed that volatilization follows Henry's law:

$$S_g = S_{aq} H \tag{1.2}$$

where the subscript, g, refers to the gaseous phase and H is the dimensionless Henry's law constant. The substrate mass in the gaseous phase is given by:

$$m_g = (S_{aq} H) V_g . \tag{1.3}$$

For our batch experiments, the substrate mass sorbed to the glassware is much smaller than the substrate mass sorbed to the aquifer material. The overall substrate mass sorbed can therefore be calculated as:

$$m_{sorb} = S_{aq} K_d m_{soil} \tag{1.4}$$

where m_{sorb} is the substrate mass sorbed [g], K_d is the distribution coefficient [cm^3/g] and m_{soil} is the mass of aquifer material [g]. However, since K_d is obtained experimentally using the same batch setup, Equation 1.4 also accounts for the mass sorbed to the glassware as explained below. The value of D can be determined as

$$D = m_{total} / m_{aq} = (m_{aq} + m_g + m_{sorb}) / m_{aq} \tag{1.5}$$

or rewritten as

$$D = (V_{aq} + H V_g + K_d m_{soil}) / V_{aq} . \tag{1.6}$$

Compounds such as m-xylene are potentially toxic substrates. To account for substrate toxicity at high concentrations, the Haldane inhibition term [S^2/K_I] (Haldane, 1930; Andrews, 1968) can be introduced where K_I [mg/L] is the Haldane inhibition concentration. The Haldane term yields a slower microbial growth and, therefore, a slower effective substrate utilization rate at higher substrate concentrations. The resulting governing equations for substrate and microbes are then given as:

$$- dS/dt = k_{max} M (S / [S + K_S + (S^2/K_I)]) / D \tag{1.7}$$

$$dM/dt = k_{max} M (S / [S + K_S + (S^2/K_I)]) Y - bM \tag{1.8}$$

where S is the organic substrate concentration [mg/L], t is time [days]; k_{max} is the maximum-utilization rate of S [day^{-1}]; M is the microbial concentration [mg/L]; K_S is the half-utilization constant of S [mg/L]; D is the mass distribution coefficient; Y is the microbial yield, the ratio of microbes grown to substrate utilized, and b is the first-order decay rate of the microbial population [day^{-1}]. The two equations are nonlinear and coupled and, therefore, must be solved iteratively.

1.5. DETERMINATION OF THE BEST FIT PARAMETERS

1.5.1. Calculation of the Distribution Coefficient (D)

The K_d value for m-xylene for Borden aquifer material was determined using sorption data presented by Patrick et al. (1985). The sorption experiments show linear isotherms with K_d values that include sorption onto both the aquifer material and the glassware surface. A K_d value of 1.55 cm^3/g for m-xylene was calculated for our experimental conditions. Using this value and H = 0.125 in Equation 1.6 yields a D value of 1.86.

Not accounting for the substrate mass which is not immediately bioavailable will result in incorrect estimations of the kinetic degradation parameters. In Figure 1.1, identical kinetic parameters are used to calculate the degradation curves for a range of D values, demonstrating the sensitivity of the solute degradation to the value of the mass distribution coefficient.

The assumptions regarding the calculation of the D value, i.e. substrate sorption and desorption follows a linear isotherm and the mass transfer between the phases is an instantaneous and reversible process, are reasonable for the low-organic carbon Borden sand (f_{OC} = 0.021%) and the BTEX compound used in the present study (Patrick et al., 1985; Hubbard et al., 1994). However, if studies are carried out using aquifer material containing large amounts of organic carbon or using more hydrophobic compounds, such as phenanthrene, sorption and volatilization kinetics of the substrate may have to be taken into account (Guha and Jaffé, 1996).

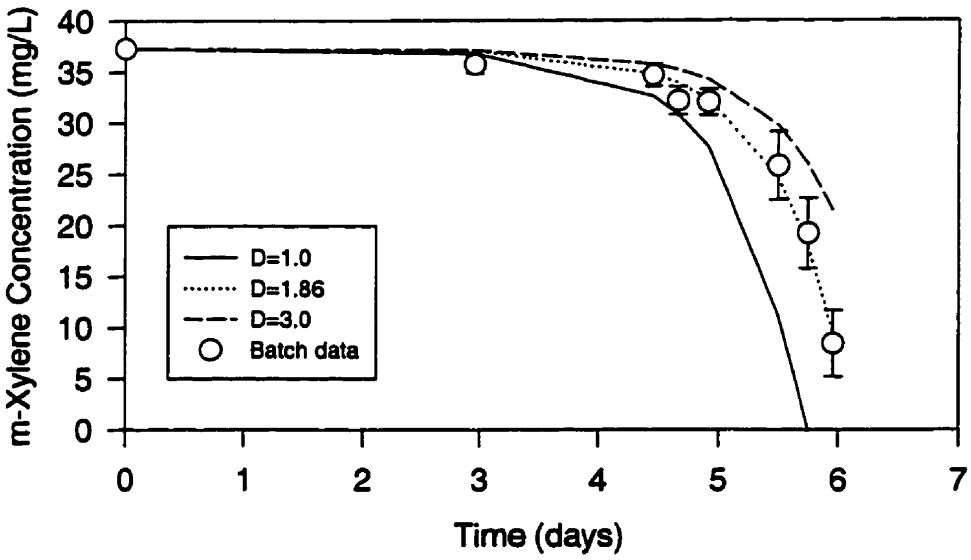

Figure 1.1. Calculated m-xylene degradation curves (lines without symbols) in comparison to measured data (symbols with error bars of one standard deviation) using identical kinetic parameters (k_{max} = 4.13 day^{-1}; K_S = 0.79 mg/L and K_I = 91.7 mg/L, the values that were found to be the unique kinetic parameters for the entire set of m-xylene data) and different mass distribution coefficients (D).

1.5.2. Calculation of the Microbial Yield (Y)

For Equations 1.7 and 1.8, with D defined, there are five unknowns (k_{max}, K_S, K_I, Y and b) that describe the system of batch experiments. The microbial concentrations were measured in the batch experiments, allowing for explicit calculation of the microbial parameters Y and b.

Since the experiments were conducted over a relatively short time (less than eight days) and the microbial population was in the exponential or, at most, the early stationary growth phase (Chapelle, 1993), we assumed that the microbial decay constant, b, was small relative to the rate of population increase. This assumption seems reasonable since no convincing evidence of the manifestation of decay in these growth phases is reported in the literature (Gaudy, 1992).

Given that we determined the final microbial concentration for each batch experiment, Y can be determined as:

$$Y = \Delta M / \Delta S \qquad (1.9)$$

for each initial substrate concentration (Table 1.1) where ΔM is the mass of microbes gained and ΔS is the mass of substrate utilized. An average Y of 0.52 was calculated for m-xylene for this set of experiments.

Not measuring Y and calibrating for it in the model would add another complication in determining unique kinetic parameters. Figure 1.2 illustrates that, holding all other parameters constant, different yield factors will give different degradation curves. This finding points out how important it is to measure the microbial yield in the experiments.

Table 1.1. Results of the best-fit Monod parameters k_{max} and K_S using BIOBATCH including the Haldane inhibition concentration K_I and the derived microbial yield Y.

Average Initial m-Xylene Conc. in mg L^{-1} [a]	Final microbial degrader population in mg L^{-1}	k_{max} in day^{-1}	K_S in mg L^{-1}	K_I in mg L^{-1}	Microbial yield Y measured	Standard deviation of microbial yield measured
4.7	3.1	4.13	0.79	91.7	0.48	0.09
8.6	10.7	4.13	0.79	91.7	0.70	0.19
17.8	12.8	4.13	0.79	91.7	0.46	0.06
37.3	23.2	4.13	0.79	91.7	0.43	0.10

[a] The average aqueous phase m-xylene concentrations of three replicates are reported in column 1. The microbial yield was calculated based on the microbial degrader mass gained and the product of the substrate mass utilized and the mass distribution coefficient (D).

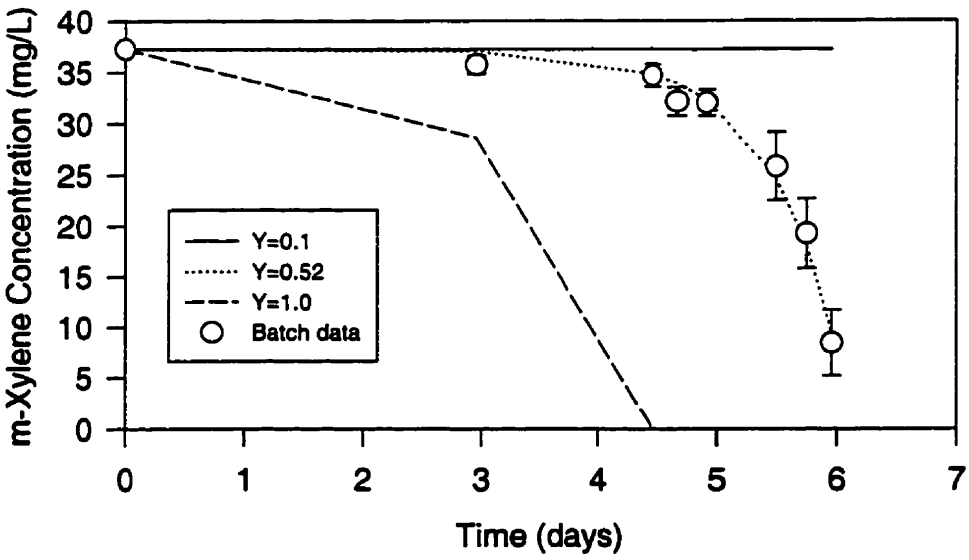

Figure 1.2. Calculated m-xylene degradation curves in comparison to measured data (symbol with error bars of one standard deviation) using microbial yields Y of 0.52 (average Y as actually measured in batch experiment), 0.1 and 1.0 and identical kinetic parameters (k_{max} = 4.13 day^{-1}; K_S = 0.79 and K_I = 91.7 mg/L, the values that were found to be the unique kinetic parameters for the entire set of m-xylene data).

1.5.3. Determination of the Best-fit Kinetic Degradation Parameters k_{max}, K_S and K_I

The three remaining unknowns, k_{max}, K_S and K_I in the Monod kinetic term, must be found. These values have to hold for the degradation curves of each initial substrate concentration. The same initial microbial concentration of 0.003 mg/L was used for each initial concentration. We can obtain the best fit k_{max}, K_S and K_I parameters by running BIOBATCH for a wide range of different k_{max} / K_S / K_I combinations, typically for $0 \leq k_{max} \leq 20$ day^{-1}, $0 \leq K_S \leq 10$ mg/L and $0 \leq K_I \leq 200$ mg/L (Figure 1.3). One parameter is changed at a time and the calculations are performed for each initial substrate concentration. The program calculates the corresponding substrate concentrations over time for each k_{max} / K_S / K_I combination and compares the results to the degradation

curves measured in the laboratory batch experiments by calculating the relative squared errors (RSE):

$$RSE = \sum_{N=1}^{z} \left(\frac{S_{mN} - S_{cN}}{S_{mN}} \right)^2 \Big/ (z-1) \qquad (1.10)$$

where z is the number of measuring points; S_{mN} is the substrate concentration measured [mg/L] and S_{cN} is the substrate concentration calculated using BIOBATCH [mg/L]. For a RSE of zero, the calculated and measured curves are identical. To maintain an even weight between the calculated errors of different substrate concentrations, the difference between S_{mN} and S_{cN} is divided by S_{mN} to normalize the error. This procedure follows the suggestion by Saez and Rittmann (1992) to use relative least squares instead of absolute ones when dealing with biodegradation batch experiments. The curve with the minimum RSE is referred to as that with the relative least squares (RLS) in the terminology of Saez and Rittmann (1992). Because we deal with several degradation curves with different numbers of measuring points and to maintain an even weight between the curves, we divide the normalized squared errors by the number of measuring point less one (z-1). The subtraction of one arises because the initial concentration is identical for all measured and calculated curves.

All calculated k_{max} / K_S / K_I combinations with their corresponding RSE values are written to a file and later plotted on a three-dimensional graph in order to find the local minimum, i.e. the best-fit parameter combination, for each initial substrate concentration.

The initial step width for the different k_{max} / K_S / K_I combinations, is 0.1 day^{-1}, 0.1 mg/L and 0.5 mg/L for k_{max}, K_S and K_I, respectively. Once a narrower range containing the RLS for the different initial concentrations is identified, the step width is refined to 0.01 day^{-1}, 0.01 mg/L and 0.1 mg/L for k_{max}, K_S and K_I, respectively, in order to obtain a more accurate result.

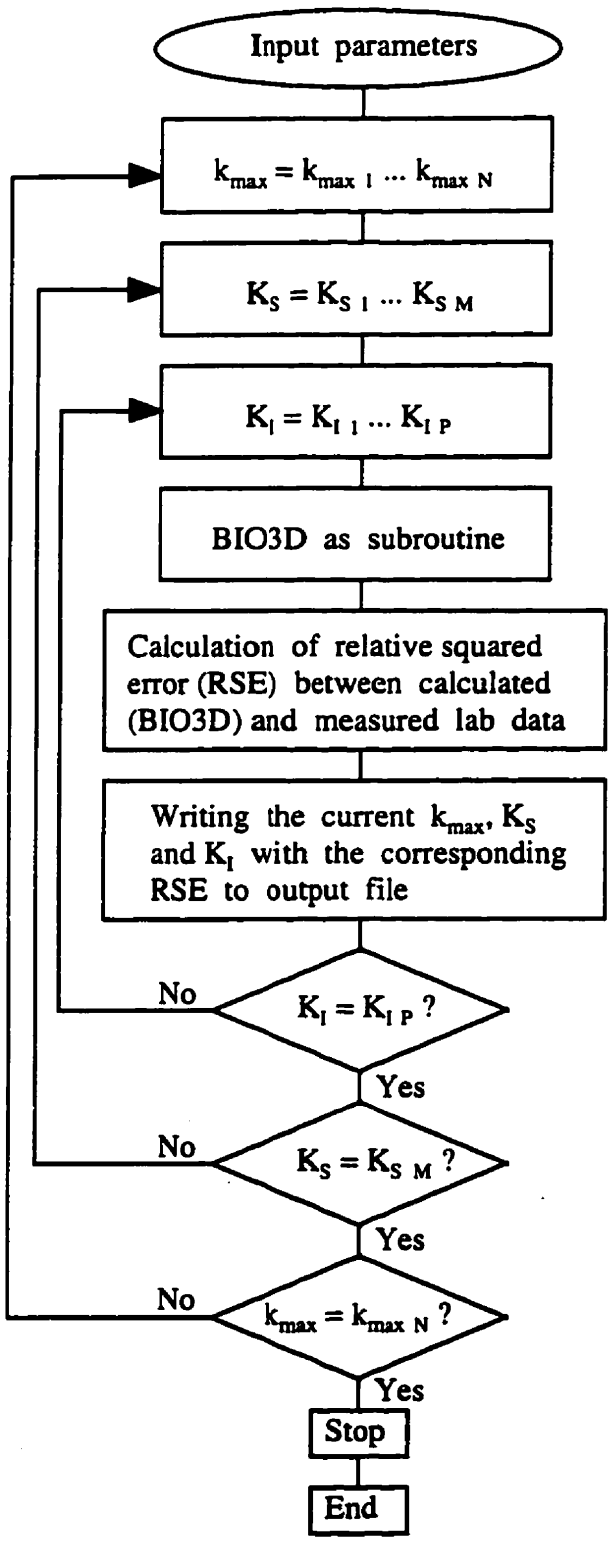

Figure 1.3. Flow chart of the numerical program BIOBATCH for the calculation of the relative squared errors (RSE) using the numerical model BIO3D as a subroutine. The RSE were later used to derive the relative least squares (RLS).

K_S and k_{max} are shown to be highly correlated, which has been demonstrated previously by other workers (e.g., Berthouex and Brown, 1994; Guha and Jaffé, 1996). Figure 1.4 presents an example where different k_{max} / K_S combinations yield an equally good fit to the measured data. This implies that degradation curves resulting from different k_{max} / K_S / K_I combinations could fit the measured values for one particular initial substrate concentration, leading to non-unique results. However, only one k_{max} / K_S / K_I combination represents the intrinsic Monod parameters for a certain set of experimental data, independent of the initial substrate concentration, ignoring the possible effects of metabolite toxicity. Therefore, degradation curves for more than one initial contaminant concentration can provide a unique k_{max} / K_S / K_I combination.

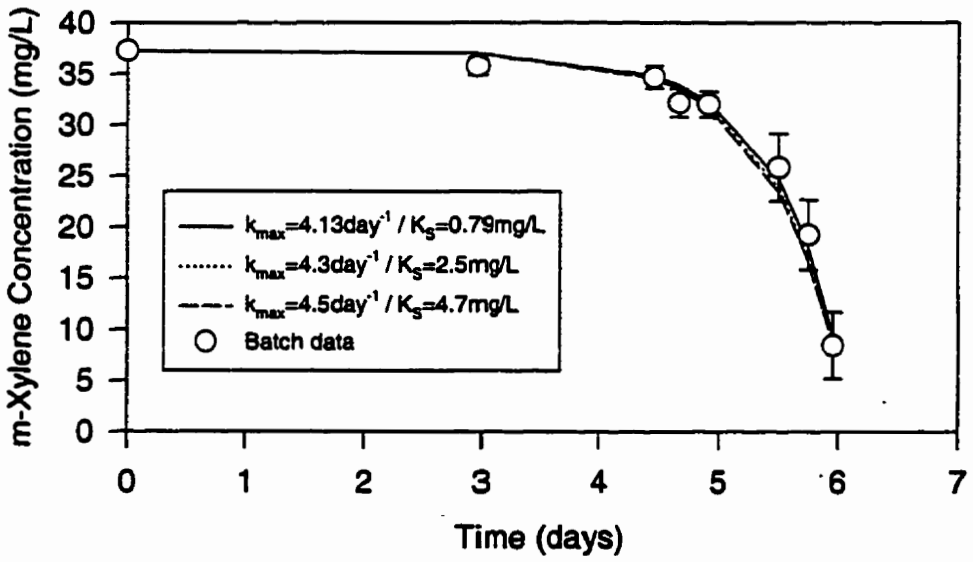

Figure 1.4. An example of modelled degradation curves calculated using different Monod parameter (k_{max} and K_S) combinations and a constant Haldane inhibition concentration K_I of 91.7 mg/L for an initial m-xylene concentration of 37.3 mg/L. Symbols represent measured data with error bars of one standard deviation.

Two examples of plotted RSE values for the aerobic m-xylene degradation are shown in Figure 1.5. For a better visualization, Figure 1.5 represents two-dimensional slices of the three-dimensional solution domain. The dark areas represent parameter combinations with small RSE, i.e. a good fit to the measured degradation curves in the batches.

The unique k_{max} / K_S / K_I combination will represent the global RLS that gives a minimal error between the measured and calculated degradation curves for all initial substrate concentrations. By overlaying the three-dimensional solution domains of the individual initial substrate concentrations by summing up the RSE for each k_{max} / K_S / K_I parameter combination (two examples of those local RSE are shown in Figure 1.5), the corresponding global RLS can be obtained (Figure 1.6).

Using the presented method to calculate a global RLS based on the local RSE of each initial substrate concentration has the advantage that it is easy to detect if the local minima do not overlap to form a global minimum. In this case, the governing equations have to be modified further to identify a global minimum.

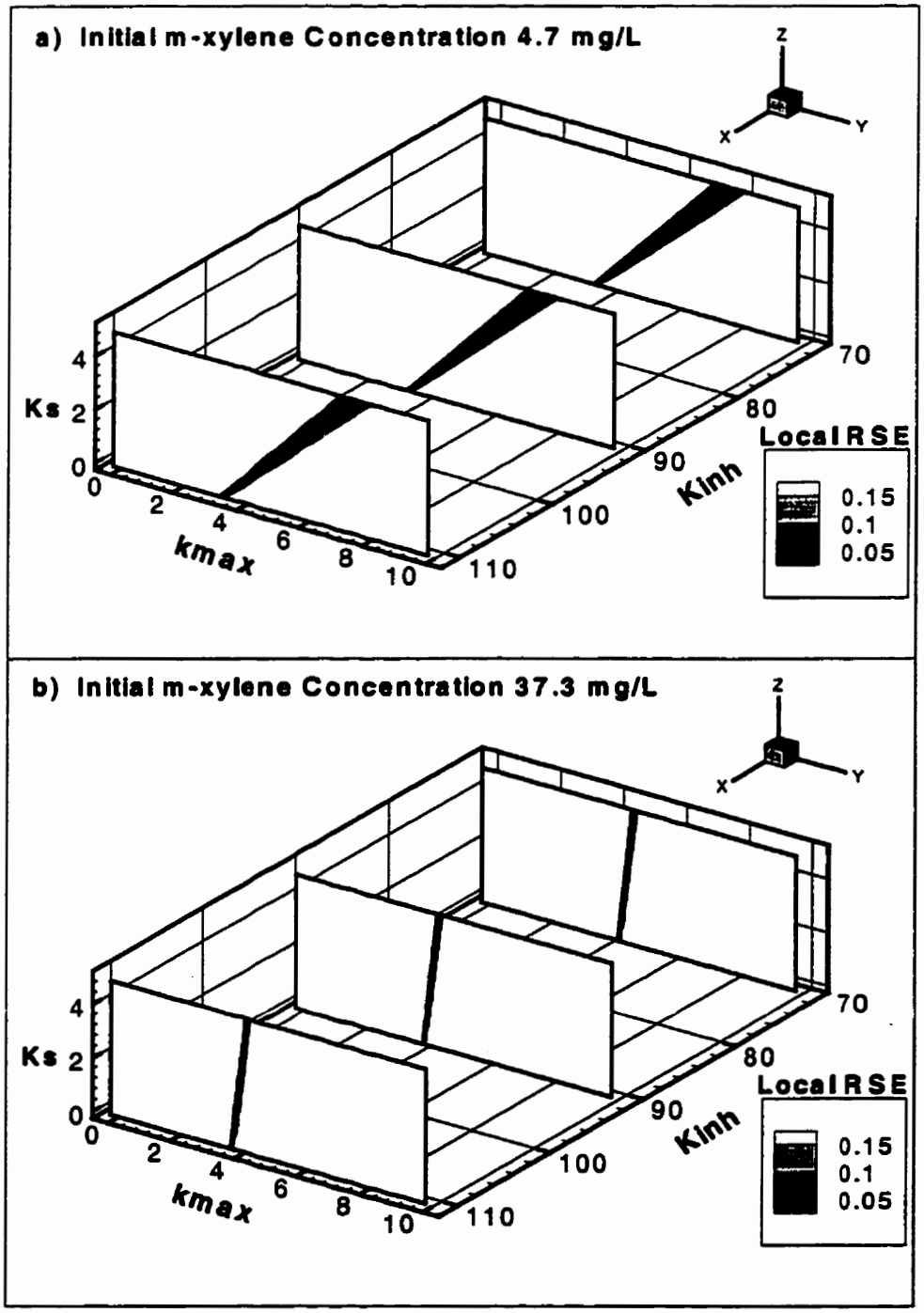

Figure 1.5. Examples of two out of four RSE (with local RLS in the dark area) between measured and calculated substrate degradation curves for the initial m-xylene concentrations (a) 4.7 mg/L and (b) 37.3 mg/L. (K_S in mg/L; k_{max} in day^{-1}; K_{inh} in mg/L).

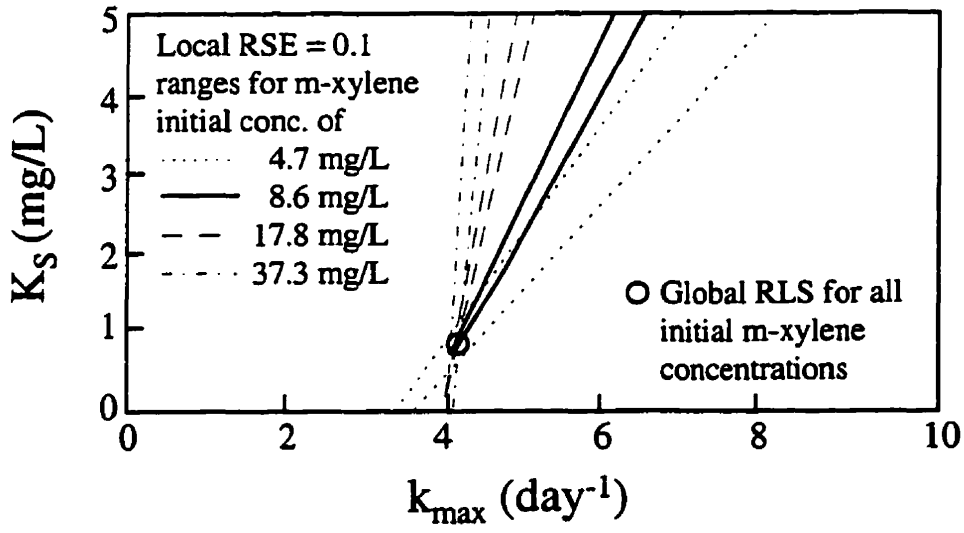

Figure 1.6. Global RLS between measured and calculated substrate degradation curves for all initial m-xylene concentrations combined. The presented two-dimensional slice of the three-dimensional solution domain represents a constant Haldane inhibition concentration K_I of 91.7 mg/L. The unique Monod degradation parameters fitting all initial m-xylene concentrations are k_{max} = 4.13 day^{-1} and K_S = 0.79 mg/L.

1.6. RESULTS AND DISCUSSION

Aerobic m-xylene biodegradation experiments were conducted in batch mode for four different initial concentrations using three replicates for each concentration. Mean values were used for the degradation curves to determine the RSE using the computer program BIOBATCH. The initial total microbial concentration was 1.474 mg/L with an experimentally determined initial degrader population of 0.2 % which yields an estimated initial degrader concentration of 0.003 mg/L.

Given that the Monod degradation parameters (k_{max} and K_S) together with the Haldane inhibition concentration (K_I) for a compound are, in theory, independent of the initial substrate concentration, we therefore calibrated the best-fit k_{max} / K_S / K_I combinations for each initial substrate concentration individually. By summing up the RSE for each Monod parameter combination and each initial concentration, the global RLS for all initial substrate concentrations was found which implies a unique fit of the Monod kinetic parameters for the set of batch experiments.

Figure 1.6 shows the global RLS for the present m-xylene study. A two-dimensional slice of the three-dimensional solution domain (for $K_I = 91.7$ mg/L) is presented. A k_{max} of 4.13 day^{-1}, a K_S of 0.79 mg/L and a K_I of 91.7 mg/L give the global RLS for all m-xylene experiments. The RLS with respect to k_{max} / K_S / K_I depends on the microbial yield Y. However, since the initial and final microbial concentrations were measured for each initial substrate concentration, Y was calculated and applied.

In the present study, the microbial decay coefficient, b, was assumed to be small and ignored. For a field application of the parameters it might be necessary to determine b using independent lab studies.

As noted by Alvarez et al. (1991), estimation of microbial numbers is a major source of variation in determining kinetic parameters in sediments, soils, etc. While direct counts are more reliable than plate counts for determining the total population, viable and nonviable cells are not distinguished, and cells active in contaminant degradation cannot be differentiated from non-growing cells, cells growing on metabolites derived from the target compound rather than the target compound itself, or cells growing on other substrates such as dead biomass or humic material present in the environment. Furthermore, microbial counts typical of aquifers are near the lower limit of detection for direct count techniques. Our approach to this difficulty in estimating the degrader population was to apply a ratio derived from viable count data (i.e., the aromatic hydrocarbon degrader : aerobic heterotroph ratio) to initial direct cell counts, to estimate that fraction of the total cell population capable of aromatic hydrocarbon degradation.

The calculated Monod parameters for m-xylene are summarized in Table 1.1 and the results applied to the biodegradation experiments are shown in Figure 1.7. There is good agreement between the calculated and measured values using the same set of k_{max} / K_S / K_I parameters for each experiment. The introduction of the Haldane inhibition term into the Monod equation was necessary to account for the slower utilization rate at higher substrate concentrations. This slower utilization rate is caused by an increased substrate toxicity to the microbial population (Peters, 1988). If this term was not introduced, the local RLS for different initial concentrations did not overlap and no global RLS would have been found.

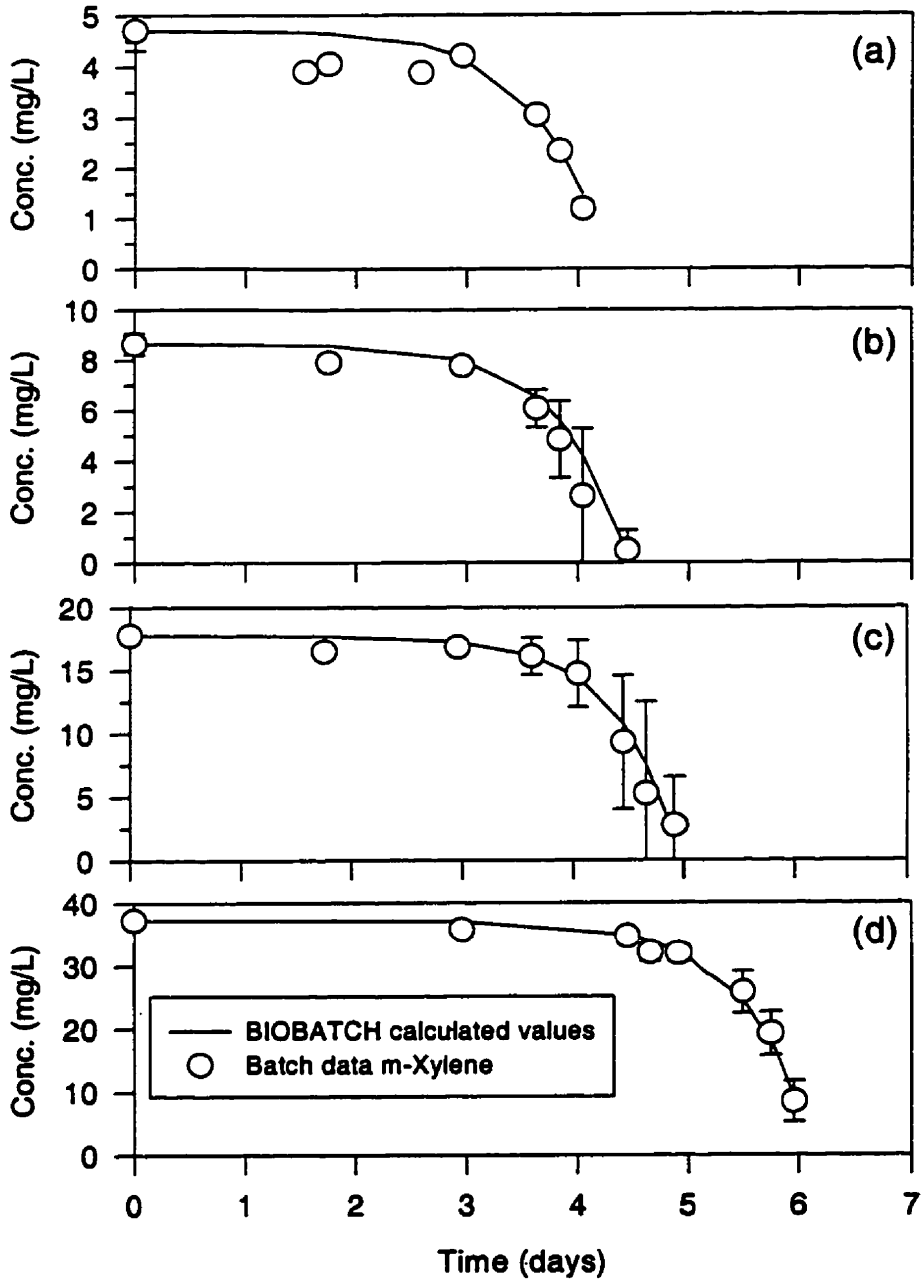

Figure 1.7. Measured m-xylene biodegradation curves (symbols with error bars of one standard deviation) compared to BIOBATCH calibrated global RLS values of $k_{max} = 4.13$ day^{-1}, $K_S = 0.79$ mg/L and $K_I = 91.7$ mg/L. Initial m-xylene concentrations are (a) 4.7 mg/L, (b) 8.6 mg/L, (c) 17.8 mg/L, and (d) 37.3 mg/L.

A range of values was obtained from the literature for the parameters k_{max} and K_S pertaining to xylene degradation (Table 1.2). The values of k_{max} and K_S obtained within this study using BIOBATCH are comparable, as all the values are within about one order of magnitude. It is important to keep in mind that the above mentioned literature values are derived from a variety of different sources using laboratory batch and column experiments.

There are many reasons for obtaining different values for kinetic parameters. They will often be site specific, since the microbial populations will vary. Different species of bacteria will differ in their biodegradation ability and possibly the pathway of metabolism. Conditions such as temperature or groundwater geochemistry will also affect the results, especially if limitations of nutrients are involved.

Since batch experiments with natural water samples appear to provide the most ecologically relevant estimates of k_{max} and K_S (Connolly et al., 1992), it is our intention to conduct additional experiments to investigate if the calculated Monod parameters also hold for BTEX mixtures. Then we will simulate a field-scale experiment that has been conducted at CFB Borden (Hubbard et al., 1994). This should give some insight into whether laboratory derived Monod parameters can be applied to the field scale.

Table 1.2. Selected literature values of Monod coefficients for aerobic xylene biodegradation.

Compound	k_{max} (day^{-1})	K_S ($mg\ L^{-1}$)	**Remark**
p-Xylene	3.12	16.0	batch test; gasoline contaminated soil [a]
p-Xylene	12.85	4.55	batch test; activated carbon fluidized-bed reactor with pure microbial culture [b]
Xylene	9.192	13.2725	batch test; creosote contaminated soil [c]
Xylene	1.488-9.00	(negative K_S)	column test; creosote contaminated soil [c]
m-Xylene	4.13	0.79	batch test; pristine sandy aquifer [d]

[a] Goldsmith and Balderson (1988); [b] Chang et al. (1993); [c] Kelly et al. (1996); [d] This study

1.7. CONCLUSIONS

Unique Monod kinetic parameters can be determined by applying computer modelling to laboratory batch experiments using different initial substrate concentrations. Measurements made for several initial substrate concentrations are crucial to overcome the problem of non-uniqueness of the fitted Monod parameters.

The calculated Monod parameters for the batch degradation experiments were reasonable and comparable to other literature values. The microbial yield is a sensitive parameter. It is very important to have information about the microbial population to accurately examine the Monod kinetic parameters. A failure to account for the microbial concentration at the beginning and the end of the experiment will result in a non-unique or erroneous estimate of the Monod parameters. Applying these erroneous values to simulate field plume behaviour may have serious implications on the predictions.

1.8. ACKNOWLEDGMENTS

This study was partially funded through a grant of the Natural Science and Engineering Research Council of Canada to J. F. Barker, B. J. Butler and E. O. Frind. We would like to thank Marit Nales, Jos Beckers, Ty Ferré and John Molson at the University of Waterloo for many thoughtful discussions, and Peter M. Huck (University of Waterloo) for the use of his microscope. Mario Schirmer was initially supported by the Gottlieb-Daimler- and Karl-Benz-Foundation (Germany) and the Canadian Government through research scholarships.

1.9. REFERENCES

Alvarez, P. J. J., Anid, P. J. and Vogel, T. M. 1991. Kinetics of aerobic biodegradation of benzene and toluene in sandy aquifer material. Biodegradation 2, 43-51.

Andrews, J. F., 1968. A mathematical model for the continuous culture of microorganisms utilizing inhibitory substrates. Biotechnol. Bioeng. 10, 707-723.

Balkwill, D. L., Leach, F. R., Wilson, J. T., McNabb, J. F. and White, D. C. 1988. Equivalence of microbial biomass measures based on membrane lipid and cell wall components, adenosine triphosphate, and direct counts in subsurface aquifer sediments. Microbial Ecology 16, 73-84.

Berthouex, P. M. and Brown, L. C. 1994. Statistics for environmental engineers. Lewis Publisher, Boca Raton, FL, pp. 201-211.

Borden, C. R., Daniel, R. A., LeBrun IV, L. E. and Davis, C. W. 1997. Intrinsic biodegradation of MTBE and BTEX. Water Resources Research 33(5), 1105-1115.

Chang, M. K., Voice, T. C. and Criddle, C. S. 1993. Kinetics of competitive inhibition and cometabolism in the biodegradation of benzene, toluene, and p-xylene by two *Pseudomonas* isolates. Biotechnol. Bioeng. 41, 1057-1065.

Chapelle, F. H., 1993. Ground-water microbiology and geochemistry. New York, John Wiley and Sons, Inc., pp. 151,152, 322-357.

Clarke, K. R. and Joint, I. R. 1986. Methodology for estimating numbers of free-living and attached bacteria in estuarine water. Appl. Environ. Microbiol. 51, 1110-1120.

Connolly, J. P., Coffin, R. B. and Landeck, R. E. 1992. Modeling carbon utilization by bacteria in natural water systems. In: Hurst, C. J. (Ed), Modeling the metabolic and physiologic activities of microorganisms. John Wiley and Sons, Inc., New York, pp. 249-276.

Frind, E. O., Sudicky, E. A. and Molson, J. W. 1989. Three-dimensional simulation of organic transport with aerobic biodegradation. In: Abriola, L. M. (Ed), Groundwater Contamination, IAHS Publ. No. 185, pp. 89-96.

Furukawa, K., Simon, J. R. and Chakrabarty, A. M. 1983. Common induction an regulation of biphenyl, xylene/toluene, and solicylate catabolism in *Pseudomonas paucimobilis*. J. Bacteriol. 154, 1356-1362.

Gaudy Jr., A. F., 1992. Introduction to modeling the metabolic and physiologic activities of microorganisms using wastewater treatment as an example. In: Hurst, C. J. (Ed), Modeling the metabolic and physiologic activities of microorganisms. John Wiley and Sons, Inc., New York, pp. 1-30.

Godsy, E. M., Goerlitz, D. F. and Grbic-Galic, D. 1992. Methanogenic degradation kinetics of phenolic compounds in aquifer-derived microcosms. Biodegradation 2, 211-221.

Goldsmith Jr., C. D. and Balderson, R. K. 1988. Biodegradation and growth kinetics of enrichment isolates on benzene, toluene, and xylene. Water Sci. Technol. 20, 505-507.

Gossett, J. M. 1987. Measurement of Henry's law constants for C1 and C2 chlorinated hydrocarbons. Environ. Sci. Technol. 21, 202-208.

Guha, S. and Jaffé, P. R. 1996. Determination of Monod kinetic coefficients for volatile hydrophobic organic compounds. Biotechnol. Bioeng. 50, 693-699.

Haldane, J. B. S. 1930. Enzymes. Longmans, Green and Company, Ltd., UK. Republished by M.I.T. Press, Cambridge, MA, 1965.

Herman, D. C., Innis, W. E. and Mayfield, C. I. 1990. Impact of volatile aromatic hydrocarbons, alone and in combination, on growth of the freshwater alga *Selenastrum capricornutum*. Aquatic Toxicology 18, 87-100.

Holm, P. E., Nielsen, P. H., Albrechtsen, H. J. and Christensen, T. H. 1992. Importance of unattached bacteria and bacteria attached to sediment in determining potentials for degradation of xenobiotic organic contaminants in an aerobic aquifer. Appl. Environ. Microbiol. 58(9), 3020-3026.

Hubbard, C. E., Barker, J. F., O'Hannesin, S. F., Vandegriendt, M. and Gillham, R. W. 1994. Transport and fate of dissolved methanol, methyl-tertiary-butyl-ether, and monoaromatic hydrocarbons in a shallow sand aquifer. Health and Environmental Science Department, API Publication Number 4601, American Petroleum Institute, Washington, DC.

Kelly, W. R., Hornberger, G. M., Herman, J. S. and Mills, A. L. 1996. Kinetics of BTX biodegradation and mineralization in batch and column systems. Journal of Contaminant Hydrology 23, 113-132.

Kepner Jr., R. L. and Pratt, J. R. 1994. Use of fluorochromes for direct enumeration of total bacteria in environmental samples: past and present. Microbiol. Rev. 58(4), 603-615.

Mackay, D. M., Freyberg, D. L., Roberts, P. V. and Cherry, J. A. 1986. A natural gradient experiment on solute transport in a sand aquifer, 1. Approach and overview of plume movement. Water Resources Research 22(13), 2017-2029.

Mayou, J. 1976. MPN - most probable number. In Speck, M.L. (ed.) Compendium of Methods for the Microbiological Examination of Foods. American Public Health Association, Washington, DC. pp. 152-162.

Monod, J., 1949. The growth of bacterial cultures. Annu. Rev. Microbiol. 3, 371-394.

Mueller, J. G., Lantz, S. E., Blattman, B. O. and Chapman, P. J. 1991. Bench-scale evaluation of alternative biological treatment processes for the remediation of pentachlorophenol- and creosote-contaminated materials: solid-phase bioremediation. Environ. Sci. Technol. 25, 1045-1055.

Nicholson, R. V., Cherry, J. A. and Reardon, E. J. 1983. Migration of contaminants in groundwater at a landfill: A case study. 6. Hydrogeochemistry. Journal of Hydrology 63, 131-176.

Norris, R. D., Hinchee, R. E., Brown, R., McCarty, P. L., Semprini, L., Wilson, J. T., Kampbell, D. H., Reinhard, M., Bouwer, E. J., Borden, R. C., Vogel, T. M., Thomas, J. M. and Ward, C. H. 1993. In situ bioremediation of ground water and geological material: a review of technologies. No. EPA/600/R 93/124. Robert S. Kerr Environmental Research Lab., Ada, OK.

Patrick, G. C., Ptacek, C. J., Gillham, R. W., Barker, J. F., Cherry, J. A., Major, D., Mayfield, C. I. and Dickhout, R. D. 1985. The behavior of soluble petroleum product derived hydrocarbons in groundwater. Petroleum Association for the Conservation of the Canadian Environment. Phase I, PACE Report No. 85-3.

Peters, R. C. 1988. The toxic effects of mononuclear aromatic hydrocarbons on ground water bacteria. M.Sc. Thesis, Department of Biology, University of Waterloo, Waterloo, ON, Canada, 137 p.

Reasoner, D. J. and Geldreich, E. E. 1985. A new medium for the enumeration and subculture of bacteria from potable water. Appl. Environ. Microbiology 49, 1-7.

Rice, D. W., Dooher, B. P., Cullen, S. J., Everett, L. G., Kastenberg, W. E., Grose, R. D. and Marino, M. A. 1995. Recommendations to improve the cleanup process for

California's leaking underground fuel tanks (LUFTs). Lawrence Livermore National Laboratory, Environmental Protection Department, UCRL-AR-121762. Report submitted to the California State Water Resources Control Board, October 16, 1995.

Saez, P. B. and Rittmann, B. E. 1992. Model-parameter estimation using least squares. Water Research 26(6), 789-796.

Schirmer, M., Frind, E. O. and Molson, J. W. 1995. Transport and Biodegradation of Hydrocarbons in Shallow Aquifers: 3D Modelling. American Petroleum Institute, Workshop: Comparative Evaluation of Groundwater Biodegradation Models, May 08-09, 1995, Hotel Worthington, Ft Worth, TX.

Simkins, S. and Alexander, M. 1984. Models for mineralization kinetics with the variables of substrate concentration and population density. Appl. Environ. Microbiol. 47, 1299-1306.

Sittig, M., 1985. Handbook of toxic and hazardous chemicals and carcinogens, 2nd ed. Noyes Publications, Park Ridge, NJ, pp. 868-870.

Wiedemeier, T. H., Swanson, M. A., Wilson, J. T., Kampbell, D. H., Miller, R. N. and Hansen, J. E. 1996. Approximation of biodegradation rate constants for monoaromatic hydrocarbons (BTEX) in ground water. Ground Water Monitoring & Remediation 16(3), Summer 1996, 186-194.

Yu, W., Dodds, W. K., Bands, M. K., Skalsky, J. and Strauss, E. A. 1995. Optimal staining and sample storage time for direct microscopic enumeration of total and active bacteria in soil with two fluorescent dyes. Appl. Environ. Microbiol. 61(9), 3367-3372.

CHAPTER 2

A STUDY OF LONG-TERM MTBE ATTENUATION IN THE BORDEN AQUIFER, ONTARIO, CANADA[1]

2.1. ABSTRACT

In 1988 and 1989, a natural gradient tracer test was performed in the shallow, aerobic sand aquifer at Canadian Forces Base (CFB) Borden. A mixture of ground water containing dissolved oxygenated gasoline was injected below the water table along with chloride (Cl^-) as a conservative tracer. The migration of BTEX, MTBE, and Cl^- was monitored in detail for 16 months. The mass of BTEX compounds in the plume diminished significantly with time due to intrinsic aerobic biodegradation, while MTBE showed only a small decrease in mass over the 16 month period. In 1995/96, a comprehensive ground water sampling program was undertaken to define the mass of MTBE still present in the aquifer. Since the plume had migrated into an unmonitored section of the Borden aquifer, numerical modeling and geostatistical methods were applied to define an optimal sampling grid and to improve the level of confidence in the results. A drive-point profiling system was used to obtain ground water samples. Numerical modeling with no consideration of degradation predicted maximum concentrations in excess of 3000 µg/L; field sampling found maximum concentrations of less than 200 µg/L. A mass balance for the remaining MTBE mass in the aquifer eight years after injection showed that only 3 % of the original mass remained. Sorption, volatilization, abiotic degradation and plant uptake are not considered significant attenuation processes for the field conditions. Therefore, we suggest that biodegradation may have played a major role in the attenuation of MTBE within the Borden aquifer.

---

[1] This paper has been published in Ground Water Monitoring and Remediation (1998) Vol. 18 (2), 113-122. Authors are M. Schirmer and J. F. Barker.

2.2. INTRODUCTION

Bioremediation is widely promoted as a possible solution to ground water contamination. As of March 1996, 33 states in the U.S. had endorsed intrinsic remediation as a viable corrective action at petroleum release sites. In California, Lawrence Livermore National Laboratories recommended that passive bioremediation be considered the primary remediation alternative at leaking fuel tank sites whenever possible (Rice et al., 1995). Intrinsic remediation of gasoline-contaminated ground water generally relies on biodegradation of benzene, toluene, ethylbenzene and the xylene isomers (BTEX) to achieve remedial objectives.

Methyl-tertiary-butyl-ether (MTBE), the most commonly used fuel oxygenate, is added to gasoline to reduce atmospheric concentrations of carbon monoxide and ozone. It appeared in gasoline in the Eastern United States in the early 1980's and in the Western States in the late 1980's (Squillace et al., 1996; Zogorski et al., 1997). It was documented in ground water contaminated by fuel leaks/spills as early as 1980 (McKinnon and Dyksen, 1984). Ground water occurrence data of MTBE were summarized by Davidson (1995).

The environmental properties, behavior and fate of MTBE have been described by Zogorski et al. (1997) and Squillace et al. (1997). MTBE has a very strong taste and odor and is likely to impair drinking water quality at aqueous concentrations of 10 - 100 μg/L. Its water solubility is about 50,000 mg/L. Its organic carbon-based partition coefficient (K_{OC}) is 11 cm^3/g which results in a minimal sorption and retardation in natural aquifers. MTBE has a moderate dimensionless Henry's law Constant (concentration in air/concentration in water) of 0.04 and, therefore, can be stripped from water by conventional air strippers, but requires a greater air flow than required for stripping of BTEX. The structure of MTBE with its ether bond suggests its resistance to degradation by microbial populations. Thus, MTBE is usually considered non-biodegradable in ground waters (e.g., Suflita and Mormile, 1993; Novak et al., 1985), although Salanitro et al. (1994, 1996) isolated a bacterial culture that could degrade MTBE under laboratory conditions. In addition, Borden and co-workers found evidence of MTBE biodegradation

at a field site in North Carolina combining information obtained by laboratory batch experiments and field monitoring (Borden et al., 1997).

Near-source concentrations of MTBE generally exceed 10 to 20 mg/L, therefore, reliance on dispersive attenuation processes alone may be insufficient to protect water well users in many cases. As a result, the occurrence of MTBE in gasoline-impacted ground water may sometimes compromise the use of intrinsic remediation because MTBE is more mobile and more persistent than BTEX in shallow aerobic aquifers.

This study investigates the fate of an MTBE plume about eight years after it was introduced into the CFB Borden aquifer to characterize and quantify the long-term persistence of this contaminant. The objectives of the study were to characterize the total mass of MTBE and its distribution in the aquifer. Numerical and analytical models and geostatistical methods were used both for the design of the sampling grid and for the analysis of the results.

2.3. THE MTBE FIELD EXPERIMENT AT CFB BORDEN, ONTARIO

In 1988, about 2800 liters of ground water, spiked with Cl^- (448 mg/L), gasoline-derived organics (including about 19 mg/L BTEX) and MTBE (269 mg/L), were injected 1.5 m below the water table into the shallow sand aquifer at CFB Borden. This mixture created a discrete slug of MTBE-contaminated ground water that then moved downgradient at about 33 m/year under natural gradient conditions.

The migration of the contaminants was monitored by detailed ground water sampling using a dense network of multilevel piezometers typically using 14 depth-points over a 2.8 - 4.2 m vertical zone. These snapshots of contaminant distribution were obtained 6, 42, 106, 317, 398, and 476 days after injection. The BTEX compounds underwent rapid aerobic biodegradation and were almost completely attenuated during the initial 16 month period. The experiment and the fate of the monitored compounds is discussed in detail by Hubbard et al. (1994).

The mass ratio MTBE/Cl^-, based on the total mass present, was about 0.59 initially and remained about the same until day 476 when it decreased to 0.43. The

MTBE/Cl^- concentration ratios for single samples ranged from 0.33 to 1.0 for the initial 476 days of the experiment. Due to the uncertainty of the field mass balance estimates, degradation of MTBE could not be demonstrated and it was concluded at the time that the compound was either persistent over the 16 months of monitoring or degrading at a rate not detectable under the experimental conditions (Hubbard et al., 1994).

In 1995 and 1996, from 2700 days to about 3000 days since the natural gradient experiment had started, additional sampling was conducted to locate and characterize the residual MTBE plume. The goal was to quantify the mass of MTBE still present in the aquifer.

2.4. METHODS OF GROUND WATER SAMPLING AND ANALYSIS

Analytical and numerical flow and transport modeling results that considered advection and dispersion predicted that by the end of 1995, the MTBE plume should have migrated 240 m beyond the injection location and about 200 m beyond the last sampling snapshot taken at 476 days. Given that the plume had traveled well beyond the 1988/89 sampling grid, no network of multilevel sampling devices was available for sampling. Rather than install a new multi-level piezometer network, the Waterloo Drive-point Profiler (Pitkin et al., 1994) was used to collect multiple ground water samples at various depths at a number of locations. With this direct-push system, a stainless steel sampling device is driven downward by pressure and vibration. De-ionized water is constantly injected to keep the sampling ports of the drive-point piezometer open and to avoid cross-contamination. Samples are collected at desired depths through stainless steel or teflon tubing connected through the drive rods to a peristaltic pump.

The sampling procedure was to advance the drive point profiler until it was driven into the aquitard underlying the aquifer (Figure 2.1). Sampling within the aquitard was attempted but in each case did not yield any sample water. In those cases where the distance between the last sampling point within the aquifer and the top of the aquitard was more than half of the vertical spacing, the sampler was slowly retrieved until ground water could be collected, presumably just above the aquitard.

Each sample was collected in a 40 mL hypovial before the water passed through the pump tubing. During sampling, three sample tube volumes plus 300 mL of ground water was flushed through the hypovials before the sample was collected. The pumping rate was less than 100 mL/min. MTBE samples for the first sampling round were acidified using two drops of a 1:1 HCl solution, packed on ice and overnight express mailed to a commercial laboratory. Following the analytical method described by Church et al. (1997), no preservatives were added to the samples for all other sampling events.

Sampling at the existing multi-level piezometers during the last sampling round was accomplished by purging at least 2 L of ground water before the sample was taken. The pumping rate during sample collection was less than 100 mL/min.

Three sampling rounds were carried out (Nov. 1995; July/Aug. 1996; Nov. 1996). Samples obtained in the first sampling round were analyzed for MTBE at a commercial laboratory using EPA's SW-846 Method 8240. Beginning in 1996, samples were analyzed at the Oregon Graduate Institute using a direct aqueous injection (DAI) GC/MS technique to determine MTBE, tert-Butyl Alcohol (TBA) and tert-Butyl Formate (TBF) (Church et al., 1997). With this method, detection limits were 0.1, 0.1 and 10 µg/L for MTBE, TBA and TBF, respectively. During the first and second sampling rounds, Cl^- was analyzed at the University of Waterloo to a detection limit of about 1 mg/L. For the final sampling round, Cl^- and sulfate analyses were performed at a commercial laboratory with detection limits of 0.5 mg/L and 2.0 mg/L, respectively. Ion chromatography was used to determine the chloride and sulfate concentrations. A CHEMETRICS™ field oxygen probe was used to measure dissolved oxygen (DO) at selected locations in the field with a detection limit of 0.1 mg/L.

2.5. DESIGN OF SAMPLING GRID

The physical properties, hydraulics and geochemistry of the Borden aquifer have been exceptionally well characterized (Nicholson et el., 1983; Mackay et al., 1986; Frind and Hokkanen, 1987; Woodbury and Sudicky, 1991; Robin et al., 1993; Schirmer et al., 1995). The aquifer is relatively homogeneous; the statistical properties describing the

hydraulic conductivity field are well defined (Sudicky, 1986; Woodbury and Sudicky, 1991; Robin et al., 1993). The aquifer lies over an extensive regional clayey and sandy silt aquitard. The aquitard is approximately 8 m thick at the field site (Foley, 1992). The mean ground water velocity in the aquifer is about 33 m/year and the northwards flow direction fluctuates seasonally over about 20^0 (e.g., Mackay et al., 1986; Frind and Hokkanen, 1987; Hubbard et al., 1994; Farrell et al., 1994). The Borden aquifer has a relatively low carbon content of 0.02 % and thus a low sorption capacity for organic compounds (Mackay et al., 1986).

2.5.1. Analytical Modeling

Based on the well-known aquifer properties and hydraulics, three-dimensional (3D) modeling was performed using the analytical solution SLUG3D (Sudicky, 1985) to estimate the MTBE plume location about seven years after injection. SLUG3D simulates 3D advective/dispersive transport in a homogeneous aquifer with a parallelopedic-shaped initial condition for the tracer mass released at time t = 0. The transport parameters used in the simulations were obtained from a previous numerical modeling study of the initial 16 months of the experiment which included an extensive sensitivity analysis of the dispersivity values (Schirmer et al., 1995). The parameters chosen were 33 m/year for the mean ground water velocity, 0.33 for the porosity, 0.25 m for the longitudinal dispersivity, 0.02 m for the transverse horizontal dispersivity and 0.005 m for the vertical transverse dispersivity. An effective diffusion coefficient of 0.027 m^2/year was chosen. The modeling showed MTBE peak concentrations of more than 3000 µg/L and movement of the plume 240 m beyond the injection site (Figure 2.1). It should be noted that a slight downward movement of the MTBE plume was observed over the initial 476 days of observation. This displacement is most likely due to recharge on top of the aquifer, which is not considered by the analytical solution.

The application of an analytical solution is very helpful to estimate peak concentrations. However, since the solution requires the assumption of a homogeneous aquifer, the expected spatial variability of solute concentrations cannot be characterized.

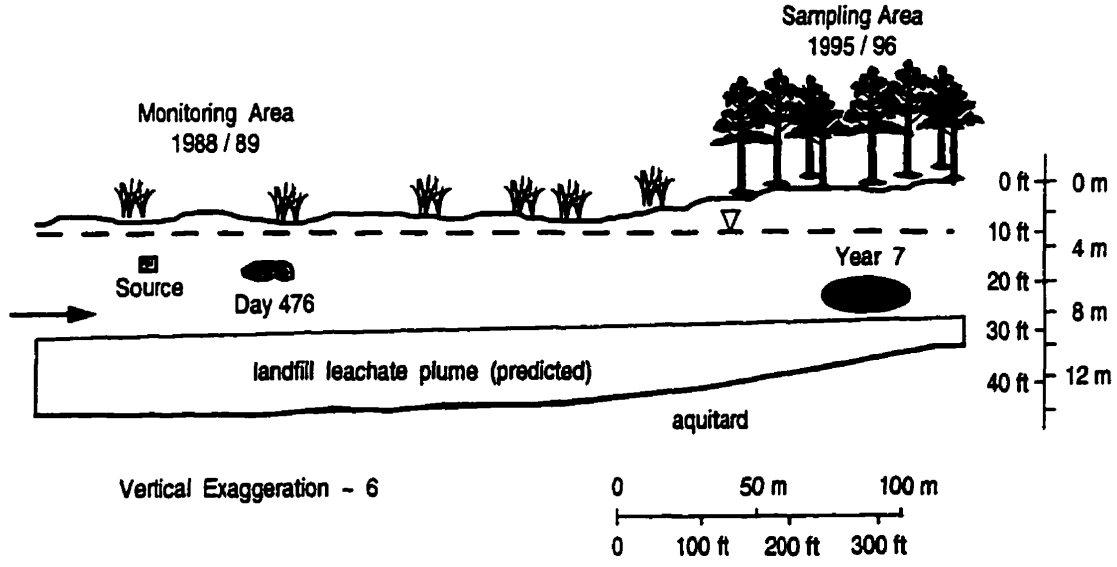

Figure 2.1. Cross section of the Borden field site with the injection area (source), the last sampling snapshot at 476 days and the anticipated plume location 7 years after injection. Note that the plume moved out of the highly monitored portion of the aquifer after day 476 into a forested area.

2.5.2. Numerical Simulations

To take advantage of the well defined statistical parameters of the Borden aquifer (Woodbury and Sudicky, 1991), numerical simulations were performed using random hydraulic conductivity (K) fields. With the computer programs available to us, it is currently computationally impossible to perform 3D analyses for 2920 days (8 years) simulation time. Therefore, we limited our analysis to two-dimensional (2D) plan-view simulations using random K fields with statistical parameters identical to those of the aquifer.

The transverse (both vertical and horizontal) dispersion of contaminants in natural aquifers is minimal (e.g., Sudicky, 1986; LeBlanc et al., 1991; Adams and Gelhar, 1992). This is consistent with observations during the first 476 days of the experiment (Hubbard et al., 1994) and other Borden field tests (e.g., Freyberg, 1986; Farrell et al., 1994). As a result, only minor additional vertical spreading of the MTBE plume was expected after

the last sampling snapshot in 1989 suggesting that the 2D modeling approach should be adequate to characterize the movement of the plume.

Plan-view 2D mathematical simulations yield depth integrated solute concentrations. Complex 3D field measurements of solute concentration can be used to construct a 2D concentration distribution by integration of vertical concentration data. The integrated concentration for equally spaced sampling points is defined as,

$$C_{integr} = \Delta z \, (c_1 /2 + \Sigma c_i + c_n/2) \qquad (2.1)$$

where C_{integr} = depth integrated concentration [ML^{-2}],

Δz = distance between sampling points [L],

c_1 = solute concentration at top point [ML^{-3}],

c_i = solute concentration at intermediary points [ML^{-3}],

c_n = solute concentration at bottom point [ML^{-3}].

In the annotations, M refers to mass and L represents a length unit. If, for example, concentrations are measured as µg/L (mg/m^3), and depths are in meters, the vertically integrated concentrations will have units of mg/m^2. If the vertical distance between the sampling points is not equally spaced, the corresponding length for a certain concentration can be found by summing up the half-distances to each neighboring point. Dividing the depth integrated concentrations by the thickness of the aquifer yields average concentrations in mg/m^3 (µg/L).

The numerical code FGEN92 (Robin et al., 1993) was applied to create several random hydraulic conductivity (K) fields. The statistical parameters used were determined by Woodbury and Sudicky (1991) as 5.14 m for the horizontal correlation length, 9.75 x 10^{-5} m/s for the geometric mean K and 0.244 for the variance of the log (K). The numerical program WATFLOW-3D (Molson et al., 1995) was used to generate the flow fields based on the random K distributions. The mean ground water velocity for all simulated cases was about 33 m/year. The numerical model BIO3D (Frind et al., 1989; Schirmer et al., 1995) was used to simulate the transport of MTBE as a

conservative solute over the 7 year period from injection to the anticipated sampling in November 1995. The applied transport parameters were equivalent to the values chosen for the analytical solution. The 2D modeling suggested peak depth integrated MTBE concentrations of more than 3500 mg/m^2. This is in agreement with the 3D results of the analytical solution SLUG3D which suggested field peak concentrations of more than 3000 µg/L, yielding vertically peak integrated concentrations of about 3600 mg/m^2.

Figure 2.2 shows outlines of three plumes determined with the numerical model using different random K fields. The three realizations shown (out of twelve realizations performed) give insight into the uncertainty of the location of the remaining MTBE, even in this very well-studied and relatively homogeneous aquifer. The plume development of all generated plumes was compared to the results of the initial 16 months of the experiment. In Figure 2.2, the plume displayed with a solid line showed the best agreement between modeled and field-observed plume until day 476 of the experiment and was used for further investigation.

In order to have confidence in the numerical simulations, it was important to assess if the assumed statistical properties for the numerical flow and transport modeling hold for the entire aquifer. Therefore, after completion of the field sampling, soil cores were taken from the aquifer portion through which the plume had moved eight years after injection. K measurements were performed to investigate if the aquifer properties in this portion of the aquifer are close to the properties used to calculate the statistics of the aquifer (Sudicky, 1986). The K values were calculated using permeameter tests at subsections of three cores (64 samples in total) and ranged from 4.5×10^{-5} to 1.49×10^{-4} m/s with a mean value of 1.04×10^{-4} m/s which compares well to the values found by Sudicky (1986) [$6 \times 10^{-6} \leq K \leq 2 \times 10^{-4}$ m/s; geometric mean $K = 9.75 \times 10^{-5}$ m/s]. Based on these results, we felt that it is appropriate to assume the same statistical hydraulic parameters for the whole study area.

Furthermore, in order to adequately describe the hydraulics at the field site and to investigate the possibility of movement of large amounts of ground water from the aquifer into the aquitard, the hydraulic properties of the aquitard were assessed. The aquifer with a mean K value of 9.75×10^{-5} m/s is underlain by a continuous, about 8 m thick

unweathered clayey till aquitard. Based on the hydraulic response to a 38 day pumping test, it was found that the aquitard does not have any significant vertical fractures (Foley, 1992). The aquitard itself overlies a semi-confined aquifer. The pressure head difference between the semi-confined aquifer and the upper aquifer is 3.5 m yielding a downwards flow component through the aquitard with a gradient of 3.5m / 8m = 0.4375. Nine consolidation tests were performed (Foley, 1992) to calculate K values for the aquitard which ranged from 1.12×10^{-10} to 5.39×10^{-10} m/s. The mean K value (2.4×10^{-10} m/s) is close to the typical values of southern Ontario lacustrine clay and thus more than five orders of magnitude lower than the mean K value of the overlying aquifer (Foley, 1992). Based on Darcy's law and the mean K value of the aquitard, a Darcy flux through the aquitard of about 3.3 mm/year was calculated. This value clearly indicates that the flux from the aquifer into the aquitard is extremely small.

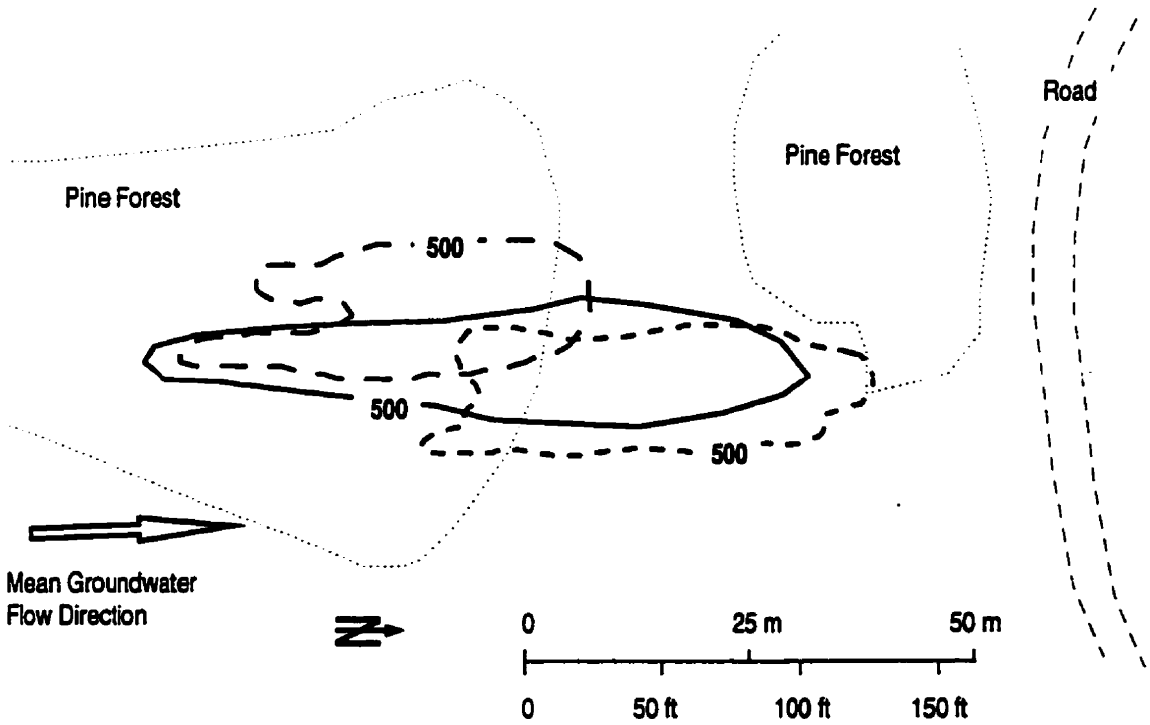

Figure 2.2. Location of a conservative MTBE plume 7 years after injection, based on modeling of twelve realizations using identical statistical Borden aquifer hydraulic properties. Three realizations are shown and the plume displayed with a solid line showed the best results in comparison to the first 16 months of the experiment. Contours are in mg/m^2.

2.6. FIELD SAMPLING STRATEGY AND MTBE RESULTS

Our sampling strategy consisted of three separate sampling rounds with additional sampling events. The task of the first sampling round was to determine if the MTBE plume could be found in the area suggested by modeling. Two more sampling rounds were required to define the vertical and lateral extent of the plume and to delineate the plume in enough detail to estimate the remaining MTBE mass. Additional sampling was performed to determine if there were shallow MTBE plume segments present in the aquifer that potentially moved faster or slower than the segment identified in the three main sampling rounds.

2.6.1. First Sampling Round - Reconnaissance Sampling

The first sampling round was carried out in November 1995. Due to weather conditions around the freezing point, samples could only be collected at thirteen locations. Three to four samples were obtained at each location with a vertical spacing of 1.5 m. Depth integrated concentrations were compared to the simulated plume which showed the best agreement with the MTBE plume over the initial 476 days (Figure 2.3). MTBE was detected at six of the sampling locations with a maximum concentration of 342 mg/m^2. The concentrations found were much lower than predicted from the modeling. The width of the plume was apparently encompassed, but not necessarily its longitudinal extent.

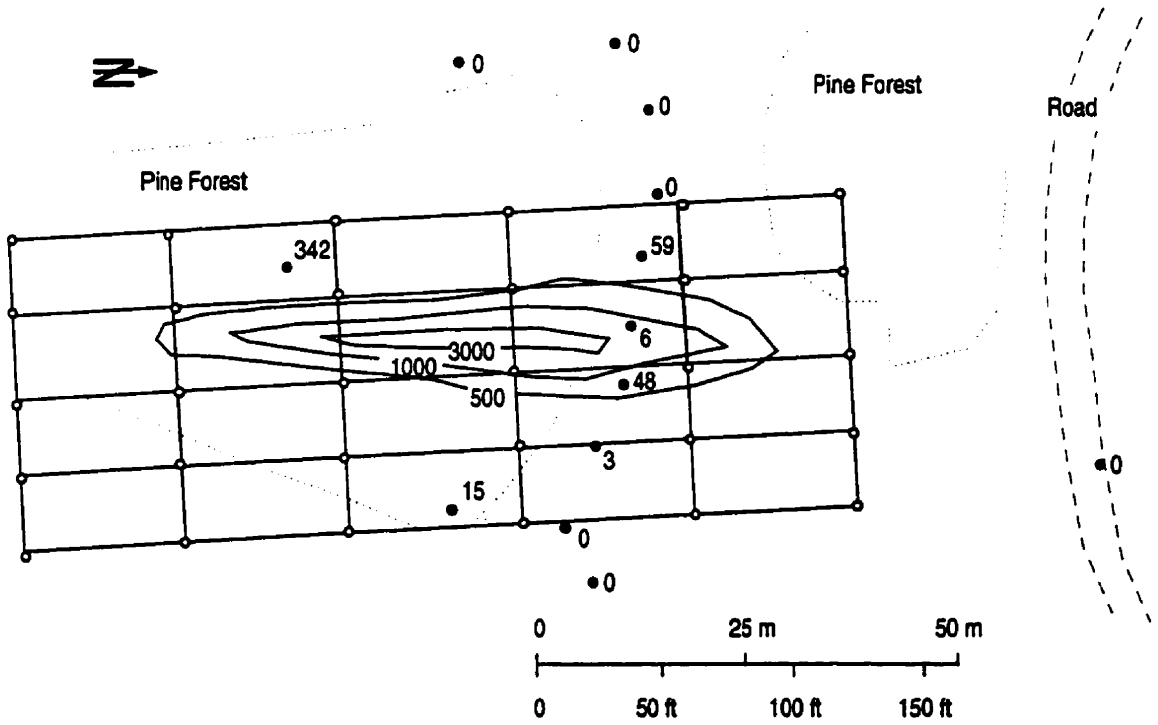

Figure 2.3. Results of the first sampling round (black dots) with the simulated MTBE plume (contours) 7 years after injection as depth integrated concentrations in mg/m^2. The simulated plume contour lines are 3000, 1000 and 500 mg/m^2. The grid with a longitudinal spacing of 20 meters and a transverse spacing of 10 meters represents the anticipated sampling locations for the second (coarse grid) sampling round.

2.6.2. Second Sampling Round - Coarse Grid Sampling

2.6.2.1. Sampling Grid Design

In preparation for the second sampling round, we needed to design an optimal sampling grid with a minimal number of sampling locations while assuring that the plume was delineated in enough detail so that a reliable MTBE mass could be calculated. We obtained the optimal grid spacing based on statistical methods. The simulated plume shown in Figure 2.3 best reproduced the field results of the initial 16 months of monitoring and was therefore chosen for the sampling grid-optimization calculations for the second sampling round. Since degradation could not be demonstrated during the initial 16 months of sampling, the mass of MTBE within the modeled domain was considered to be conservative, providing the opportunity to calculate the mass of MTBE that would be measured if different sampling grid spacings were used. The selected

sampling network would then be the network which recovered the largest percentage of the initial MTBE mass with the fewest monitoring locations while clearly delineating the lateral extent of the plume. We chose a recovery of 30 % of the mass as the objective of the second, coarse grid sampling round. A subsequent fine grid sampling was planned to fill in sampling locations to produce a reliable mass balance.

The KRIGING routine together with the GRIDVOL (grid volume) option of the geostatistical software package GEOSOFT™ were used to determine the recovery of the known mass of MTBE for different grid spacings. We tested three different spacings in the transverse direction [5 m, 7.5 m and 10 m] and in the longitudinal direction [10 m, 15 m and 20 m] yielding nine different grids. With each grid, a large enough area had to be covered so that the lateral extent of the plume was encountered. The corresponding number of sampling locations was 30, 42 and 55 for longitudinal spacings of 20 m, 15 m and 10 m, respectively. Each grid was overlain on the simulated plume to determine the concentration for each sampling location. Then the KRIGING option was used to interpolate MTBE concentrations between the grid points; the mass recovery was found from the interpolated values. In addition, each grid was shifted over the domain of the simulated plume. The recovered mass was calculated for each grid placement to ensure that a reasonable mass recovery was not dependent on the location of the grid. The lowest recovered mass for each grid configuration was reported to give a conservative estimate. For large grid spacings, fewer sampling points are located within or close to the plume center and less mass is recovered. Since the numerically generated plume (Figure 2.3) is long and thin, the mass recovery is much more sensitive to the transverse spacing than to the longitudinal spacing. Regardless of the exact position of the grid, at least a third of the mass was obtained with the coarsest grid spacing of 20 m in the longitudinal and 10 m in the transverse direction (Table 2.1).

Table 2.1. Minimum mass recovered from a simulated MTBE plume using different sampling grid designs.

	Longitudinal Spacing		
Transverse Spacing	**20 m**	**15 m**	**10 m**
10 m	36%	38%	44%
7.5 m	38%	40%	49%
5 m	61%	63%	81%

2.6.2.2. Coarse Grid Sampling

Based on the calculations above and considering the uncertainties in flow direction and average ground water flow velocity, we sampled over a coarse grid, covering a 100 m x 40 m area with 30 sampling locations spaced 20 m apart longitudinally and 10 m apart transversely (Figure 2.3). Four to eight sampling points were distributed vertically at each location with 0.25 - 1.0 m spacing.

The coarse grid sampling was performed in July/August 1996. Figure 2.4 shows the depth integrated MTBE concentrations obtained during this sampling round. If the entire plume lay within the covered area, at least 36 % of the plume mass should have been recovered assuming that MTBE behaves conservatively (Table 2.1). Due to time constraints, one sampling transect (between the pine forests; Figure 2.4) could not be completed. Only five of the 21 locations sampled contained measurable MTBE concentrations. Unfortunately, the outermost sampling points were not uniformly non-detects, therefore, we could not define the longitudinal extent of the plume.

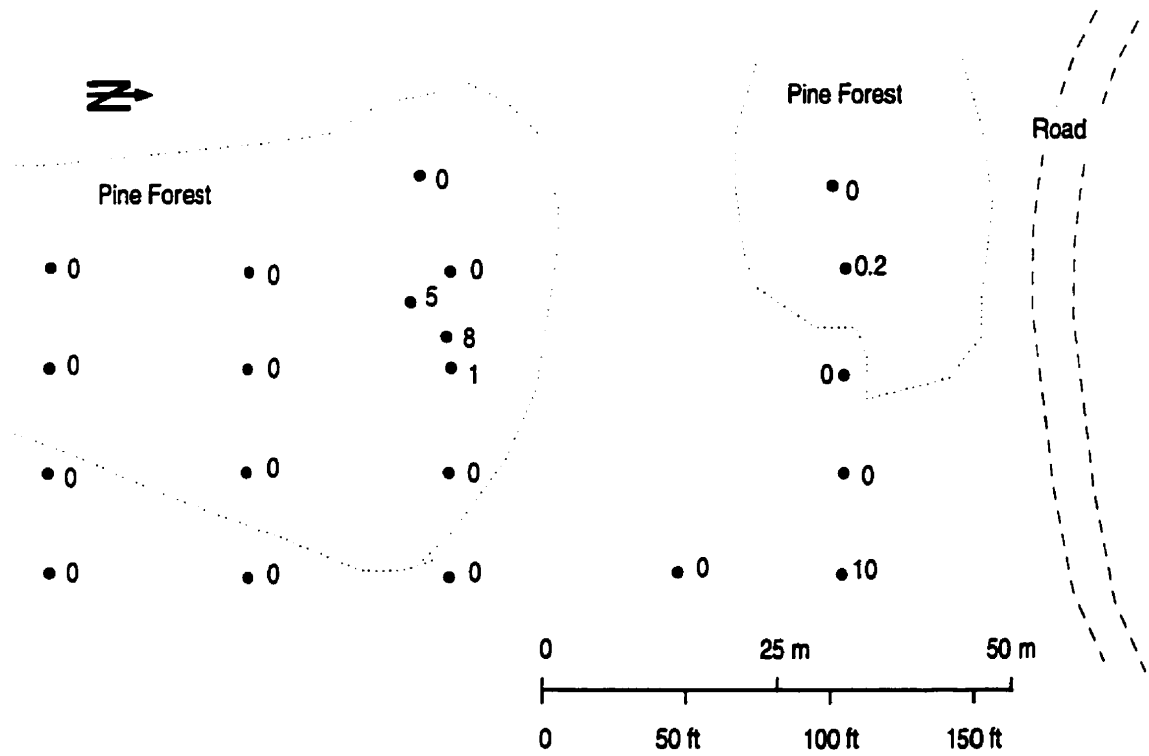

Figure 2.4. Sampling locations with depth integrated MTBE concentrations for the coarse grid sampling round. A longitudinal spacing of 20 meters and a transverse spacing of 10 meters was chosen. Concentrations are in mg/m^2.

2.6.3. Third Sampling Round - Fine Grid Sampling

The fine grid sampling was carried out in November 1996 to increase the confidence in the mass balance calculations. Given that the coarse grid sampling did not encounter the downgradient edge of the plume, the first priority of this round was to ensure that the entire plume was delineated. To test the degree of plume capture, several locations were placed beyond the coarse sampling grid in the vicinity of the road (Figure 2.5). Non-detects in the downgradient sampling locations indicate that the plume was most likely within the sampled area. The sampling grid was then refined to ensure sufficient coverage to perform a mass balance. The vertical spacing at the sampling locations was 0.25 - 0.75 m. Figure 2.5 shows the locations and depth integrated MTBE concentrations for the fine grid sampling round. Nine of the 25 locations sampled contained measurable MTBE concentrations.

As during all of the previous sampling rounds, we found MTBE only at the deepest sampling points, closest to the aquitard. Figure 2.6 presents the vertical MTBE concentration distributions along transect A-A' shown in Figure 2.5. The locations where MTBE was found generally coincided with elevated sulfate concentrations (> 10 mg/L) and dissolved oxygen concentrations of less 1.8 mg/L (data not shown). However, it was not possible to define a boundary between background ground water and the expected landfill leachate plume (Figure 2.1). The leachate plume is apparently very dilute in that area.

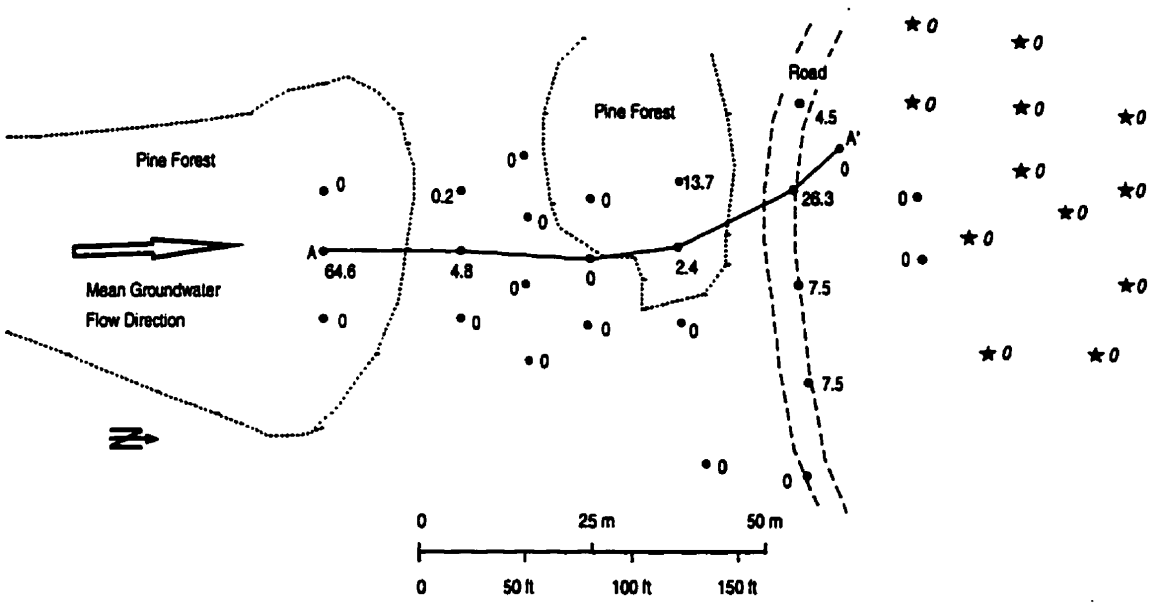

Figure 2.5. Sampling locations with depth integrated MTBE concentrations for the fine grid sampling round. MTBE depth profiles along transect A - A' are shown in Figure 2.6 below. Stars indicate sampling locations where existing multilevel piezometers were sampled in depths of 0.3 - 3.5 meters below the water table. Concentrations are in mg/m^2.

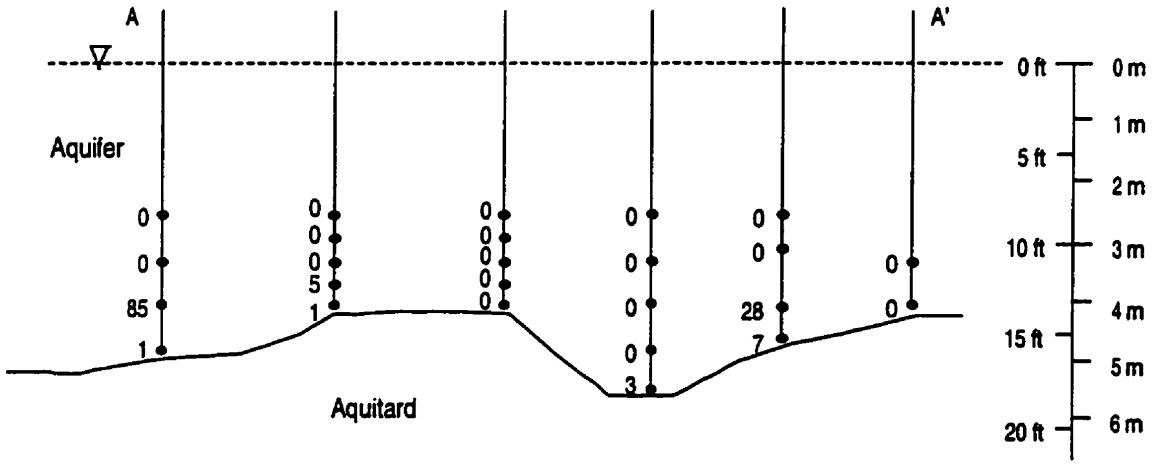

Figure 2.6. Examples of MTBE depth profiles for the transect A - A'. MTBE is only measured at the deepest sampling locations close to the aquitard. Concentrations are in µg/L.

2.6.4. Additional Sampling

At the Borden field site, vertical splitting of injected slugs into faster and slower moving segments has been noted (e.g., Sudicky et al., 1983). In November 1996, additional sampling sought such a shallow MTBE slug, moving faster than the slug identified in the above sampling rounds. Twelve multilevel piezometers, located in the area north of the road (Figure 2.5), with sampling ports 0.3 - 3.5 m below the water table were sampled. Two samples at each piezometer were collected. There was no detection of MTBE in any of those samples. These data show that there is no fast moving MTBE slug with high MTBE concentrations in the upper portion of the aquifer.

In addition, sampling is still ongoing at three locations (A, B and C in Figure 2.7) where new multilevel piezometers were installed. These piezometers penetrate the whole aquifer down to the aquitard at a spacing of 25 cm. These piezometers are sampled on a bimonthly basis to detect a potentially slower moving plume with high MTBE concentrations. Until September 1997, ten months after the last (third) sampling round, no MTBE was detected in the upper part of the aquifer and only small MTBE concentrations of less than 30 µg/L were found close to the aquitard, as expected from the

previous sampling events. To date, this data shows that there is no slow moving slug with high MTBE concentrations (Schirmer et al., 1998).

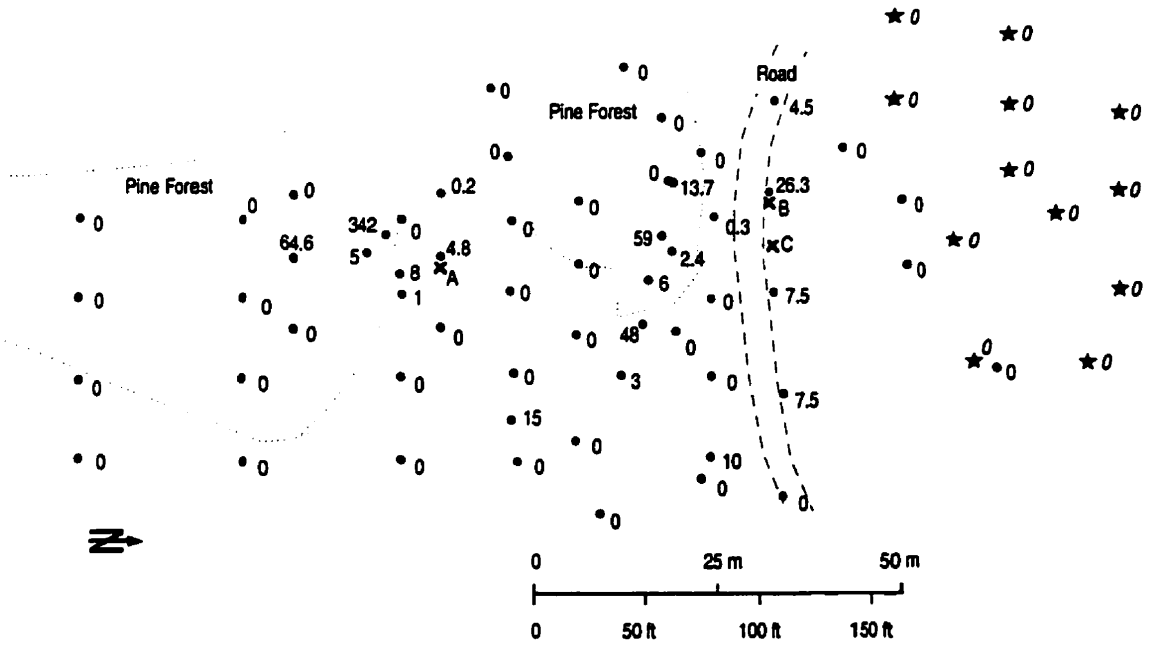

Figure 2.7. Depth integrated and time corrected MTBE concentrations for all sampling rounds. These concentrations are used to perform a mass balance. Stars indicate sampling locations where existing multilevel piezometers were sampled in depths of 0.3 - 3.5 meters below the water table. Crosses (A, B, and C) indicate sampling locations with ongoing sampling. Concentrations are in mg/m^2.

2.7. MASS ESTIMATION PROCEDURE

We performed an MTBE mass balance using the results from all three sampling rounds. Data from sampling rounds one and two were time corrected to sampling round three. Given that the aquifer is relatively homogeneous, we displaced the concentration data obtained during the first and second sampling rounds downgradient at the mean ground water velocity of 33 m/year to the locations that they would have occupied during the final sampling round (Figure 2.7). Since any decline of the MTBE concentration data of sampling rounds one and two due to attenuation processes is not accounted for in the time correction procedure, the mass estimate will be conservative.

The KRIGING routine together with the GRIDVOL option of GEOSOFT™ were applied to the MTBE concentration distribution shown in Figure 2.7. For the KRIGING, a spherical interpolation function was used for the variogram with a blanking distance of 50 m, a grid cell size of 2.5 m and a range of 5 m, respectively. The recovered total MTBE mass in the aquifer was only 22 g while a mass of 752 g of MTBE was introduced in 1988. A second geostatistical method was applied to verify the calculations. The inverse distance method of GMS™ was used to calculate the total mass. With this method an MTBE mass of 24.5 g was obtained. This is in agreement with the previous results, suggesting that only about 3 % of the initial MTBE mass was found.

2.8. SUMMARY AND DISCUSSION

An MTBE plume was characterized in three major sampling rounds (November 1995, July/August 1996 and November 1996). These events were planned with the use of analytical and numerical flow and transport modeling and statistical analyses. The main goal was to delineate the MTBE plume in enough detail to perform a reliable mass balance. The Borden aquifer is exceptionally well characterized and the measured MTBE plume location is, considering all the uncertainty involved in modeling such a long-term experiment, in good agreement with the location suggested by numerical modeling. The MTBE concentrations, however, were more than an order of magnitude lower than expected based on numerical modeling that considered dispersion and diffusion as the only attenuation mechanisms.

MTBE was present only in the deepest portion of the aquifer, close to the underlying aquitard. This observation may suggest that the dilute anaerobic landfill leachate plume, presumably present in this part of the aquifer, had mixed with the MTBE plume and MTBE persisted under these conditions.

MTBE/Cl^- concentration ratios were calculated for each sampling point and found to be between 0.001 and 0.008, much lower than the ratios of 0.33 to 1.0 calculated during the initial 16 months of the experiment. This drop in the MTBE/Cl^- ratio could either suggest that MTBE had undergone transformation or that additional Cl^- from other

sources, such as the landfill leachate plume, had mixed with the plume. Neither TBA nor TBF, two potential MTBE degradation products, was found in any of the samples. This could suggest that MTBE had not been transformed or that these compounds, if they are formed, transform readily. Finding potential degradation products is usually a good indication of transformation, however, in the case of very slow degradation rates, as expected for MTBE, those compounds might be found at concentrations too small to be measured.

Figure 2.6 shows that the full vertical extent of the plume was measured. Generally, non-detect levels of MTBE were found at the peripheries of the sampling grid (Figures 2.3, 2.4 and 2.5), suggesting that the full lateral extent of the plume was delineated as well.

The mass balance suggests a significant loss of MTBE in the Borden aquifer, which could potentially be attributed to biodegradation, abiotic degradation, volatilization, plant uptake or sorption. To our best knowledge, abiotic MTBE degradation involving subsurface material was only shown in one set of experiments by Yeh and Novak (1995). These researchers found MTBE to hydrolyze when hydrogen peroxide was added but iron was needed to act as a catalyst. This reaction is insufficient in aerobic or near-neutral (pH > 6.5) environments (Squillace et al., 1997) such as the Borden aquifer with a mean pH value of 7 - 8. We therefore rule out the possibility of abiotic MTBE degradation at the Borden field site. Furthermore, the MTBE was introduced into the aquifer 1.5 m below the water table; therefore, volatilization was also not an attenuation factor in this experiment.

Plant uptake or phytoremediation is another potential attenuation factor. At the site, two forested areas exist with predominantly Aspen and Pine trees and ferns. Contrary to a common perception, the main orientation of tree roots is horizontal, not vertical. In fact, tree roots generally spread horizontally as far as 1-3 times the tree height, while almost 90 % of a tree's roots can be found within the upper 0.6 m of soil (Dobson and Moffat, 1995). Root growth has been found to stop completely when air space dropped to 2 %. The reduced root growth at higher water content can be attributed to the fact that oxygen diffuses in solution about 10,000 times less rapidly than in the gas phase, thereby

restricting the gas exchange in soil (Dobson and Moffat, 1995). Thus, at the Borden field site, where the top of the capillary fringe is found 2 - 3 m below ground, it is doubtful that vertical root penetration extends beyond this depth and reaches the water table. In conclusion, it is very unlikely that plant uptake influenced the MTBE plume introduced 1.5 m below the water table.

Based on linear sorption, the calculated MTBE retardation factor is 1.02 for the Borden aquifer (Schirmer et al., 1998). This low value suggests that sorption cannot account for the large discrepancy between the initial and final MTBE mass.

Although the possibility exists that we missed part of the MTBE plume, we feel that the extensive sampling in a well-characterized aquifer, with the location of MTBE where it was anticipated, suggests otherwise.

Only about 3 % of the initial MTBE mass was found and we hypothesize that biodegradation played an important role in the attenuation of the MTBE within the Borden aquifer. Nevertheless, additional lines of evidence of biodegradation, such as laboratory batch and column experiments, are necessary to confirm this possibility. Studies are underway, but no confirmatory laboratory evidence has been found to date. Thus, while we are confident that MTBE mass has been lost, we cannot yet confirm biodegradation as the process.

The interpretation of major MTBE mass loss after 3000 days seems to contradict the suggestion of conservative behavior during the initial 476 days of transport (Hubbard et al., 1994). Therefore, we re-examined the trend in the recovered mass in the aquifer over the initial 476 days of the experiment. Using the statistical program SYSTAT™, a regression analysis was performed on the MTBE mass calculations of the initial 476 days of the experiment, leading to the following equation:

$$\text{Mass of MTBE (time)} = 736\ \text{g} - 0.327\ \text{g/day} \cdot \text{time (in days)} \qquad (2.2)$$

The slope of 0.327 g/day was found to be significant at a level of alpha = 0.1 (Figure 2.8). This interpretation suggests that there was a small but statistically significant mass loss during the first 476 days of the MTBE monitoring.

The slope of the line through the initial and the final MTBE mass is 0.243 g/day and therefore slightly flatter than the slope of the initial MTBE masses only (Figure 2.8). We suggest biodegradation as the main attenuation factor of MTBE in the Borden aquifer, however, the presented slopes represent only apparent field mass loss rates and not necessarily true rates of biodegradation.

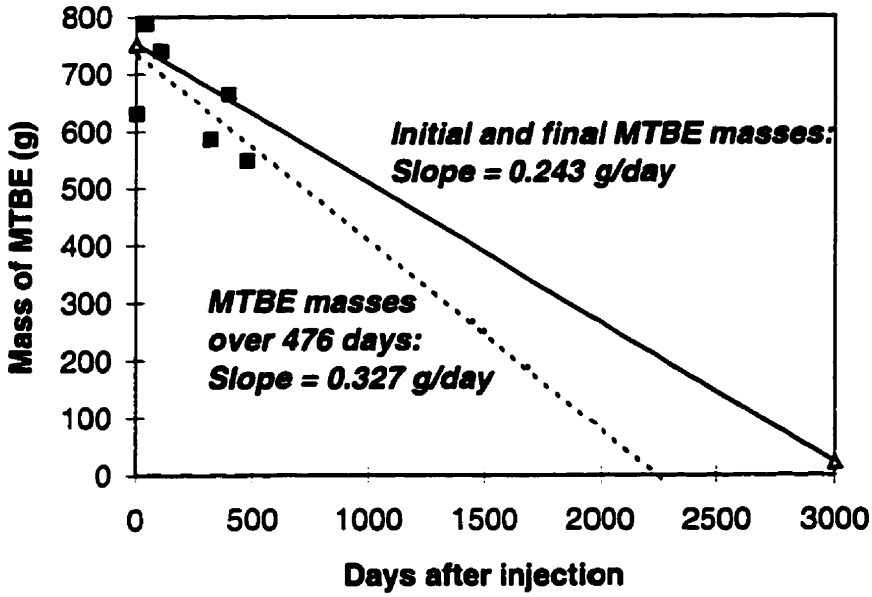

Figure 2.8. MTBE field mass estimates with the initial sampling rounds (up to 476 days) and the final sampling round about eight years (3,000 days) after injection. The dashed line represents the regression line based on the initial sampling rounds up to 476 days only.

This study provides field evidence of MTBE mass loss. Consideration of possible mass loss mechanisms leads us to the suggestion that MTBE within the Borden aquifer was biodegraded over a 3000 day period, which disagrees with the prevailing paradigm of MTBE resistance to biodegradation. Research is now needed to determine which types of subsurface environments do support MTBE biodegradation, and to define the microbiological and geochemical factors which influence MTBE biodegradation. This understanding is necessary before biodegradation can be considered for intrinsic remediation of MTBE in ground water.

2.9. ACKNOWLEDGMENTS

This research was supported by the American Petroleum Institute, Health and Environmental Sciences Department. Particularly, I would like to thank the members of the API Soil and Groundwater Technical Task Force for their ongoing support and advice. The views expressed here are those of the author, however. I thank Tina Hubbard for many insightful discussions on the initial part of the experiment as well as for her advice and careful review of the manuscript. I would also like to thank Clint Church, Jim Pankow and Paul Tratnyek of the Oregon Graduate Institute for the analyses of the samples and many helpful discussions. I thank Ty Ferré, Bob Cleary and Bob Borden for their careful review of the manuscript and many helpful discussions. As always, a large group at University of Waterloo contributed advice, assistance and support.

2.10. REFERENCES

Adams, E. E., and Gelhar, L. W. 1992. Field Study of dispersion in a heterogeneous aquifer, 2. Spatial moments analysis. Water Resources Research 28(12), 3293-3307.

Borden, C. R., Daniel, R. A., LeBrun IV, L. E. and Davis, C. W. 1997. Intrinsic biodegradation of MTBE and BTEX. Water Resources Research 33(5), 1105-1115.

Church, C. D., Isabelle, L. M., Pankow, J. F., Rose, D. L. and Tratnyek, P. G. 1997. Method for determination of methyl tert-butyl ether and its degradation products in water. Environmental Science & Technology 31(12), 3723-3726.

Davidson, J. M. 1995. Fate and transport of MTBE - The latest data. In Proceedings of the Petroleum Hydrocarbons and Organic Chemicals in Ground Water: Prevention, Detection, and Remediation Conference, Houston, Texas, November 1995, 285-301.

Dobson, M. C. and Moffat, A. J. 1995. A re-evaluation of objections to tree planting on containment landfills. Waste Management & Research 13(6), 579-600.

Farrell, D. A., Woodbury, A. D., Sudicky, E. A. and Rivett, M. O. 1994. Stochastic and deterministic analysis of dispersion in unsteady flow at the Borden tracer test site, Ontario, Canada. Journal of Contaminant Hydrology 15(3), 159-185.

Foley, S. L. 1992. Influence of sand microbeds on hydraulic response on an unweathered clay aquitard. M.Sc. Project, Department of Earth Sciences, University of Waterloo, Ontario, Canada.

Freyberg, D. L. 1986. A natural gradient experiment on solute transport in a sand aquifer. 2. Spatial moments and the advection and dispersion of nonreactive tracers. Water Resources Research 22(13), 2031-2046.

Frind, E. O., and Hokkanen, G. E. 1987. Simulation of the Borden plume using the alternating direction Galerkin technique. Water Resources Research 23(5), 918-930.

Frind, E. O., Sudicky, E. A. and Molson, J. W. 1989. Three-dimensional simulation of organic transport with aerobic biodegradation. In Groundwater Contamination, IAHS Publ. No. 185, Ed. Abriola, L. M., 89-96. Wallingford, Oxfordshire, UK: IAHS Press.

Hubbard, C. E., Barker, J. F., O'Hannesin, S. F., Vandegriendt, M. and Gillham, R. W. 1994. Transport and fate of dissolved methanol, methyl-tertiary-butyl-ether, and monoaromatic hydrocarbons in a shallow sand aquifer. American Petroleum Institute Publ. 4601, Health & Environmental Sciences Department., Washington, D.C., 226 p.

LeBlanc, D. R., Garabedian, S. P., Hess, K. M., Gelhar, L. W., Quadri, R. D., Stollenwerk, K. G., and Wood, W. W. 1991. Large-scale natural gradient tracer test in sand and gravel, Cape Cod, Massachusetts, 1. Experimental design and observed tracer movement. Water Resources Research 27(5), 895-910.

Mackay, D. M., Freyberg, D. L., Roberts, P. V. and Cherry, J. A. 1986. A natural gradient experiment on solute transport in a sand aquifer, 1. Approach and overview of plume movement. Water Resources Research 22(13), 2017-2029.

McKinnon, R. J. and Dyksen, J. E. 1984. Removing organics from groundwater through aeration plus GAC. Journal American Water Works Association 76(5), 42-47.

Molson, J. W., Martin, P. J. and Frind, E. O. 1995. WATFLOW-3D: A 3D numerical flow model for saturated porous media. User Guide. Waterloo Centre for Groundwater Research, University of Waterloo, Waterloo, ON, Canada.

Nicholson, R. V., Cherry, J. A. and Reardon, E. J. 1983. Migration of contaminants in groundwater at a landfill: A case study. 6. Hydrogeochemistry. Journal of Hydrology 63(1/2), 131-176.

Novak, J. T., Goldsmith, C. D., Benoit, R. E. and O'Brien, J. H. 1985. Biodegradation of methanol and tertiary butyl alcohol in subsurface systems. Water Science Technology 17(9), 71-85.

Pitkin, S., Ingleton, R. A. and Cherry, J. A. 1994. Use of a drive point sampling device for detailed characterization of a PCE plume in a sand aquifer at a dry cleaning facility. In Proceedings of the Outdoor Action Conference, 395-412, by National Ground Water Association. Dublin, Ohio: NGWA.

Rice, D. W., Dooher, B. P., Cullen, S. J., Everett, L. G., Kastenberg, W. E., Grose, R. D. and Marino, M. A. 1995. Recommendations to improve the cleanup process for California's leaking underground fuel tanks (LUFTs). Lawrence Livermore National Laboratory, Environmental Protection Department, UCRL-AR-121762. Report submitted to the California State Water Resources Control Board, October 16, 1995.

Robin, M. J. L., Gutjahr, A. L., Sudicky, E. A. and Wilson, J. L. 1993. Cross-Correlated Random Field Generation with the Direct Fourier Transform Method. Water Resources Research 29(7), 2385-2397.

Salanitro, J. P., Diaz, L. A., Williams, M. P. and Wisniewski, H. L. 1994. Isolation of a bacterial culture that degrades methyl t-butyl ether. Applied and Environmental Microbiology 60(7), 2593-2596.

Salanitro, J. P., Wisniewski, H. L. and Williams, M. P. 1996. Observation on the biodegradation and bioremediation potential of methyl t-butyl ether. In Proceedings of SETAC 17th Annual Meeting, November 17-21, 1996, p.115. Washington, D.C.: Society of Environmental Toxicology and Chemistry.

Schirmer, M., Frind, E. O. and Molson, J. W. 1995. Transport and biodegradation of hydrocarbons in shallow aquifers: 3D modeling. API Workshop: Comparative Evaluation of Groundwater Biodegradation Models, Fort Worth, Texas, May 8-9, 1995.

Schirmer, M., Barker, J. F. and Hubbard, C. D. 1998. Delineation and characterization of the Borden MTBE plume: An evaluation of 8 years of natural attenuation processes. American Petroleum Institute Publ. 4668. Washington, D.C.: Health & Environmental Sciences Department.

Squillace, P. J., Zogorski, J. S., Wilber, W. G. and Price, C. V. 1996. Preliminary assessment of the occurrences and possible sources of MTBE in groundwater in the United States, 1993-1994. Environmental Science and Technology 30(5), 1721-1730.

Squillace, P. J., Pankow, J. F., Korte, N. E. and Zogorski, J. S. 1997. Review of the environmental behavior and fate of Methyl tert-Butyl Ether. Environmental Toxicology and Chemistry 16(9). 1836-1844.

Sudicky, E. A., Cherry, J. A. and Frind, E. O. 1983. Migration of contaminants in groundwater at a landfill: A case study. 4. A natural-gradient dispersion experiment. Journal of Hydrology 63(1/2), 81-108.

Sudicky, E. A. 1985. A collection of analytical solutions for solute transport in porous and fractured porous media. Report, Institute for Groundwater Research, University of Waterloo, Ontario, Canada.

Sudicky, E. A. 1986. A natural gradient experiment on solute transport in sand aquifer: spacial variability of hydraulic conductivity and its role in the dispersion process. Water Resources Research 22(13), 2069-2082.

Suflita, J. M. and Mormile, M. 1993. Anaerobic biodegradation of known and potential gasoline oxygenates in the terrestrial subsurface. Environmental Science and Technology 27(5), 976-978.

Woodbury, A. D. and Sudicky, E. A. 1991. The geostatistical characteristics of the Borden aquifer. Water Resources Research 27(4), 533-546.

Yeh, C. K. and Novak, J. T. 1995. The effect of hydrogen peroxide on the degradation of methyl and ethyl tert-butyl ether in soils. Water Environment Research 67(5), 828-834.

Zogorski, J. S., Morduchowitz, A., Baehr, A. L., Bauman, B. J., Conrad, D. L., Drew, R. T., Korte, N. E., Lapham, W. W., Pankow, J. F. and Washington, E. R. 1997. Fuel oxygenates and water quality: current understanding of sources, occurrence in natural waters, environmental behavior, fate, and significance. Chapter 2 in: Interagency assessment of oxygenated fuels. The White House Office of Science & Technology Policy, Executive Office of the President, Washington, DC 20500, July 2, 1997.

CHAPTER 3

INFLUENCE OF SEASONAL CHANGES IN FLOW DIRECTION ON PLUME SHAPE AND APPARENT DISPERSION OF BIODEGRADABLE AND CONSERVATIVE COMPOUNDS[1]

3.1. ABSTRACT

The rate of biodegradation in contaminated aquifers depends to a large extent on dispersive mixing processes that are now generally accepted to result from spatial variations in the velocity field. It has been shown, however, that transient flow fields can also contribute to this dispersive mixing process. The influence of transient flow on biodegrading contaminants is particularly important since it can enhance mixing with possible electron acceptors, further promoting the reactive process. The effect of transient flow on the behaviour of a biodegradable contaminant is here evaluated both with respect to the development of apparently large horizontal transverse dispersion and with respect to enhanced mixing between substrate and electron acceptor. The numerical model BIO3D, which solves for advective-dispersive transport coupled with Monod-type biodegradation of substrates in the presence of an electron acceptor, was used for the simulations. The model was applied in a two-dimensional plan view mode considering a single substrate (electron donor). Changes in flow direction were found to yield larger apparent transverse dispersion because the longitudinal dispersivity also acts transverse to the mean flow direction. In the reactive case, the transient flow field increases substrate-oxygen mixing, which in turn enhances the rate of biodegradation. The results suggest that in the case of moderate changes of flow directions, for many practical applications a steady-state flow field is justified, thereby avoiding the higher computational costs of a fully transient simulation. Rather, the use of a higher transverse horizontal dispersivity in a steady flow field can, under these conditions, adequately forecast plume development.

---

[1] This paper is for submission to Ground Water. Authors are M. Schirmer, G. C. Durrant, E. O. Frind and J. W. Molson.

3.2. INTRODUCTION

Pollution of aquifers by contaminant spills or landfill leachate is a widespread environmental problem with characteristic fan-shape plumes often observed downgradient of contaminant sources. The cause of this large horizontal transverse plume spreading has been the subject of several past studies (see for example, Kinzelbach and Ackerer, 1986; Naff et al., 1989; Goode and Konikow, 1990; Sudicky and Huyakorn, 1991; Rehfeldt and Gelhar, 1992; Farrell et al., 1994; Bellin et al., 1996).

The rate of biodegradation of contaminants in aquifers depends to a large extent on the mixing processes caused by dispersion. Large-scale dispersion of solutes in groundwater (referred to here as macrodispersion) is now generally accepted to result from spatial variations in the velocity field caused by spatial variability in aquifer properties, mainly due to hydraulic conductivity variations. However, groundwater velocity and flow direction are also functions of the hydraulic gradient, which can change over time because of changes in the relative magnitudes and locations of hydraulic stresses imposed on an aquifer. These transient gradients can be the result of temporal fluctuations of recharge, changes in vegetation cover, as well as changing boundary conditions, such as fluctuating surface water levels and pumping wells. Changing flow directions primarily act to increase the apparent transverse horizontal dispersion because the longitudinal dispersivity is acting in a direction that is not the mean flow direction. This increase is a function of the angle between the true transient flow vector and the assumed steady-state flow direction system (Goode and Konikow, 1990).

Several research groups (e.g., Kinzelbach and Ackerer, 1986; Naff et al., 1989; Goode and Konikow, 1990; Rehfeldt and Gelhar, 1992; Farrell et al., 1994; Bellin et al., 1996) have investigated the phenomena of transient flow fields using both deterministic and stochastic numerical tools. Kinzelbach and Ackerer (1986) showed that transient flow yields a larger transverse dispersivity, but an equally smaller longitudinal dispersivity when compared with the steady-state case. Goode and Konikow (1990) found that hydraulic transients can lead to enhanced lateral dispersion and that directional variation is more important than changes in the magnitude of the hydraulic gradient. Naff

et al. (1989) showed that temporal variability in the flow field could account for the observed lateral spreading in the Stanford-Waterloo tracer experiment at the Borden field site (Freyberg, 1986). Rehfeldt and Gelhar (1992) used a stochastic approach to account for the enhanced asymptotic macrodispersivity which results from the presence of transients in a flow field. They assumed hydraulic gradient fluctuations and their results compare reasonably well with Freyberg's 1986 data. Farrell et al. (1994) investigated the Borden emplaced source experiment (Rivett et al., 1994) using deterministic and stochastic tools applying measured transients of the flow field. They showed that flow transients contribute to the transverse horizontal macrodispersivity at the Borden field site. Bellin et al. (1996) revisited Freyberg's (1986) data using a stochastic modelling approach incorporating transients in the flow field. These workers found as well that due to the unsteadiness of the mean head gradients, additional transverse horizontal spreading of the plume occurs. However, it can not fully explain the spreading as observed in the experiment. They conclude that defining a Fickian transverse dispersion coefficient may not be a simple task for transport occurring under natural flow conditions.

These previous studies show quantitatively that transient flow can lead to enhanced transverse horizontal dispersion for conservative transport problems. However, the implications of these transient flow fields on mass loss due to biodegradation have not yet been investigated.

Cirpka et al. (in sub.) revisited the macrodispersivity theory with respect to reactive transport by using a two-dimensional steady-state streamtube model. They conclude that macrodispersivity values should not be used in the direction transverse to flow because large dispersivity values introduce artificial mixing between the contaminant and the electron acceptor and thus actually enhance the rate of biodegradation. Furthermore, they conclude that grid orientation and large element spacing can introduce significant numerical dispersion yielding erroneous results.

The objective of this research was to determine the influence of changing flow directions on the development of apparently large transverse horizontal dispersion of plumes developing from an areal contaminant source and to assess its effect on the rate of biodegradation. The focus is on biodegradable contaminants and for each case a

corresponding conservative tracer is simulated to provide a benchmark for the overall rate of biodegradation. Changing flow directions are simulated with the assumption that only molecular diffusion is acting in the transverse flow direction and consequently set the horizontal transverse dispersivity to zero. For the steady-state flow case, a horizontal transverse dispersivity value larger than zero was introduced to match closely the results of the changing flow direction runs.

3.3. SIMULATION APPROACH

3.3.1. Theory

The numerical model BIO3D solves for the coupled advective-dispersive transport and biodegradation of multiple substrates in the presence of an electron acceptor (in this case dissolved oxygen) and includes the growth and decay of a stationary microbial population (Frind et al., 1989; Schirmer et al., 1995). The model was applied in a two-dimensional mode considering a single substrate (electron donor).

The respective equations governing behaviour of the substrate, oxygen and microbes are given by:

$$-\frac{dS}{dt} = \frac{v_i}{R_S}\frac{\partial S}{\partial x_j} - \frac{\partial}{\partial x_i}\left(\frac{D_{ij}}{R_S}\frac{\partial S}{\partial x_j}\right) + k_{max}\frac{M}{R_S}\frac{S}{S+K_S}\frac{A}{A+K_A} \qquad (3.1)$$

$$-\frac{dA}{dt} = \frac{v_i}{R_A}\frac{\partial A}{\partial x_j} - \frac{\partial}{\partial x_i}\left(\frac{D_{ij}}{R_A}\frac{\partial A}{\partial x_j}\right) + k_{max}\frac{M}{R_A}X\frac{S}{S+K_S}\frac{A}{A+K_A} \qquad (3.2)$$

$$+\frac{dM}{dt} = k_{max}MY\frac{S}{S+K_S}\frac{A}{A+K_A}\left(1-\frac{M}{M_{max}}\right) - bM \qquad (3.3)$$

where x_i are the spatial coordinates (L), v_i is the velocity vector (L/T), D_{ij} is the hydrodynamic dispersion tensor (L^2/T) as defined below, t is time (T), k_{max} is the maximum utilization rate (T^{-1}), S is the concentration of the primary organic substrate (M/L^3), A is the electron acceptor (oxygen) concentration (M/L^3) and M represents the

total microbial biomass concentration (M/L^3). Furthermore, K_S is the organic half-utilization constant (M/L^3), K_A is the electron acceptor (oxygen) half-utilization constant (M/L^3), X is the ratio of oxygen to organic substrate consumed, Y is the microbial yield per unit organic substrate consumed, M_{max} is the maximum microbial concentration at which the microbial population reaches a steady state, b is the first-order microbial decay coefficient (T^{-1}), R_S is the retardation factor of organic substrate and R_A is the retardation of the electron acceptor (which is equal to unity in the case of oxygen).

Unrealistically high cell numbers in the numerical model are avoided by introducing the term $[1-(M/M_{max})]$ in Equation 4.3. This term restricts the microbial population from growing beyond the maximum concentration M_{max}, the concentration at which the microbial population reaches a quasi steady-state. To our knowledge, the inhibition term concept was first introduced by Levenspiel (1980) as $[1-(P/P_{max})]^{\alpha}$ to account for product (P) toxicity. Luong (1987) extended this concept to describe substrate (S) inhibition with a term $[1-(S/S_{max})]^{\alpha}$. The power function α serves as an additional degree of freedom to account for a slow or rapid increase of inhibition with higher concentrations. For simplicity, an α value of one is applied. If microbial growth in the model was not restricted, simulated microbial concentrations may reach very high numbers, especially in source areas with continuous substrate and electron acceptor supply. In real aquifers, the size of microbial populations is limited due to lack of space, production of inhibitory metabolites, lack of some nutrients, protozoal grazing, sloughing of microbial mass and viral attack, for example, and consequently clogging of aquifers due to large microbial populations has not been observed in nature (Schäfer, 1992). Other workers suggested similar inhibition terms to describe the decrease in biomass accumulation with higher microbial concentrations (e.g., Kindred and Celia, 1989).

The hydrodynamic dispersion tensor D_{ij} (L^2/T) in two dimensions was first developed by Scheidegger and Bear and is given, after Bear (1988), by:

$$D_{xx} = \alpha_L \frac{v_x^2}{v} + \alpha_{TH} \frac{v_y^2}{v} + D^* \quad (3.4)$$

$$D_{yy} = \alpha_{TH} \frac{v_x^2}{v} + \alpha_L \frac{v_y^2}{v} + D^* \quad (3.5)$$

$$D_{xy} = D_{yx} = (\alpha_L - \alpha_{TH}) \frac{v_x v_y}{v} \quad (3.6)$$

$$v = \sqrt{v_x^2 + v_y^2} \quad (3.7)$$

where α_L is the longitudinal dispersivity (L), α_{TH} is the horizontal transverse dispersivity (L), D^* is the effective diffusion coefficient (L^2/T) and v_x and v_y are the velocity components (L/T) in the x- and y-direction, respectively.

Since it has been shown that microbial populations form essentially stationary colonies with minimal migration (Ghiorse and Balkwill, 1983), the mobile component of the microbial population has been neglected in Equation 3.3, and the microbes are assumed to be governed by exponential growth and decay functions. Further assumptions include using identical components of the dispersion tensor D_{ij} for both the organic substrate and the electron acceptor. Linear, reversible sorption is assumed for the substrate and the electron acceptor.

The retardation factor R_S represents the average velocity of the groundwater relative to that of the organic substrate. It is assumed that $R_A = 1$ since the electron acceptor is oxygen. Equation 3.1 implies that the sorbed substrate is not available for microbial consumption. Temperature, pH and other factors are neglected.

The nonlinear Equations 3.1-3.3 are coupled through the dual-Monod (decay) terms. The solution is obtained following a Picard-type iterative method. The transport boundary conditions can include first type (Dirichlet), second type (Neumann) and third type (Cauchy). Initial conditions must also be defined for the organic substrate, as well as for the electron acceptor and the microbial population.

The transient flow field is simulated by multiplying the velocity vectors of the

mean flow direction by the angle of the actual flow direction over each time step. This implies that the change in the flow direction is instantaneous. The aquifer storage is assumed to be zero.

3.3.2. Model parameters

The model domain measures 120 or 140 m long and 15 or 20 m in width to prevent the organic plume from reaching the domain boundaries. The model input parameters are summarized in Table 3.1. The element lengths in the x- and y-direction were 0.6 and 0.05 m, respectively. Cirpka et al. (in sub.) stress that a coarse grid spacing, especially in the transverse direction of flow, can introduce significant numerical dispersion which in turn yields an artificial mixing of the substrates. In their simulations, a grid spacing of 0.1 m in the transverse direction reduced numerical dispersion considerably in comparison to their streamtube modelling approach. Therefore, simulations under changing flow conditions by applying an α_{TH} value of zero with refined grid spacings of 0.3 and 0.025 m in the x- and y-directions, respectively, were performed to ensure that the grid spacing of 0.6 and 0.05 m was sufficient for the simulations. The results were almost identical, with a maximum discrepancy of about 4 % between single calculated concentration values, suggesting that numerical dispersion is minimal. The time step was 1 day for the conservative cases and 0.1 days for the biodegradation simulations. The stoichiometric ratio of X = 3.07 corresponds to the oxygen-to-benzene utilization ratio.

In order to calculate a reasonable maximum microbial concentration (M_{max}) for our simulations, literature values of microbial counts from several contaminated sites were reviewed. Ghiorse and Wilson (1988) summarized a large number of studies with respect to types, abundances and activities of microorganisms in the subsurface ranging from pristine to highly contaminated sites. The viable microbial counts at the contaminated sites ranged from 10 to 10^7 cells/g aquifer material. Assuming a cell weight of 1.72×10^{-10} mg (Balkwill et al., 1988), a soil density of 2.67 g/cm^3 and a porosity of 0.33, the microbial concentration in the pore space is about 13.92 mg/L for the highest

cell count. In the present study, we therefore chose a M_{max} value of 14 mg/L.

The model BIO3D was used to examine and compare several different parameters and conditions within a groundwater flow system approximating the hydraulic conditions of the Borden field site (Rivett et al., 1994). These cases involved a) homogeneous and heterogeneous flow fields; b) steady and transient flow, and c) retardation factors of 1 and 5. The simulated transient flow fields are approximations of those observed at the Borden (Rivett et al., 1994) and Columbus field sites (Boggs et al., 1992) (Figure 3.1). Each case was simulated with both a biodegradable substrate and a conservative tracer to provide a benchmark for comparison of mass removal.

3.4. RESULTS - HOMOGENEOUS AQUIFER

3.4.1. Benchmark Cases - Conservative Tracer

A base case simulation is first considered assuming a non-reactive tracer and applying average Borden aquifer conditions (Sudicky, 1986; Table 3.1). After three years under steady flow conditions with a transverse dispersivity (α_{TH}) of 0.0025 m and R = 1, a long, narrow plume develops and its 1 µg/l contour line extends about 128 m downgradient from the source (Figure 3.2a). Microbial and oxygen concentrations remain unchanged at background levels throughout the domain due to the non-degradability of the compound. Figure 3.2b shows the same case, modified using a transient flow field from the Borden site (Figure 3.1) and with a α_{TH} set to zero. A second transient flow scenario, simulated with α_{TH} set to zero as well is shown in Figure 3.2c. This scenario is based on an idealized flow pattern observed at the Columbus field site (Boggs et al., 1992), displaying a range of 30 degrees over the course of one year (Figure 3.1).

Table 3.1. Input values for the numerical simulations.

Initial Source Conc.	**Transport Parameters**	**Degradation Parameters**	**Grid Spacing**
S = 3.0 mg/l	v = 0.09 m/day	k_{max} = 0.0 day^{-1}	Δx: 0.60 m
A = 3.0 mg/l	(homogeneous case; mean	(conservative case)	Δy: 0.05 m
M = 0.02 mg/l	v for heterogeneous case)	k_{max} = 0.1 day^{-1}	
Initial Background Conc.	α_L = 0.36 m	(biodegradation case)	**Source Size**
S = 0.0 mg/l	α_{TH} = 0.0 m and 0.0025 m	K_S = 0.1 mg/l	x: 1.8 m
A = 3.0 mg/l	D^* = 7.4 x 10^{-4} m^2/day	K_A = 0.1 mg/L	y: 1.0 m
M = 0.02 mg/l	porosity = 0.35	X = 3.07	
Inflow Boundary Conc.	R_S = 1.0 and 5.0	Y = 0.4	
S = 0.0 mg/l	R_A = 1.0	b = 0.01 day^{-1}	
A = 3.0 mg/l		M_{max} = 14 mg/l	

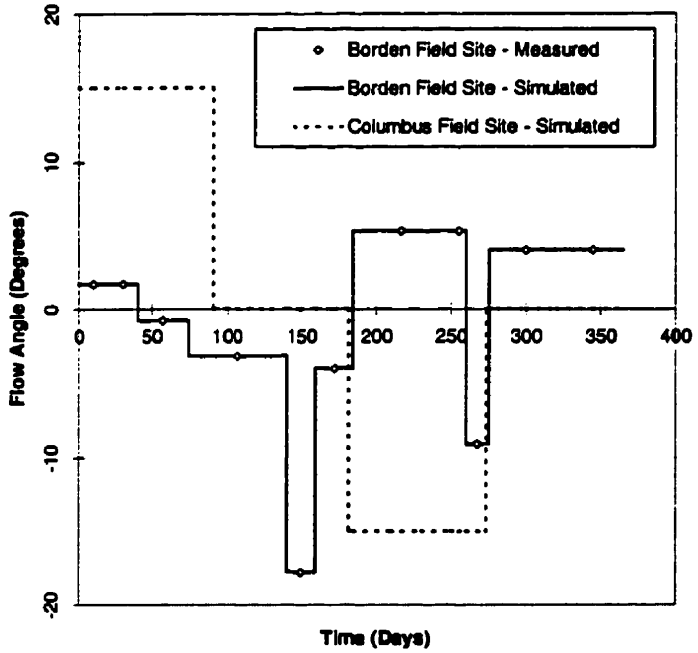

Figure 3.1. The angles of the changing flow directions over the course of one year as applied in the simulations representing Borden field conditions and idealized flow conditions as measured during the Columbus field experiment.

The plumes in Figure 3.2a for the steady flow case and Figure 3.2b for the Borden transient case ("Borden case") are similar maintaining relatively narrow profiles with high peak concentrations (Figure 3.3). The α_{TH} value of 0.0025 m was selected among numerous trial values (0.03 m, 0.025 m, 0.02 m, 0.015 m, 0.01 m, 0.005 m, 0.0025 m and 0.001 m) as producing the closest representation to the transient flow case. The

Columbus transient flow plume ("Columbus case") shows slightly greater lateral spreading and therefore lower peak concentrations than the other cases (Figure 3.2c). The 1000 μg/L contour line did not travel as far as for the other two cases and is not centred downgradient of the source area due to the relatively large changes in flow directions.

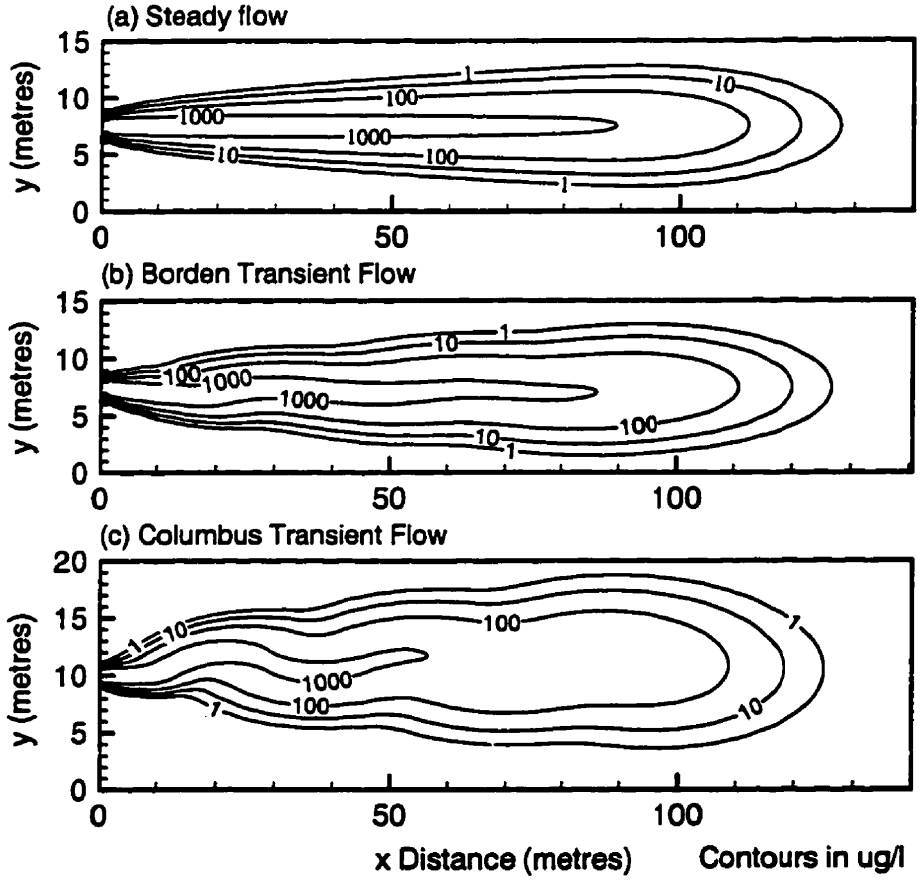

Figure 3.2. Plan view concentration distribution of a conservative tracer after three years simulation time with a retardation factor of 1. a) a steady flow field with a horizontal transverse dispersivity α_{TH} of 2.5 mm is applied. b) changing flow directions simulating Borden field conditions are applied. The horizontal transverse dispersivity α_{TH} is set to zero. c) changing flow directions simulating Columbus field conditions are applied. The horizontal transverse dispersivity α_{TH} is set to zero.

3.4.2. Biodegradation Cases

Biodegradation was incorporated into the model applying kinetic parameters as presented in Table 3.1. The substrate, microbes and oxygen plumes for the Borden case with R = 1 are shown in Figure 3.4. As compared to the conservative case (Figure 3.2b), the reactive substrate plume (Figure 3.4a) is narrower, shorter, and has a lower peak contaminant concentration. The microbes have developed within the domain of the plume, showing higher microbial concentrations along the edges of the substrate plume and at the source where the mixing between the contaminant and the oxygen occurs (Figure 3.4b). The highest microbial concentrations were about 10,000 μg/l and occurred within the source area. Dissolved oxygen has been consumed by biodegradation and shows a low concentration depletion plume, limiting microbial growth within the plume core (Figure 3.4c). Asymmetry observed in the substrate and microbial plumes (Figure 3.4a and 3.4b) even within these homogeneous hydraulic conductivity fields can be attributed to the transient flow field and the resulting irregular microbial growth. Cross-sections 40 m and 80 m downgradient of the source area and the longitudinal peak concentrations are represented along with the corresponding conservative cases in Figure 3.3. The peak concentration in the biodegrading Columbus case is, again, not in the centre line due to transient flow conditions. As with the conservative case, setting α_{TH} = 0.0025 m approximates the Borden case in plume width as well as peak concentration and gradient. However, the plume geometry of those two cases appears slightly different.

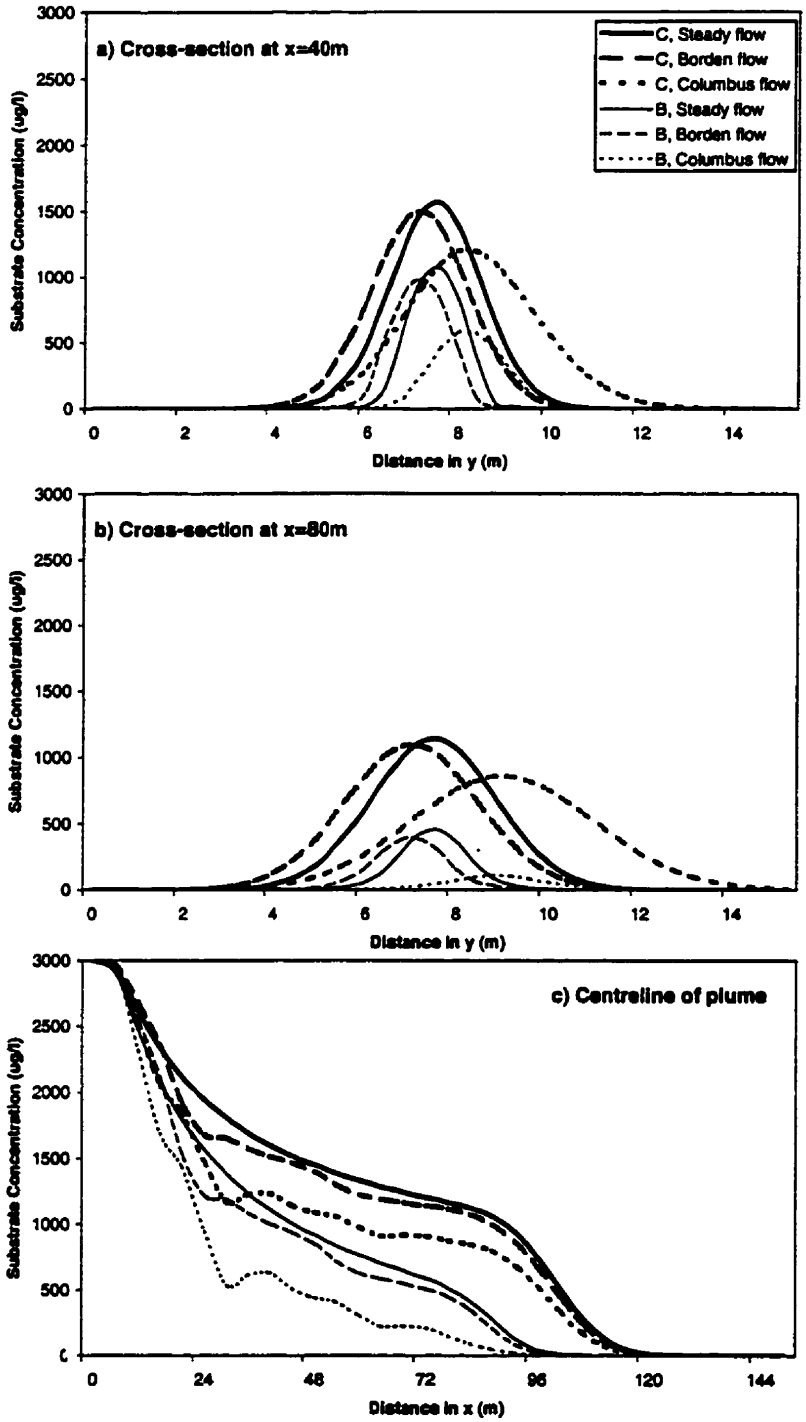

Figure 3.3. Transverse substrate concentrations after three years at a) 40 m downgradient and b) 80 m downgradient of the source area; c) peak concentrations along the plume centre line. Biodegrading and conservative cases; simulations of three years with a retardation factor of 1. (C – conservative compound; B- biodegradable substrate).

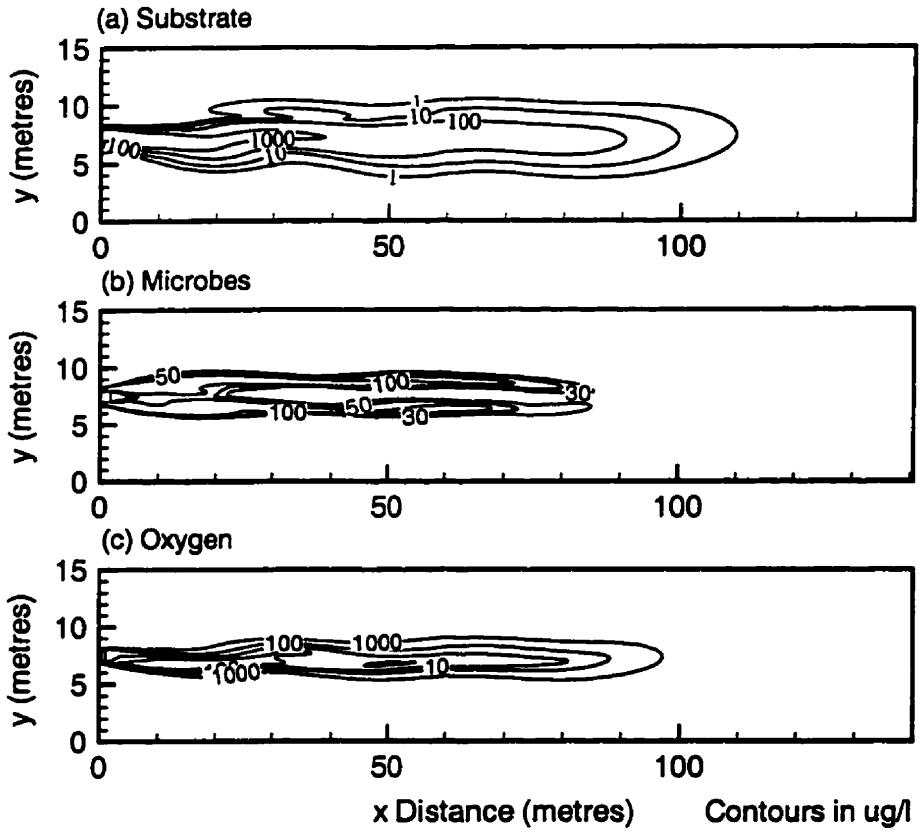

Figure 3.4. Plan view concentration distribution of a biodegradation case after three years simulation time with a retardation factor of 1. Changing flow directions applied as observed at the Borden field site. The horizontal transverse dispersivity α_{TH} is set to zero. a) biodegrading substrate; b) microorganisms; c) electron acceptor (oxygen).

3.4.3. Influence of Retardation

Similar plume shapes were observed when the retardation factor, R, was increased to 5. The six cases above were repeated with this higher retardation factor, for a duration of five years. Cross sections of those cases at 15 m and 30 m downgradient of the source area and the longitudinal peak concentrations are shown in Figure 3.5. Increasing the retardation factor decreases the effect of the transient flow field significantly with respect to the plume shape. The Borden and Columbus plumes are closer to the centre line of flow in comparison to the R = 1, three-year cases, a characteristic which is likely due to a damping effect of the retardation on the transient flow directions.

3.4.4. Effects on Rate of Biodegradation

Figure 3.6 demonstrates the effect that biodegradation has had on the mass removed in each of the scenarios modelled. The percent of mass biodegraded was calculated by taking the difference between mass in the system, at a given time, in a conservative case versus the mass in the system for the corresponding biodegradation case, divided by the conservative mass. The R = 1, three-year cases display similar trends, reaching approximately 61 and 63% of mass biodegraded for the steady and Borden cases, respectively, and 71% of mass biodegraded for the Columbus case.

The results for the R = 5 simulations show much less biodegradation when compared to the R = 1 simulations. After three years simulation time, only 26, 28 and 37% of mass biodegraded in the steady, the Borden and the Columbus cases, respectively. Even after five years, the percentage of contaminants biodegraded does not reach the level of the R = 1 cases of three years simulation time. These results indicate that biodegradation is less effective when the retardation factor increases.

For both simulated retardation factors, the Columbus case shows the largest percentage biodegraded. This demonstrates that a transient flow field can induce greater mixing between the substrate and the electron acceptor and can therefore enhance the rate of biodegradation.

Figures 3.2a, 3.2b and 3.3 demonstrate that the Borden case with $\alpha_{TH} = 0.0$ and changing flow directions and the steady flow field with $\alpha_{TH} = 0.0025$ m for a simulation time of three years give similar results with respect to peak concentrations, plume shape and mass loss in the biodegrading case (Figure 3.6) indicating that the physical mixing is similarly represented by these two modelling approaches. Based on these results and considering the uncertainty inherent in field measurements together with the limited number of field sampling locations, it is suggested that for many practical applications it is not necessary to simulate moderate changes in flow direction; using a slightly larger transverse horizontal dispersivity will adequately forecast plume development.

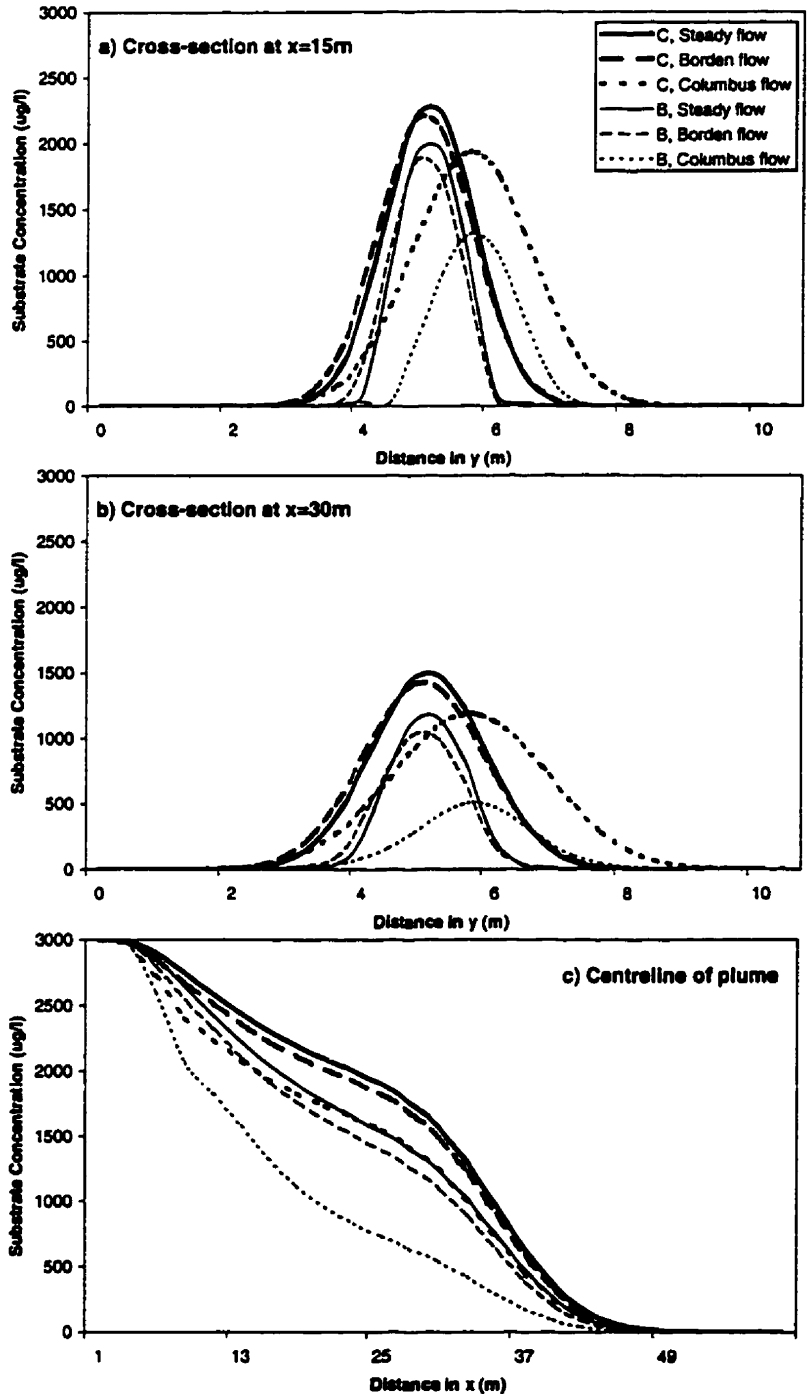

Figure 3.5. Transverse substrate concentrations at a) 15 m downgradient and b) 30 m downgradient of the source area; c) peak concentrations along the plume centre line. Biodegrading and conservative cases; simulations of five years with a retardation factor of 5. (C – conservative compound; B- biodegradable substrate).

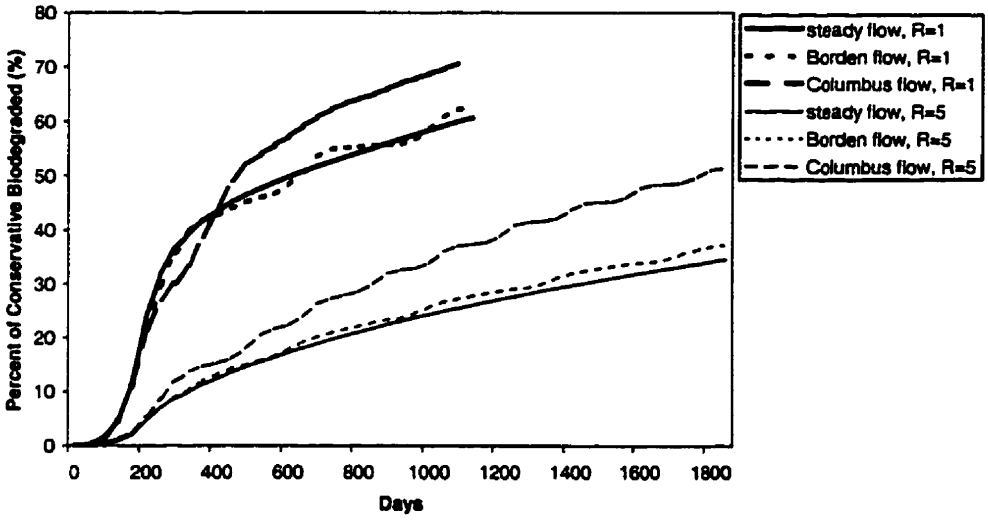

Figure 3.6. Mass loss calculations due to biodegradation. Percent difference between biodegrading and conservative cases in a homogeneous aquifer.

3.5. RESULTS - HETEROGENEOUS AQUIFER

Because heterogeneities can significantly influence the flow field and therefore the rate of biodegradation, a heterogeneous flow field was introduced into the system with parameters representative of the Borden aquifer. The mean hydraulic conductivity was maintained at the same value as in the previous cases, but a variance of 0.244 and an isotropic horizontal correlation length of 5.14 m (Woodbury and Sudicky, 1991) were applied to generate a random hydraulic conductivity field using the numerical program FGEN92 (Robin et al., 1993). The modelling domain was increased to 20 m in the transverse direction to accommodate the greater transverse spreading that was observed with the heterogeneous simulations.

3.5.1. Biodegradation versus Conservative Cases

An identical suite of simulations to those described in the previous section for the Borden and steady flow field cases was completed with the random heterogeneous flow field. The conservative, Borden flow case, R = 1, at t = 3 years is shown in Figure 3.7.

The plume travelled only about 100 m for the 1 μg/l contour line, not as far as it did under homogeneous flow conditions (Figure 3.2a). Figure 3.8 shows the cross sections of these plumes at 40 m and 80 m downgradient of the source area and the longitudinal peak concentrations. The match between the Borden conditions and the steady flow case with α_{TH} = 0.0025 m, among the conservative and among the biodegradation simulations, is as close as it was for the homogenous hydraulic conductivity simulations presented above (Figure 3.3).

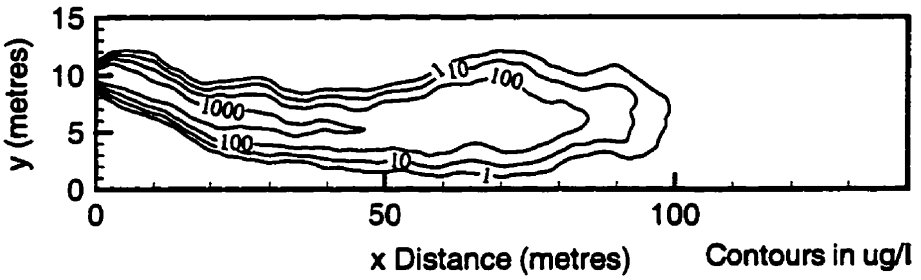

Figure 3.7. Plan view concentration distribution of a conservative tracer after three years simulation time with a retardation factor of 1. A steady flow field in a random hydraulic conductivity field as observed at the Borden field site with a horizontal transverse dispersivity α_{TH} of 2.5 mm is applied.

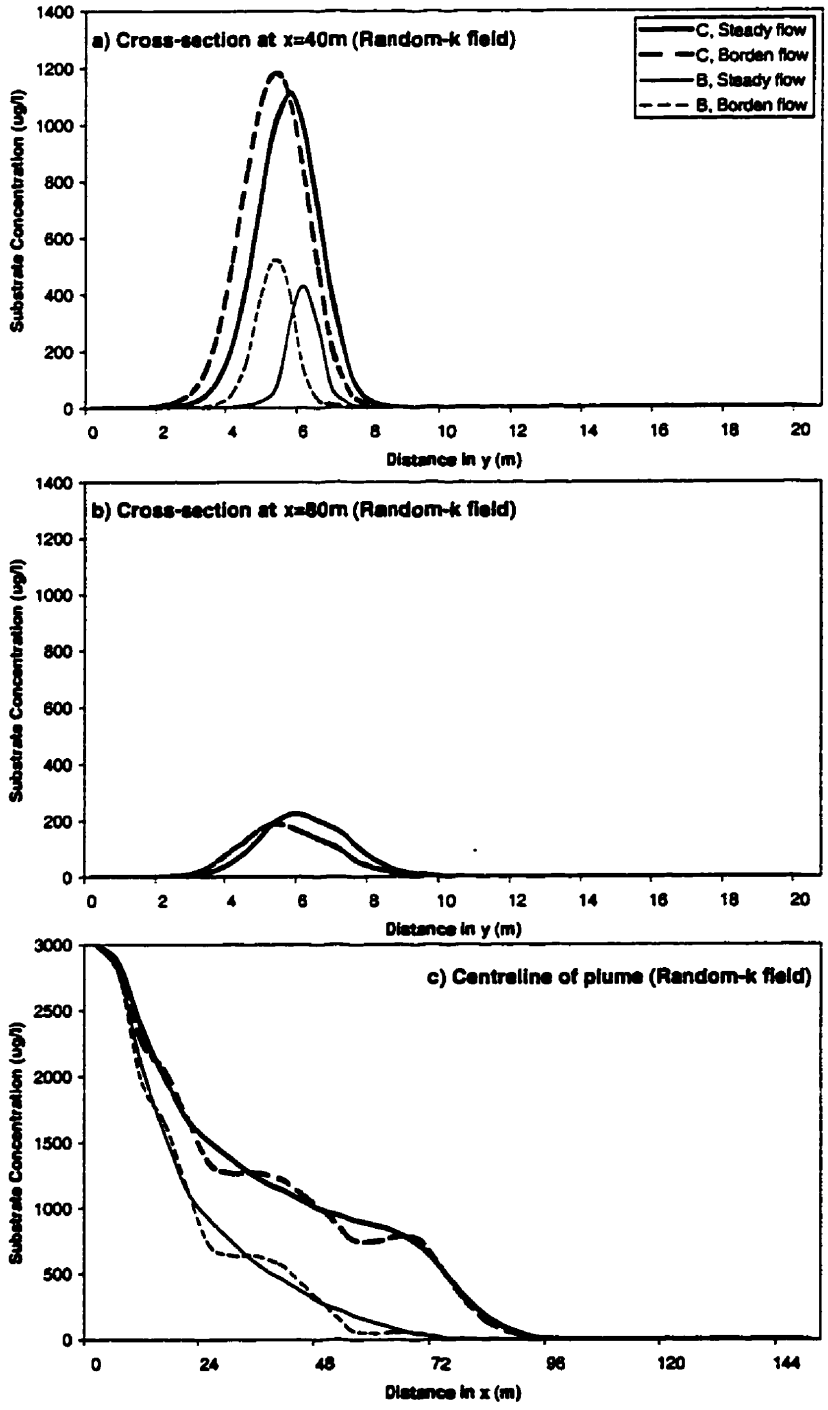

Figure 3.8. Transverse substrate concentrations at a) 40 m downgradient and b) 80 m downgradient of the source area; c) peak concentrations along the plume centre line. Biodegrading and conservative cases; simulations of three years in a random hydraulic conductivity field as observed at the Borden field site with a retardation factor of 1. (C – conservative compound; B- biodegradable substrate).

3.5.2. Effects on Rate of Biodegradation

Biodegradation has a more significant overall effect in the heterogeneous case than in the case of a homogeneous flow field, due to greater mixing between the substrate and the electron acceptor in the heterogeneous aquifer. In this respect, these simulations confirm the observations made in earlier work by MacQuarrie and Sudicky (1990). The plume generated with the steady flow field and the Borden case show similar shapes and peak concentrations (results not shown). Figure 3.9 demonstrates the percent mass biodegraded in the heterogeneous field. For the R = 1 case, the Borden transient and the steady flow cases have very similar degrees of biodegradation over the three-year simulation time (Figure 3.9). Also the extent of the two plumes is similar (results not shown).

Slightly more biodegradation occurs in the transient flow case in comparison to the steady case with an α_{TH} value of 0.0025 m when the retardation factor is increased to R = 5 (Figure 3.9). This is to be expected because in the transient case, unretarded oxygen is transported into the edges of the substrate plume while in the steady flow case, the oxygen will be replenished in the plume core.

The results presented here for the non-retarded substrate in the heterogeneous aquifer confirm the findings of the homogeneous simulations that for many practical applications it is not necessary to simulate moderate changes in flow directions; using a slightly larger transverse horizontal dispersivity will adequately forecast plume development. Quantifying the relationship between flow angle, frequency and dispersivity is beyond the scope of this work. It will be attempted in future analyses by using numerical simulations of slugs with an analysis of spatial moments.

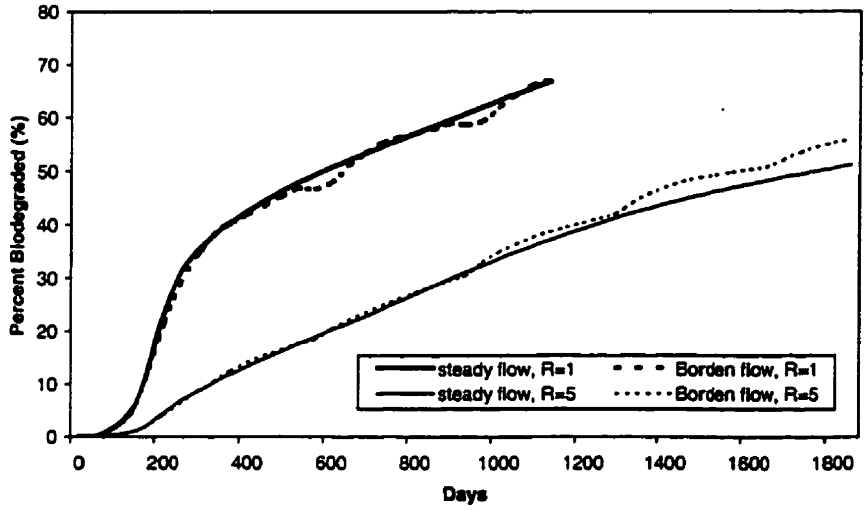

Figure 3.9. Mass loss calculations due to biodegradation. Percent difference between biodegrading and conservative cases in a random hydraulic conductivity field as observed at the Borden field site.

3.6. SUMMARY

This study showed that similar reactive plumes can be generated under transient flow conditions with $\alpha_{TH} = 0.0$ and under steady flow conditions with an α_{TH} value greater than zero. The mixing of substrate and oxygen appears to be similar for these two modelling approaches and therefore similar rates of biodegradation are predicted in the two approaches. This suggests that for many practical applications it is not necessary to incorporate moderate changes in flow direction into the model; using a slightly higher transverse dispersivity will adequately forecast plume development. This is an important outcome because it is usually difficult and time consuming to accurately measure transient flow directions at field sites at reasonable time intervals.

The results show that greater variations in flow directions cause larger transverse spreading of the plume and therefore smaller substrate peak concentrations. Due to the increased mixing of substrate and oxygen, the rate of biodegradation can be significantly enhanced.

Transient flow together with biodegradation can cause asymmetric plume shapes due to the non-uniform growth of the microorganisms, which is highest where the

substrate and the oxygen mix. As expected, a higher retardation factor reduces the rate of biodegradation.

Care must be taken when choosing the numerical solution strategy because there is the potential of introducing considerable numerical dispersion which in turn enhances the mixing between substrate and oxygen causing artificial biodegradation. Small grid spacings, on the order of 5 cm, particularly in the transverse direction to flow, help to minimize this problem.

3.7. ACKNOWLEDGMENT

This study was partially funded through a grant of the Natural Science and Engineering Research Council of Canada to J. F. Barker, E. O. Frind and B. J. Butler. I thank Dominique Sorel (now at Geomatrix Consultants, San Francisco) and Suzanne O'Hara (University of Waterloo) for their contributions in the early stages of this research. I thank Kerry MacQuarrie (now at the University of New Brunswick), as well as Ed Sudicky and John Cherry for many helpful discussions.

3.8. REFERENCES

Balkwill, D. L., Leach, F. R., Wilson, J. T., McNabb, J. F. and White, D. C. 1988. Equivalence of microbial biomass measures based on membrane lipid and cell wall components, adenosine triphosphate, and direct counts in subsurface aquifer sediments. Microbial Ecology 16, 73-84.

Bear, J. 1988. Dynamics of fluids in porous media (Reprint ed.). Mineola, NY: Dover Publications, Inc.

Bellin, A., Dagan, G. and Rubin, Y. 1996. The impact of head gradient transient on transport in heterogeneous formations: Application to the Borden field site. Water Resources Research 32(9), 2705-2713.

Boggs, J. M., Young, S. C., Beard, L. M., Gelhar, L. W., Rehfeldt, K. R. and Adams, E. E. 1992. Field study of dispersion in a heterogeneous aquifer. 1. Overview and site

description. Water Resources Research 28(12), 3281-3291.

Cirpka, O., Frind, E. O. and Helmig, R. In submission. Numerical simulation of mixing-controlled biodegradation in heterogeneous aquifers. Submitted to Water Resources Research in August 1997.

Farrell, D. A., Woodbury, A. D., Sudicky, E. A. and Rivett, M. O. 1994. Stochastic and deterministic analysis of dispersion in unsteady flow at the Borden tracer-test site, Ontario, Canada. Journal of Contaminant Hydrology 15, 159-185.

Freyberg, D. L. 1986. A natural gradient experiment on solute transport in a sand aquifer. 2. Spatial moments and the advection and dispersion of nonreactive tracers. Water Resources Research 22(13), 2031-2046.

Frind, E. O., Sudicky, E. A. and Molson, J. W. 1989. Three-dimensional simulation of organic transport with aerobic biodegradation. In: Groundwater Contamination, IAHS Publ. No. 185, (Ed. L. M. Abriola), 89-96.

Ghiorse W. C. and Balkwill, D. L. 1983. Enumeration and morphological characterization of bacteria indigenous to subsurface environments. Dev. Ind. Microbiology 24, 215-224.

Ghiorse, W. C. and Wilson, J. T. 1988. Microbial ecology of the terrestrial subsurface. In: Advances in Applied Microbiology 33, Academic Press, Inc., San Diego, (Ed. Allen I. Laskin), 107- 172.

Goode, D. J. and Konikow, L. F. 1990. Apparent dispersion in transient groundwater flow. Water Resources Research 26(10), 2339-2351.

Kindred, J. S. and Celia, M. A. 1989. Contaminant transport and biodegradation. 2. Conceptual model and test simulations. Water Resources Research 25(6), 1149-1159.

Kinzelbach, W. and Ackerer, P. 1986. Modélisation de la propagation d'un champ d'écoulement transitoire, Hydrogéologie 2, 197-206.

Levenspiel, O. 1980. The Monod equation: A revisit and a generalization to product inhibition situations. Biotechnol. Bioeng. 22, 1671-1687.

Luong, J. H. T. 1987. Generalization of Monod kinetics for analysis of growth data with substrate inhibition. Biotechnol. Bioeng. 39, 242-248.

MacQuarrie, K. T. B. and Sudicky, E. A. 1990. Simulation of biodegradable organic

contaminants in groundwater. 2. Plume behavior in uniform and random flow fields. Water Resources Research 26(2), 223-239.

Naff, R. L., Yeh, T.-C. and Kemblowski, M. W. 1989. Reply. Water Resources Research 25(12), 2523-2525.

Rehfeldt, K. R. and Gelhar, L. W. 1992. Stochastic analysis of dispersion in unsteady flow in heterogeneous aquifers. Water Resources Research 28(8), 2085-2099.

Rivett, M. O., Feenstra, S. and Cherry, J. A. 1994. Comparison of Borden natural gradient tracer tests. Proceedings of the IAHR/AIRH Symposium on Transport and Reactive Processes in Aquifers, Zurich, Switzerland, April 11-15, 1994, 283-288. In: Transport and Reactive Processes in Aquifers, Eds. Th. Dracos and F. Stauffer, Balkema, Rotterdam, Brookfield.

Robin, M. J. L., Gutjahr, A. L., Sudicky, E. A. and Wilson, J. L. 1993. Cross-Correlated Random Field Generation with the Direct Fourier Transform Method. Water Resources Research 29(7), 2385-2397.

Schäfer, W. 1992. Numerische Modellierung mikrobiell beeinflußter Stofftransportvorgänge im Grundwasser. München Wien: R. Oldenbourg Verlag GmbH. (German text).

Schirmer, M., Frind, E. O. and Molson, J. W. 1995. Transport and Biodegradation of Hydrocarbons in Shallow Aquifers: 3D Modelling. American Petroleum Institute, Workshop: Comparative Evaluation of Groundwater Biodegradation Models, May 08-09, 1995, Hotel Worthington, Ft Worth, Texas.

Sudicky, E. A. 1986. A natural gradient experiment on solute transport in sand aquifer: spacial variability of hydraulic conductivity and its role in the dispersion process. Water Resources Research 22(13), 2069-2082.

Sudicky, E. A. and Huyakorn, P.S. 1991. Contaminant migration in imperfectly known heterogeneous groundwater systems. Reviews of Geophysics, Supplement, 240-253, April 1991.

Woodbury, A. D. and Sudicky, E. A. 1991. The geostatistical characteristics of the Borden aquifer. Water Resources Research 27(4), 533-546.

CHAPTER 4

APPLICATION OF LABORATORY-DERIVED KINETIC DEGRADATION PARAMETERS AT THE FIELD SCALE

4.1. ABSTRACT

Estimating the intrinsic remediation potential of an aquifer typically requires the accurate assessment of the biodegradation kinetics, the level of available electron acceptors and the flow field. Unlike in the dispersion case, there is no known macroscale parameter the biodegradation process will converge towards in the field. Zero- and first-order degradation rates derived at the laboratory scale generally overpredict the rate of biodegradation when applied to the field scale because limited electron acceptor availability and microbial growth are typically not considered. On the other hand, field-estimated zero- and first-order rates are often not suitable to forecast plume development because they may be an oversimplification of the processes at the field scale and ignore several key processes, phenomena and characteristics of the aquifer. This study uses the numerical model BIO3D to link the laboratory and field-scale by applying laboratory-derived Monod kinetic degradation parameters to simulate a dissolved gasoline field experiment at Canadian Forces Base (CFB) Borden. All additional input parameters were derived from laboratory and field measurements or taken from the literature. The simulated results match the experimental results reasonably well without having to calibrate the model. An extensive sensitivity analysis was performed to estimate the influence of the most uncertain input parameters and to define the key controlling factors at the field scale. It is shown that the most uncertain input parameters have only a minor influence on the simulation results. Furthermore it is shown that the flow field, the amount of electron acceptor (oxygen) available and the Monod kinetic parameters have a significant influence on the simulated results. Under the field conditions modelled and the assumptions made for the simulations, it can be concluded that laboratory-derived Monod kinetic parameters can adequately describe field-scale degradation processes if all controlling factors that are not necessarily observed at the lab scale are incorporated in the field-scale modelling. In this way, there are no scale relationships to be found

that link the laboratory and the field scale. Accurately incorporating the additional processes, phenomena and characteristics, such as a) advective and dispersive transport of one or more contaminants, b) advective and dispersive transport and availability of electron acceptors, c) mass transfer limitations and d) spatial heterogeneities, at the larger scale and applying well defined lab-scale parameters should accurately describe field-scale processes.

4.2. INTRODUCTION

Biological, chemical and physical phenomena which control the rate of biodegradation of organics in groundwater are typically scale dependent. Representative elemental volumes (REV; Bear, 1988) with dimensions which differ over orders of magnitude are used by different research disciplines to describe biodegradation and transport processes. REVs at a larger scale are an assembly of many REVs at the smaller scale; therefore, there must be a link between observations made at different scales. Additional scale-dependent phenomena may play a role in the biogeochemical reactions as the size of an REV increases, i.e. complexities which are influential at a larger scale may not play a role at the smaller one. The processes, phenomena, and characteristics that can play a role and that may be scale-dependent include:

- advective and dispersive mass transport of one or more contaminants;
- non-equilibrium and equilibrium sorption;
- advective and dispersive transport and availability of one or more electron acceptors;
- population dynamics of microorganisms;
- influence of different microbial populations;
- nutrient supply;
- mass transfer limitations;
- spatial heterogeneities.

If we do not understand and account for these scale-dependent complexities, a poor estimate of intrinsic biodegradation abilities of a certain environment or an inappropriate configuration of bioremediation designs may result (Sturman et al., 1995).

Biodegradation modelling can be a helpful tool to link results of different measuring scales and to fill gaps or inadequacies in our current understanding of the governing processes.

Modelling, for example, can help to answer several important questions: a) what should I measure?; b) where and when should I measure?; c) what uncertainty do I have to expect?; and (d) which parameters are most sensitive to the final results?. In combination with modelling, batch and column test series performed in the laboratory as precursors to field-scale applications can be made more efficient and meaningful. On the other hand, the numerical model as a tool has to be developed and defined further as our knowledge of the involved processes expands.

The present work will be one step towards the goal of understanding the link between laboratory-scale experiments and controlled field tests with the possible link to "real world" problems. The aim is to provide a framework from which to assess the importance of observations at different scales and how particular results and conclusions can be used at other scales. The modelling intends to give an integrated approach to the scaling process. My intention was to use the results obtained at the smaller scale and incorporate these into the larger scale simulations where additional processes, phenomena, and characteristics can be taken into account.

4.3. RESEARCH OBJECTIVES

The research objectives of this chapter are:

- To use a mathematical model incorporating groundwater transport, and biodegradation interactions and apply the model to the field scale by using laboratory-derived kinetic degradation parameters;
- To determine the sensitivity of the model with respect to the various controlling parameters and to define the key controlling factors at the field scale;
- To investigate scale relationships, and to interpret and explain interactions observed in the transport and biodegradation of BTEX (benzene, toluene, ethylbenzene, m-xylene, o-xylene, and p-xylene).

4.4. BACKGROUND

Environmental pollution by organic compounds is a serious and widespread problem. In the subsurface, major organic contaminants include petroleum fuels (gasoline, diesel), petroleum byproducts (coal tar, coal-tar creosote), and chlorinated solvents. A large number of contaminated sites have been reported in the scientific literature. In many cases, groundwater at study sites contains a mixture of organic contaminants, either due to the complex mixture in many NAPLs (non-aqueous phase liquids; e.g., gasoline) or due to co-disposal/co-spillage (e.g., landfill leachates). Many NAPLs are toxic at concentrations exceeding drinking water standards. The degradation of these contaminants is controlled to a large extent by the biological and geochemical conditions in the groundwater. Fortunately, biodegradation tends to attenuate at least some organics during groundwater transport.

Organic contaminants generally occur as mixtures of several components, which tend to interact with each other in the groundwater as they migrate by advection and dispersion. The availability of electron acceptors (e.g. oxygen, nitrate, iron and sulphate) in microbially-mediated biotransformation processes is also crucial in the biodegradation of organics. The literature abounds with examples of organic substrate interaction in groundwater (e.g., Alvarez and Vogel, 1991; Major et al., 1991, Acton and Barker, 1992, Butler et al., 1992, Semprini and McCarty, 1992; Chang et al., 1993; Oh et al., 1994; Stringfellow and Aitken, 1995; Millette et al., 1995, 1998).

In static microcosms, biodegradation rates can be determined, controlling microbial factors identified, and interactions between organic substrates at least demonstrated, if not fully understood (e.g., Alvarez and Vogel, 1991; Godsy et al., 1992; Millette et al., 1995, 1998). Dynamic column experiments include the advection process, and can therefore simulate flowing groundwater. However, these column tests are more complex than static microcosm experiments, and biological processes are less precisely explained (e.g., Millette et al., 1998). When organic contaminant plumes are evaluated (e.g. Borden et al., 1986; Fry and Istok, 1994) or when field experiments are interpreted (Barker et al. 1989; Acton and Barker, 1992; MacIntyre et al., 1993), the biodegradation process is often represented as a first-order decay process, which may not be valid.

An understanding of the seriousness of contamination and whether active remediation is required, or whether natural processes of attenuation (passive remediation) will be sufficient are important questions in "real world" situations. Passive or intrinsic remediation is generally preferred, if feasible, due to the potential to: a) permanently eliminate contaminants through biochemical transformation or mineralization; b) avoid expensive biological, chemical, and physical treatments; and c) operate in situ. However, the possible attenuation of organic compounds and the impact of that contamination on a groundwater resource is difficult to predict since field sampling limitations make it difficult to develop an accurate mass balance. If sufficient data are available, a numerical model can be used to help answer these questions, predict the evolution of the plume, and evaluate factors limiting biodegradation (Essaid et al., 1995). However, a predictive capability facilitating justified decisions can only be found in contaminant transport models that include the full range of the controlling processes.

As described above, natural attenuation phenomena involve complex interactions of biological, chemical and physical processes, and require integration of phenomena operating at scales ranging from 10^{-6} metres (microbial cell diameter, diffusion layer thickness) up to 10 or even 1000 metres (field sites). For practical reasons, laboratory experiments are performed at a small scale. But, unfortunately, the transition from laboratory-scale observations to field-scale applications often introduces: (a) additional mass transport mechanisms and possibly mass transfer limitations; (b) the presence of multiple phases, contaminants and competing microorganisms; (c) spatial heterogeneities; and (d) one or more factors which may inhibit bacterial growth, such as lack of nutrients or unfavourable pH, redox conditions or temperature (Sturman et al., 1995). Therefore, care must be taken in extrapolating laboratory results to the field scale. On the other hand, results obtained at the field scale, in almost all cases, do not conclusively prove that contaminant loss is due to microbial activity and not some abiotic process or a measuring error (Madsen, 1991).

A representative example of how a numerical model can be used to link observations at different scales is the study by Frind et al. (1987). Frind and co-workers applied a 2D model with microscale dispersivity values at a very fine grid spacing (2 cm - 13 cm) to simulate plume evolution in heterogeneous media. The results indicate convergence of the effective dispersivity

at the microscale to the theoretical macrodispersivity value at the macroscale by taking the medium heterogeneity, a large-scale characteristic, into account.

The National Research Council (1990) defined mathematical modelling of groundwater systems as an attempt to understand the "real world" processes and represent these in mathematical terms. The first step in developing a mathematical model is the initial identification of the processes of interest and their mathematical formulation. The identification can come from laboratory and/or field observations or through theoretical analyses. Careful analysis and description must follow the initial process identification, since a precise mathematical formulation needs details about how the process works and about the characteristic parameters. Process description can usually only be done by controlled laboratory and field experiments. The mathematical model can serve to provide a sensitivity analysis. When a process and its controlling parameters are thoroughly understood and the mathematical description of the process represents the behaviour of the real system, it is possible to use the model to solve practical problems.

Once the key controlling parameters are identified for further research, the requirement for additional research, in most cases, revolves around developing theoretical, experimental, and field-based approaches for determination of model parameters. Because both the complexity of processes and our knowledge of them vary, it is no surprise that there is also broad variability in our state of knowledge with respect to model parameter estimation (API Biodegradation Workshop, 1995).

A detailed overview of existing transport and biodegradation models is given, for example, by Baveye and Valocchi (1989) and Essaid et al. (1995), and representative models are described by a number of researchers (e.g., Widdowson et al., 1988; MacQuarrie et al., 1990; Schäfer, 1992; Chen et al., 1992). In general, most of these models can deal with advection, dispersion, sorptive retardation, and chemical or biological reactions in one, two or three dimensions, where the biodegradation is based on single or multiple substrates.

A drawback of the above models is that none takes substrate interactions into account. This shortcoming has been recognized by a few researchers and substrate interaction models are now starting to appear in the scientific literature. Chang and Alvarez-Cohen (1995) and Ely et al. (1995) describe non-dimensional models dealing with cometabolic biodegradation of chlorinated

organics. McNab and Narasimhan (1995) present a model capable of handling geochemical interactions between organics and inorganic species but apply only first-order degradation reactions. Another non-dimensional model is presented by Tan et al. (1996) that describes substrate inhibition of microbial growth by using several different equations to adequately describe the involved processes. Two 1D models, one by Semprini and McCarty (1992) and the other by Malone et al. (1993), take substrate interactions into account using a modified form of the Monod equation. Recently, a 3D model was developed by MacQuarrie (1997) that takes substrate as well as geochemical interactions into account.

Modelling and experimental work, at laboratory as well as field scale, can be seen as an evolutionary procedure. I am now able to take advantage of research that has been completed at the University of Waterloo to link results obtained at the laboratory and field scale using a numerical model. The goal is to find scale relationships and to identify the most limiting factors of biodegradation at the field scale.

4.5. SCALE DEFINITIONS AND PHENOMENA

Because research is performed at scales that differ several orders of magnitude in size, the results concern REVs of different sizes. Therefore, defining different observation scales serves as a conceptual structure for approaching scale-dependent problems (Figure 4.1). Table 4.1 shows the scale-dependent processes, phenomena and characteristics and their observation methods. Scale definitions are arbitrary and I will use a modified approach proposed by Sturman et al. (1995). In the present work, I have defined the terms micro-, meso-, and macroscale as follows:

The **microscale** is taken as the scale at which chemical and microbiological species and reactions can be characterized independently of transport processes other than diffusion. Microscale parameters can only be measured in the laboratory. The magnitude of this scale is in the order of 10^{-6} to 10^{-5} metres, which is equivalent to the approximate diameter of a microbial cell and the thickness of a diffusion layer. Phenomena like the composition of microbial consortia, reactions with soil or aquifer matrix, diffusion and sorption belong to the microscale. Detailed laboratory experiments can give insight into microscale processes. Performing

microbial plate counts to determine the percentage of a certain microbial degrader population is an example of a microscale characterization method.

At the **mesoscale**, system geometry is becoming a dominant influencing factor. Advection, dispersion, interphase mass transfer, as well as diffusion and sorption, may be physical processes at the mesoscale. The influencing parameters at the mesoscale include the size of bacterial microcolonies, diameter of soil particles, lengths of pore channels, and characteristic diffusion lengths. The dimensions range from 10^{-5} to 10^{-1} metres and processes can be determined using batch and column experiments. Laboratory batch tests to determine microbial degradation kinetics are an example for mesoscale experiments.

Spatial heterogeneity, as well as advection and dispersion, are dominating factors at the **macroscale**. The corresponding dimensions range from 10^{-1} to 10^{2} metres or larger. Field or large-scale laboratory experiments are required to obtain information at this scale of interest.

The description above assumes that there are no fixed boundaries between the different scales and it has to be pointed out that phenomena observed at a smaller scale fully apply at a larger scale. However, additional phenomena at the larger scale have to be taken into account as well when modelling larger scale processes. Half-lives measured at the field scale, for example, tend to be longer than laboratory-derived values (Barker et al., 1987; Chiang et al., 1989; and Hubbard et al., 1994) because the latter are often determined under optimized conditions. The answers derived at one scale need to be extended to another scale using our knowledge of the biogeochemical/physical processes in order to be useful for field biodegradation/bioremediation applications. The numerical model will facilitate this transfer among various scales by taking additional phenomena at larger scales into account.

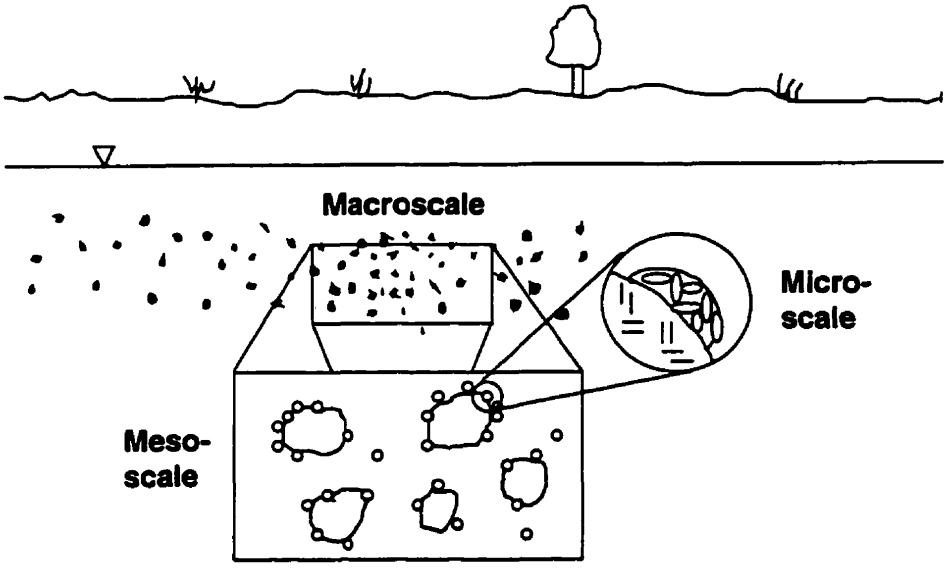

Figure 4.1. Schematic diagram of the scale of observation (modified after Sturman et al., 1995).

Table 4.1. Scale-dependent processes, phenomena and characteristics and their observation methods. The assumption is made that small-scale processes fully apply at the larger scale where the additional processes at the appropriate scale play a role as well.

Scale	Observation method
Microscale	
Microbial concentrations	plate counts
Microbial populations	gene probes, plate counts
Sorption characteristics	electron-microscopy
Mesoscale	
Reaction kinetics (e.g., Monod)	batch experiments
Degradation pathways	batch experiments
Toxicity and inhibition	batch experiments
Electron acceptors	batch experiments
Diffusion	batch experiments
Sorption (equilibrium)	batch experiments
Sorption (non-equilibrium)	column experiments
Mass transfer rates and limitations	column experiments
Microbial populations (transport, clogging)	column experiments
Advection and dispersion	column experiments
Macroscale	
Advection and dispersion	large-scale lab and field experiments
Spatial and temporal electron acceptor distribution	field measurements
Spatial heterogeneities	deterministic and stochastic aquifer analysis

4.6. LABORATORY AND FIELD EXPERIMENTS

My approach to investigate scale relationships is to integrate microbial biodegradation research at the laboratory and field scale, as well as numerical modelling within the context of transport and remediation of the organic contaminants in groundwater. Although the diversity of organic contaminants in groundwater provides many systems worthy of research, significant but relatively straightforward systems need to be selected initially.

Detailed laboratory batch experiments were evaluated to derive unique microbial degradation kinetics for m-xylene and benzene using Borden aquifer material (Chapter 1 and Appendix A). In addition, a controlled 16-month field experiment at Borden (Hubbard et al., 1994) involving dissolved PS-6 gasoline was analyzed in order to evaluate field-scale degradation processes.

In summer 1988, a natural gradient experiment was performed at CFB Borden to investigate the effect of methanol and MTBE on the mobility and persistence of BTEX from gasoline in groundwater (Hubbard et al., 1994). Three separate dissolved PS-6 gasoline plumes containing BTEX (1. dissolved PS-6 gasoline 100%; 2. dissolved PS-6 gasoline 15% and methanol 85%; and 3. dissolved PS-6 gasoline 90% and MTBE 10% [see Chapter 2 for the MTBE plume investigation]) were established below the water table. All three plumes contained a chloride (Cl^-) tracer in order to establish a mass balance. The progress of the contaminants and the Cl^- tracer was mapped by conducting "snap shot" sampling of 400 to 800 groundwater monitoring points at 6, 42, 106, 317, 398 and 476 days after injection. The control plume containing dissolved gasoline suffered from 70% to 100% mass loss for benzene, toluene, ethylbenzene, m-xylene, o-xylene, and p-xylene. This control plume is the subject of the present study.

In order to compare the field-plume evolution to the modelling results, a moment analysis for the different field plumes was performed. The mass of the contaminants, the centre of mass and the variances were calculated based on the three-dimensional concentration distributions. For numerical simulation results, performing a moment analysis for a slug is a straightforward procedure. The calculation procedure along with the equations is described in detail elsewhere (e.g., Freyberg, 1986; MacQuarrie et al., 1990). On the other hand, for three-dimensional (3D)

field data, a moment analysis requires a regular 3D grid with an interpolated concentration distribution that can be used to calculate the moments. Because the flow direction of the slug does not necessarily align with the chosen coordinate system of the regular grid, the resulting second moment tensor has to be transformed to obtain the variance of the concentration distribution in the principal directions of flow.

4.7. THE NUMERICAL MODEL BIO3D

4.7.1. Equations and Assumptions

The numerical model BIO3D solves for the coupled advective-dispersive transport and biodegradation of multiple organic substrates in the presence of an electron acceptor (in this case oxygen) and includes the growth and decay of an attached microbial population in a steady-state saturated groundwater system. The model evolved from an original 2D principal direction formulation by MacQuarrie et al. (1990), and from a 3D single-substrate finite-element model presented by Frind et al. (1989). The aerobic biodegradation process is assumed to be governed by dual-Monod kinetics under oxygen-limiting conditions. A Picard iteration scheme is used for the competing substrates, while a threshold concentration can be applied to prevent biodegradation for low substrate and electron acceptor concentrations. The groundwater flow and multiple mass transport equations are solved using the Galerkin finite-element technique with Leismann time-weighting to maintain matrix symmetry (Leismann and Frind, 1989). The technique provides second-order accuracy in time. Complex aquifer geometry can be accommodated using deformable brick elements, and an efficient preconditioned conjugate gradient solver is used to solve the matrix equation (Schmid and Braess, 1988). The respective governing equations for the substrates, the electron acceptor, and the microbial population are given by:

$$-\frac{dS_\beta}{dt} = \frac{v_i}{R_{S\beta}}\frac{\partial S_\beta}{\partial x_j} - \frac{\partial}{\partial x_i}\left(\frac{D_{ij}}{R_{S\beta}}\frac{\partial S_\beta}{\partial x_j}\right) + k_{\max\beta}\frac{M}{R_{S\beta}}\frac{S_\beta}{S_\beta + K_{S\beta} + \frac{S_\beta^2}{K_{I\beta}}}\frac{A}{A+K_A} \qquad \beta = 1, \ldots, N \quad (4.1)$$

$$-\frac{dA}{dt} = \frac{v_i}{R_A}\frac{\partial A}{\partial x_j} - \frac{\partial}{\partial x_i}\left(\frac{D_{ij}}{R_A}\frac{\partial A}{\partial x_j}\right) + \sum_{\beta=1}^{N} k_{\max\beta}\frac{M}{R_A}X_\beta\frac{S_\beta}{S_\beta + K_{S\beta} + \frac{S_\beta^2}{K_{I\beta}}}\frac{A}{A+K_A} \quad (4.2)$$

$$+\frac{dM}{dt} = \sum_{\beta=1}^{N} k_{\max\beta} M Y_\beta\left(1 - \frac{M}{M_{\max}}\right)\frac{S_\beta}{S_\beta + K_{S\beta} + \frac{S_\beta^2}{K_{I\beta}}}\frac{A}{A+K_A} - bM \quad (4.3)$$

where S_β is the concentration of organic substrate β (ML^{-3}), t is time (T); v_i is the velocity vector (LT^{-1}), $R_{S\beta}$ is the retardation factor of organic substrate β, x_i and x_j are the spatial coordinates (L), D_{ij} (L^2T^{-1}) is the hydrodynamic dispersion tensor (Burnett and Frind, 1987) with its components α_L as the longitudinal dispersivity (L), α_{TH} as the horizontal transverse dispersivity (L), α_{TV} as the vertical transverse dispersivity (L) and D* as the effective diffusion coefficient (L^2T^{-1}); $k_{max\,\beta}$ is the maximum utilization rate of substrate β (T^{-1}); M is the microbial concentration (ML^{-3}); $K_{S\beta}$ is the half-utilization constant of the substrate β (ML^{-3}); $K_{I\beta}$ is the Haldane inhibition concentration of substrate β (ML^{-3}); A is the electron acceptor (oxygen) concentration (ML^{-3}); K_A is the electron acceptor (oxygen) half-utilization constant (ML^{-3}), N is the number of substrates, R_A is the retardation factor of the electron acceptor; X_β is the mass ratio of oxygen to organic substrate β consumed; Y_β is the microbial yield per unit organic substrate β consumed, M_{max} is the maximum microbial concentration (ML^{-3}) and b is the first-order decay rate of the microbial population (T^{-1}).

The substrate Monod term in Equations 4.1 to 4.3 was extended by introducing the Haldane inhibition term ($S_\beta^2/K_{I\beta}$) as proposed by Haldane (1930) and Andrews (1968). The Haldane term yields a slower microbial growth and, therefore, a slower effective substrate utilization rate at higher substrate concentrations (see also Chapter 1 and Appendix A).

Intensive research is ongoing to determine the influence of microbial migration on biodegradation processes. It is commonly accepted that the major portion of the microbial population is attached to the soil particles (Holm et al., 1992; McCaulon et al., 1995; Johnson et al., 1995) and that these microorganisms are the principal users of organic matter. Hence, the

mobile component of the microbial population has been neglected in Equation 4.3 and the microbes are assumed to be governed by exponential growth and decay functions. A microbial threshold concentration at each node within the numerical model will ensure that a minimum microbial population is maintained at all times.

Unrealistically high cell numbers in the numerical model are avoided by introducing the term $[1-(M/M_{max})]$ in Equation 4.3. If microbial growth in the model was not restricted, simulated microbial concentrations may reach very high numbers, especially in source areas with continuous substrate and electron acceptor supply. In real aquifers, the size of microbial populations is limited due to lack of space, production of inhibitory metabolites, lack of some nutrients, protozoal grazing, sloughing of microbial mass and viral attack, for example, and consequently clogging of aquifers due to large microbial populations has not been observed in nature (Schäfer, 1992). M_{max} represents the maximum microbial concentration at which the microbial population reaches a quasi steady state. Other workers suggested similar inhibition terms to describe the decrease in biomass accumulation at higher microbial concentrations (e.g., Kindred and Celia, 1989).

Microbial population dynamics in natural systems are complex, difficult to monitor and thus not well known, and some simplifying assumptions have been made for the model. Equation 4.3 implies, for example, that a single microbial population utilizes all substrates without interactions other than electron acceptor limiting effects. Further assumptions include using identical components of the dispersion tensor D_{ij} for both the organic substrates and the electron acceptor. Assuming linear sorption for each organic substrate, the retardation factors $R_{S\beta}$ can be calculated as (Freeze and Cherry, 1979)

$$R_{S\beta} = 1 + (\rho_b \; K_{d\beta}) / \theta \qquad (4.4)$$

where ρ_b is the bulk mass density of the porous medium (M/L^3), $K_{d\beta}$ is the distribution coefficient for substrate β and θ is the porosity. It is assumed that $R_A = 1$ because the electron acceptor is oxygen. Equation 4.1 implies that the sorbed substrates are not available for microbial consumption. Temperature, pH or other factors are neglected.

The boundary conditions can include first type (Dirichlet), second type (Neumann) and third type (Cauchy). Initial conditions must also be defined for each organic substrate, as well as for oxygen and the microbial population.

4.7.2. Verification of BIO3D Against Analytical Solution SLUG3D

In order to verify the numerical model BIO3D, the results were compared to the results of the analytical solution SLUG3D (Sudicky, 1985). SLUG3D is an analytical model to simulate three-dimensional mass transport that includes an instantaneous input of mass. The model was modified to include simple first-order degradation of the substrate. Because the analytical solution can only handle first-order degradation for a single substrate by ignoring oxygen and microbial concentrations, the problem to be solved has to be relatively simple. A homogeneous, isotropic 3D aquifer was assumed with $v = 0.09$ m/day, $\alpha_L = 0.36$ m, $\alpha_{TH} = 0.03$ m, $\alpha_{TV} = 0.0$ m and $D^* = 7.4\ 10^{-5}$ m^2/day, $R = 1$ and a porosity θ of 0.35. To simulate the degradation process, a first-order degradation rate of 0.01 day^{-1} was applied to the substrate which had an initial source concentration of 10 mg/L. The full slug source dimensions for SLUG3D were 2.8 m in longitudinal, 1.95 m in transverse horizontal and 1.5 m in transverse vertical direction, respectively. Because the solution is symmetrical about the axes perpendicular to flow, only a quarter of the source has to be simulated. Accordingly, the numerical quarter source dimensions of BIO3D are 2.1 m in longitudinal, 0.9 m in transverse horizontal and 0.7 m in transverse vertical direction, respectively. A constant grid spacing of 0.7 m, 0.15 m and 0.1 m was applied in the longitudinal, transverse horizontal and vertical directions, respectively. In this way, the numerical and the analytical sources are closely represented. The first-order degradation process can be approximated in the numerical solution by maintaining constant microbial and electron acceptor (oxygen) concentrations and selecting $K_S >> S$ and $K_A << A$.

Figures 4.2. - 4.4 show the comparison between BIO3D and SLUG3D for a simulation time of 50 days based on concentration profiles. In the longitudinal direction, the contaminant front calculated with the analytical solution is slightly advanced in comparison to the numerical solution but generally shows good agreement (Figure 4.2). The peak concentration of the numerical solution is slightly higher, however the difference is less than 1%. The discrepancy in

the profile can be attributed to the slightly different ways by which the source is represented in the analytical and numerical solution. Concentration profiles in the directions perpendicular to flow, close to the centre of mass show a very good agreement between the analytical and the numerical solution (Figure 4.3 and 4.4) indicating minimal numerical dispersion. Figure 4.5 presents a comparison of the mass loss of the substrate. The mass loss curves for the analytical and the numerical solution are also in good agreement. These results verify the accuracy of the numerical solution BIO3D, at least for this simplified case of first-order degradation.

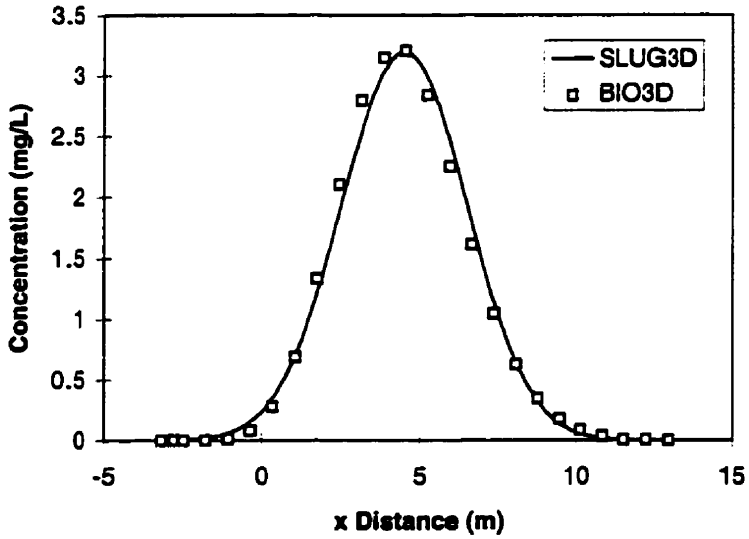

Figure 4.2. Longitudinal profiles along the plume centre line comparing the analytical solution (SLUG3D) and the numerical solution (BIO3D) for a simulation time of 50 days. A first-order degradation rate of 0.01 day^{-1} was applied.

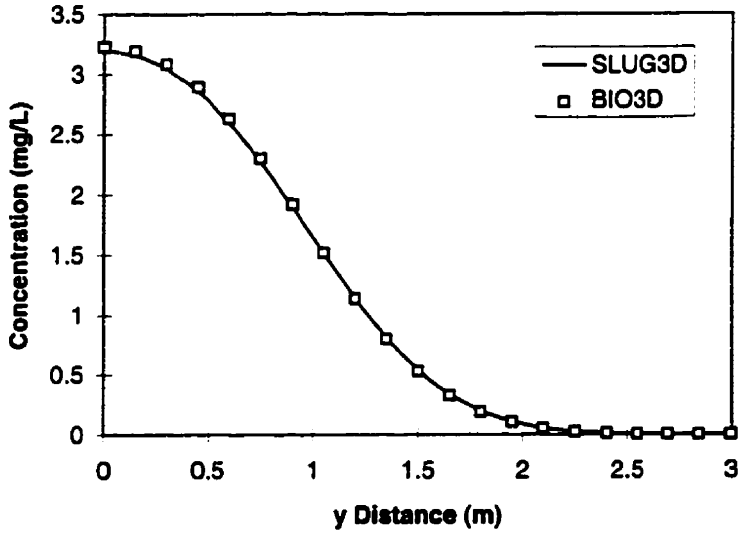

Figure 4.3. Transverse horizontal profiles close to the centre of mass comparing the analytical solution (SLUG3D) and the numerical solution (BIO3D) for a simulation time of 50 days. A first-order degradation rate of 0.01 day^{-1} was applied.

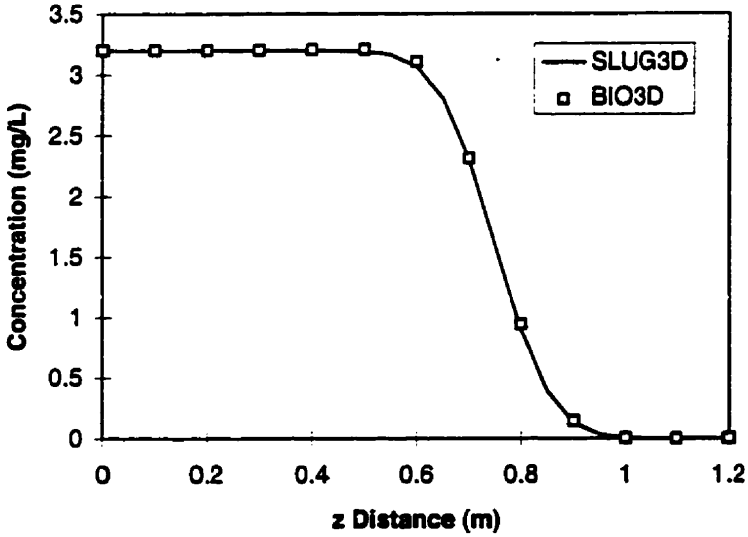

Figure 4.4. Vertical profiles close to the centre of mass comparing the analytical solution (SLUG3D) and the numerical solution (BIO3D) for a simulation time of 50 days. A first-order degradation rate of 0.01 day^{-1} was applied.

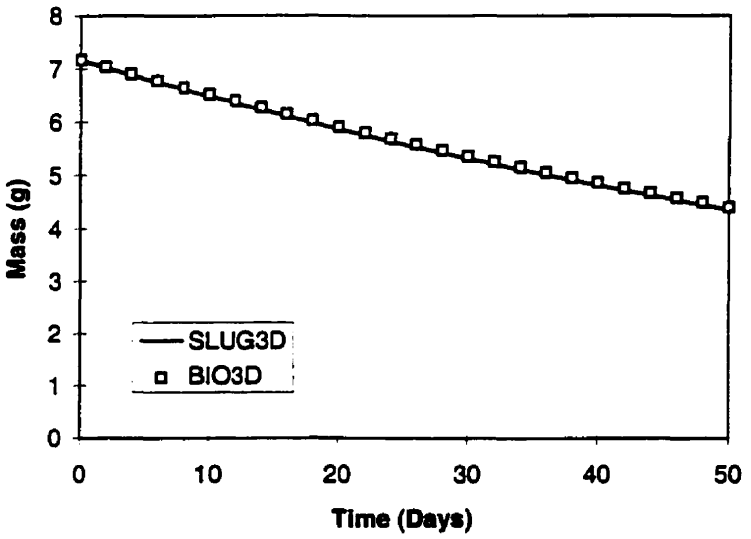

Figure 4.5. Total mass of substrate versus time comparing the analytical solution (SLUG3D) and the numerical solution (BIO3D). A first-order degradation rate of 0.01 day^{-1} was applied.

4.8. SIMULATION OF FIELD EXPERIMENT USING LABORATORY KINETIC PARAMETERS

The hypothesis of this research is that all parameters measured at a smaller scale fully apply at the larger scale. The validity of this hypothesis will be assessed using the numerical model as a tool. Field-scale processes, phenomena, and characteristics, such as sorption, transport and availability of the electron acceptor, spatial and temporal distribution of electron donors, spatial and temporal distribution of the microbial population and spatial heterogeneities, will play a role at the field scale and need to be identified and taken into account. All of the above-mentioned factors, including the micro-, meso- and macroscale phenomena, will be incorporated into the numerical model and considered as required. The intention is to run the model at the field scale with micro-, meso- and macroscale parameters (Chapter 1 and Appendix A), using small discretizations in the cm range and let the model develop the large-scale phenomena. The outcome will be compared to the results of the Borden dissolved gasoline field

experiment and no attempt will be made to calibrate the model. Instead, an extensive sensitivity analysis will be performed to identify the controlling factors.

This work will provide insight into the applicability of the multiple substrate model to "real world" sites. It will also give a better understanding of the data that are required for successful modelling of transport with multiple substrate biodegradation at the field scale. This insight might be helpful in the design of future cost-effective field or large-scale laboratory experiments and in the design of remedial actions at contaminated sites.

4.9. BIO3D INPUT PARAMETERS AND SIMULATION APPROACH

4.9.1. Input Parameters

In order to simulate the Borden dissolved gasoline field experiment (Hubbard et al., 1994), only previously calculated and measured input parameters from laboratory and field studies as well as values from the literature are applied. This information is used to simulate the BTEX field-plume behaviour without attempting to calibrate the results. The three-dimensional BTEX concentration distribution as measured by Hubbard et al. (1994) was used to calculate the zeroth (mass of the contaminants), first (the centre of mass) and second (the variances of the concentration distribution) moments of the contaminants in order to compare them to the moments as simulated using BIO3D. A homogeneous and five different random heterogeneous aquifers with identical statistics are used to perform the simulations.

Hubbard et al. (1994) measured all six BTEX compounds (benzene, toluene, ethylbenzene, m-xylene, o-xylene and p-xylene) during six sampling snapshots at 6, 42, 106, 317, 398 and 476 days after injection. In addition, oxygen concentrations were measured prior to the experiment.

The transport and geometry parameters, including the source of information, are summarized in Table 4.2. The 3D random hydraulic conductivity fields were generated using the program FGEN92 (Robin et al., 1993) and applying statistical parameters of the Borden field site as calculated by Woodbury and Sudicky (1991). The parameters used to describe the structure of

the heterogeneity include the mean of $\hat{Y}$, where $\hat{Y}$ = ln (hydraulic conductivity in cm/s), the variance of $\hat{Y}$ ($\sigma_{\hat{Y}}^2$) and the correlation lengths (λ_H and λ_V) in horizontal and vertical direction, respectively. The corresponding parameters are $\hat{Y}$ = -4.68, $\sigma_{\hat{Y}}^2$ = 0.244, λ_H = 5.14 m and λ_V = 0.209 m in an exponential covariance function (Woodbury and Sudicky, 1991). It is assumed that the hydraulic conductivity field is stationary and log-normally distributed, with point-to-point hydraulic conductivities being locally isotropic. The groundwater flow model WATFLOW-3D (Molson et al., 1995) was used to simulate the random 3D groundwater flow field and to create a velocity vector field within the solution domain of BIO3D.

Table 4.2. Transport and geometry parameters for the base-case BIO3D simulations.

Parameters	Comments
Porosity θ = 0.35	Sudicky (1986)
Homogeneous:	
v = 0.09 m/day	Sudicky (1986)
Heterogeneous:	
mean K = 8.052 m/day	Sudicky (1986)
Gradient = 0.00391	Sudicky (1986)
Grid Spacing	
X: 0.70 m	See Section "Verification of Grid Spacing" below
Y: 0.15 m	See Section "Verification of Grid Spacing" below
Z: 0.10 m	See Section "Verification of Grid Spacing" below
Full Source Size	
X: 2.1 m	Approximation of simulated injection using WATFLOW-3D (Molson et al., 1995)
Y: 1.8 m	Approximation of simulated injection using WATFLOW-3D (Molson et al., 1995)
Z: 1.4 m	Approximation of simulated injection using WATFLOW-3D (Molson et al., 1995)
Dispersivities/Diffusion	
A_L = 0.36 m	Sudicky (1986)
A_{TH} = 0.03 m	Sudicky (1986)
A_{TV} = 0.00 m	Sudicky (1986)
D^* = 7.4 x 10^{-5} m^2/day	Hubbard et al. (1994)

All six BTEX compounds were measured in the field but because no accurate laboratory kinetic degradation data are available for toluene, ethylbenzene, o-xylene and p-xylene, and in order to keep computational costs manageable, those compounds were lumped together into one compound (TEX) for all simulations. Furthermore, the BTEX compounds were not the only contaminants dissolving from the original gasoline source. Another lumped compound, including more than 100 individual compounds that are generally less soluble than BTEX, has to

be introduced. These compounds were not measured in the field, however, ignoring them in the simulations might overpredict the available oxygen for the BTEX compounds. Thus, four co-existing substrates (1 - benzene, 2 - m-xylene, 3 - TEX, 4 - all other dissolved gasoline constituents) are simulated along with oxygen as the electron acceptor and the microbial population. An estimate of the amount of available oxygen under the field conditions yielded sufficient oxygen to degrade all the injected substrate mass. Therefore, it is assumed that oxygen is the only electron acceptor. Within a single time step, the oxygen available to each substrate will decrease to levels dependent on that consumed previously and that being consumed during the time step by the other substrates present. It is assumed that all substrates are degraded by the same microbial population. This assumption seems reasonable in this case of BTEX compounds being the primary electron donors. The microbial, oxygen and substrate related input parameters and information about where each of the parameters was obtained, are summarized in Table 4.3.

Table 4.3. Microbial, oxygen and substrate related input parameters for the base case BIO3D simulations.

Initial Source Conc.	**Comments**
S_{S1} = 7.117 mg/L	calculated based on measured field data (Hubbard et al., 1994)
S_{S2} = 2.023 mg/L	calculated based on measured field data (Hubbard et al., 1994)
S_{S3} = 7.675 mg/L	calculated based on measured field data (Hubbard et al., 1994)
S_{S4} = 4.204 mg/L	calculated based on measured laboratory data (Brookman et al., 1985) [see text]
A_S = 2.55 mg/L	Hubbard et al. (1994)
M_S = 0.003 mg/L	measured in the laboratory (Chapter 1)
Initial Backgr. Conc.	
S_{B1} = 0.0 mg/L	Hubbard et al. (1994)
S_{B2} = 0.0 mg/L	Hubbard et al. (1994)
S_{B3} = 0.0 mg/L	Hubbard et al. (1994)
S_{B4} = 0.0 mg/L	Hubbard et al. (1994)
A_B variable	calculated based on measured field data (Hubbard et al., 1994) [see text]
M_B = 0.003 mg/L	measured in the laboratory (Chapter 1)
Degradation Parameters	
$K_{max\,1}$ = 1.56 day^{-1}	measured in the laboratory (Appendix A)
$K_{max\,2}$ = 4.13 day^{-1}	measured in the laboratory (Chapter 1)
$K_{max\,3}$ = 4.00 day^{-1}	estimated based on measured benzene and m-xylene degradation data (Chapter 1; Appendix A) [see text]
$K_{max\,4}$ = 0.20 day^{-1}	assumed due to lack of information [see text]
K_{S1} = 0.0 mg/L	measured in the laboratory (Appendix A)
K_{S2} = 0.79 mg/L	measured in the laboratory (Chapter 1)
K_{S3} = 0.79 mg/L	estimated based on measured benzene and m-xylene degradation data (Chapter 1; Appendix A) [see text]
K_{S4} = 2.0 mg/L	assumed due to lack of information [see text]
K_A = 0.1 mg/L	MacQuarrie et al. (1990)
K_{I1} = 95.0 mg/L	measured in the laboratory (Appendix A)

K_{I2} = 91.7 mg/L	measured in the laboratory (Chapter 1)
K_{I3} not applied	inhibition concentration not applied due to lack of information [see text]
K_{I4} not applied	inhibition concentration not applied due to lack of information [see text]
X_1 = 3.072	oxygen to benzene mass ratio assuming complete mineralization
X_2 = 3.209	oxygen to m-xylene mass ratio assuming complete mineralization
X_3 = 3.156	oxygen to TEX mass ratio assuming complete mineralization
X_4 = 3.460	oxygen to mass of remaining constituents ratio assuming complete mineralization (Brookman et al., 1985) [see text]
Retardation Factors	
R_1 = 1.5	Hubbard et al. (1994) based on measured laboratory K_d values
R_2 = 2.0	Hubbard et al. (1994) based on measured laboratory K_d values
R_3 = 1.6	Hubbard et al. (1994) based on measured laboratory K_d values
R_4 = 2.8	estimated based on measured laboratory distribution coefficients (Brookman et al., 1985)
R_A = 1.0	Hubbard et al. (1994)
Microbial Parameters	
Y_1 = 1.24	measured in the laboratory (Appendix A)
Y_2 = 0.52	measured in the laboratory (Chapter 1)
Y_3 = 0.50	estimated based on measured benzene and m-xylene degradation data (Chapter 1; Appendix A)
Y_4 = 0.25	assumed due to lack of information [see text]
B = 0.0 day^{-1}	Chapter 1 and Appendix A [see text]
M_{max} = 14 mg/L	Chapter 3

Subscripts: 1 - benzene; 2 - m-xylene; 3 - TEX (see text); 4 - Other constituents (see text)

Most of the model input parameters in Table 4.3 were calculated or obtained from measured laboratory or field data. However, some of the parameters had to be estimated or assumed using best professional judgement. Nevertheless, all parameters were obtained prior to the start of the simulations.

Hubbard et al. (1994) measured the background oxygen concentration in the aquifer one week prior to the injection of the dissolved gasoline. They found oxygen concentrations below the average concentration of about 4.5 mg/L in a zone close to the injection interval. Even small pockets of 2 mg/L oxygen and less were identified. In order to simulate the available oxygen in the aquifer as realistically as possible, a variable initial background oxygen distribution was estimated. An oxygen concentration of 3 mg/L was estimated for the horizontal plane through the centre line of the plumes with linearly increasing concentrations to 4.5 mg/L oxygen for the horizontal planes 0.5 m below and 0.5 m above the centreline plane. Outside this zone of variable background oxygen, a constant oxygen background concentration of 4.5 mg/L was assumed.

The Monod parameters for the TEX compounds (toluene, ethylbenzene, o-xylene and p-xylene) were not measured in the lab. But the degradation behaviour of all BTEX compounds is fairly similar, therefore, $k_{max\,3}$ and $K_{S\,3}$ were estimated based on the degradation parameters of benzene and m-xylene (Table 4.3). However, no Haldane inhibition concentration was introduced for the lumped TEX compound due to the relative uncertainty of the estimated kinetic parameters and due to lack of better information. A sensitivity analysis is performed below to investigate the influence of the estimated TEX Monod parameters.

Defining the initial substrate concentration, the Monod parameters, the oxygen demand and the microbial yield of the second lumped compound, which includes more than 100 individual substrates, such as n-butane, n-butene, n-pentene, propane, cyclopentane, cyclohexane, isobutane, isopentane, different trimethylbenzenes, different ethylbenzenes, isobutane and isopentane (Brookman et al., 1985), has to be attempted. Brookman et al. (1985) investigated the aqueous solubilities and average aqueous concentrations of all measurable compounds of the PS-6 gasoline, as used for the field study by Hubbard et al. (1994). Based on this, an estimate can be made of how large the mass percentage of all compounds is in comparison to BTEX. It was found that all compounds other than BTEX comprise about 20% of the total dissolved gasoline mass. Because the injected mass of benzene, m-xylene and TEX were 20.4, 5.8 and 22 g, respectively, the mass of all remaining compounds lumped together is approximately 12.05 g. This yields an initial source concentration for the simulations of $S_{S4} = 4.204$ mg/L.

An extensive literature review was undertaken to define Monod kinetic parameters for at least some of the remaining compounds beside BTEX. Although a relatively large number of studies present Monod parameters for BTEX, no groundwater-related Monod parameters for any of the other compounds were found. To the best of my knowledge, only one study by Hardison et al. (1997) measured n-butane degradation; however, a fungus was utilizing the substrate in this case. Therefore, only an estimate for the Monod parameters and the microbial yield can be made for the lumped compound. It is believed that the majority of the compounds are not degraded as readily as the BTEX compounds, therefore, a maximum degradation rate $k_{max\,4} = 0.2\ day^{-1}$ with a half-utilization constant $K_{S\,4} = 2.0$ mg/L was assumed. A sensitivity analysis on the degradation parameters is performed below to investigate their influence on the overall results. Furthermore, some of the compounds are only degraded by cometabolism, therefore, it is expected that the

microbial yield is smaller than for the BTEX compounds. For this study, a microbial yield Y_4 = 0.25 is assumed and a sensitivity analysis will be performed.

Because the chemical structure of the remaining compounds is known, the oxygen required for complete mineralization of those compounds to CO_2 and H_2O can be calculated as X_4 = 3.46. Assuming complete mineralization of all compounds is likely to overestimate the oxygen demand and thus represents the worst case scenario from the remediation point of view.

The microbial decay coefficient, b, was assumed to be negligible for the short-term laboratory study (Chapter 1; Appendix A) performed to derive the Monod parameters. In the field, this parameter might be of some significance. MacQuarrie et al. (1990) calculated a best-fit microbial decay coefficient of 7.63 x 10^{-13} day^{-1}, essentially zero, in their attempt to simulate a column experiment involving toluene. Other researchers have chosen higher microbial decay coefficients in their modelling efforts. Decay coefficients of 0.01 day^{-1} were applied, for example, by Borden and Bedient (1986), Malone et al. (1993) and Essaid et al. (1995). For simplicity, b = 0 was assumed and a sensitivity analysis will be performed for this value.

4.9.2. Verification of Grid Spacing and Simulation Approach

Defining of the appropriate grid spacing for the simulations is an important task because numerical and biogeochemical constraints have to be met. In order to minimize numerical dispersion that would induce artificial mixing and thus artificial degradation, the Peclet criterion has to be satisfied. To my knowledge, no rigorous Peclet criterion exists to define the grid spacing in the directions transverse to flow. Therefore, the appropriate grid spacings in transverse-horizontal and vertical directions of flow have to be defined by sensitivity analysis. Furthermore, the reactions between the substrates and the electron acceptor are affected by the grid spacing because it defines the size of the REV and thus the degree of mixing between the substrates and the electron acceptor.

The base case grid (longitudinal, transverse-horizontal and vertical grid spacings of 70, 15 and 10 cm, respectively) with the base case parameters as described in the previous section was run and compared to the results obtained by a coarser and a finer grid where the transverse grid spacings were doubled and cut in half, respectively. For the fine grid, the longitudinal grid

spacing was also cut in half. For the coarse grid, to double the longitudinal grid spacing with respect to the base case, results in element lengths of 1.4 m which violates the Peclet criterion. Severe oscillations were observed and therefore, the longitudinal base-case grid spacing of 70 cm was applied to the coarse grid. The results as presented for benzene in Figure 4.6 indicate that the fine and base-case grids are almost identical whereas the mass loss in the case of the coarser grid spacing increases presumably due to the larger element sizes and therefore higher degree of mixing. The volume of the microcosms used to derive the Monod-kinetic parameters was 0.16 L (Chapter 1; Appendix A). The volume of the base-case and fine grid REV is 10.5 L and approximately 1.31 L, respectively, but the numerical results are essentially the same. Based on these results, it is indicated that a grid spacing of 70, 15 and 10 cm longitudinally, transverse-horizontally and vertically, respectively, is sufficient to adequately describe the reactions and to minimize numerical dispersion.

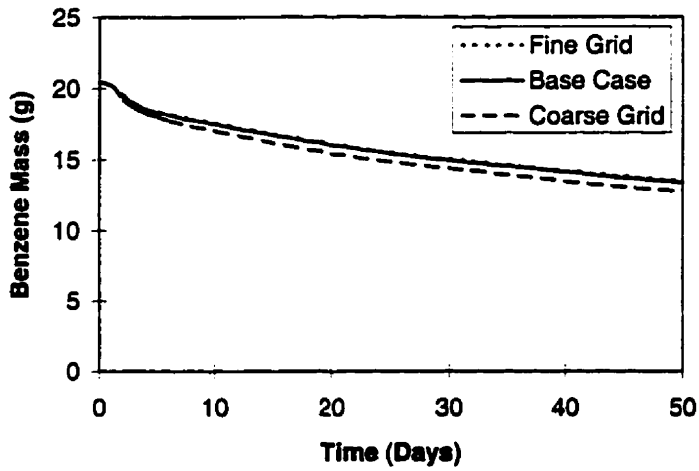

Figure 4.6. Three different grid spacings (fine grid: 35, 7.5 and 5 cm, base case: 70, 15 and 10 cm, coarse grid: 70, 30 and 20 cm longitudinally, transverse horizontally and vertically, respectively) for a homogeneous medium are compared for the case of benzene.

4.10. RESULTS AND DISCUSSION

4.10.1. Simulation Results

Several simulations were performed using the same base case input parameters (Table 4.1 and 4.2) but different generated random hydraulic conductivity fields as well as a homogeneous aquifer. For the homogeneous aquifer, the solution is symmetrical about the y- and z-axes, therefore, simulating a quarter of the source is appropriate. Due to the relatively large utilization rates and especially the large microbial yields, a time step of 0.01 days has to be applied initially. After a simulation time of about 10 days, the microbial population grew well above the initial concentration of 0.003 mg/L, reaching peak concentrations of more than 7 mg/L. At this point the time step was increased to 0.02 days. A further increase to 0.05 days after about 50 days simulation time and again to 0.1 days after about 100 days of simulation time was allowed. The small time steps in the beginning of the simulations are required to avoid numerical oscillations when the growth of the microbial population is exponential in the presence of high substrate and oxygen concentrations. Later, when oxygen is depleted in the centre of the plumes and the different substrate plumes start to separate, the time step can be relaxed.

A full scale simulation (homogeneous medium [quarter source] with 64 x 33 x 25 [= 52800] elements, four substrates, oxygen and the microbial population over 7760 time steps) up to 476 days requires a CPU time on the order of 4 days on a Pentium II (333 MHz). For the heterogeneous runs, dependent on the random hydraulic conductivity field chosen, an increase of up to 25% in CPU time was experienced. This increase arises from the larger number of iterations required to obtain the solution.

In order to keep computational costs manageable, only one full source heterogeneous run was performed. In addition, five different heterogeneous simulations with a quarter source were run to investigate the variability of the outcome based on different hydraulic conductivity fields with the same statistical parameters. Examples of simulated plan view benzene and m-xylene plumes using a homogeneous aquifer in comparison to the field derived contour lines are presented in Figures 4.7 and 4.8. The benzene field plume advances slightly faster than the simulated plume (Figure 4.7), however, the plume shapes are similar. The speed of the simulated

m-xylene plume mirrors very well the field plume behaviour (Figure 4.8). At Day 476, a small amount of m-xylene mass is still remaining in the simulated plume, although no m-xylene was measured in the field at this time. The reason for this discrepancy could be that the model underpredicts the field degradation but it is also possible that such a small mass of m-xylene was missed by the sampling network. For a more detailed analysis, the simulated mass losses (zeroth moments), centres of mass (first moments) and variances of the concentration distributions (second moment) for benzene and m-xylene for all seven cases in comparison to the measured field moments are presented in Figures 4.9 to 4.18.

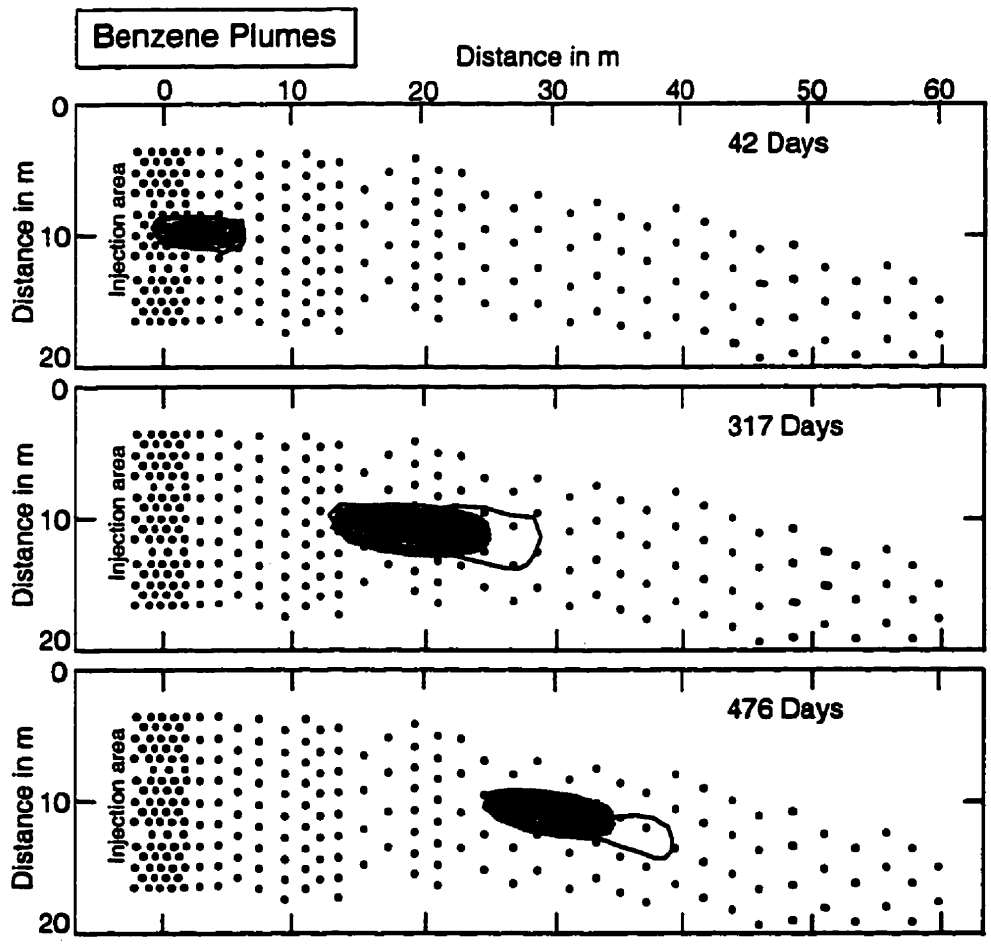

Figure 4.7. Field measured (solid lines) and simulated (shaded areas) benzene plumes applying a homogeneous medium in plan view using peak concentrations. Values of the contour lines are in 0.1 and 1.0 mg/L for 42 days and 0.1 mg/L for 317 and 476 days. The black dots represent the locations of the multi-level piezometers with 14 sampling points vertically.

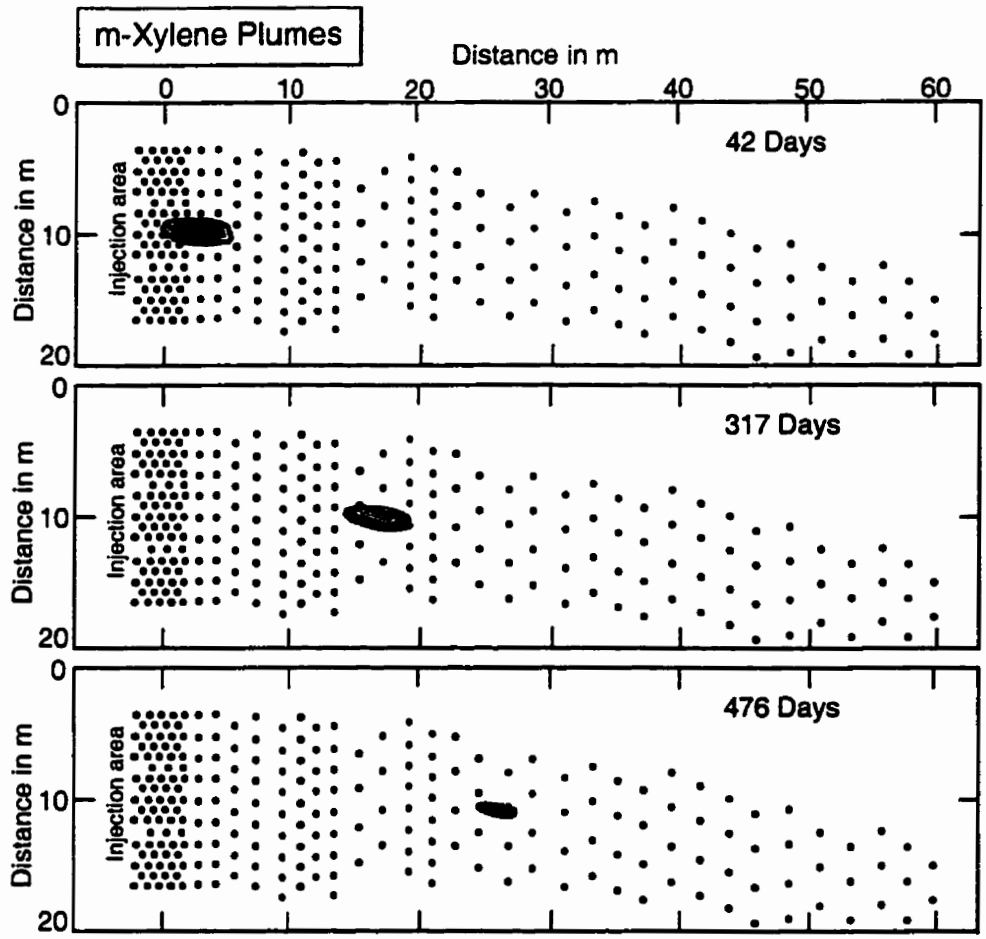

Figure 4.8. Field measured (solid lines) and simulated (shaded areas) m-xylene plumes applying a homogeneous medium in plan view using peak concentrations. Values of the contour lines are in 0.1 and 1.0 mg/L for 42 days and 0.1 mg/L for 317 and 476 days. The black dots represent the locations of the multi-level piezometers with 14 sampling points vertically.

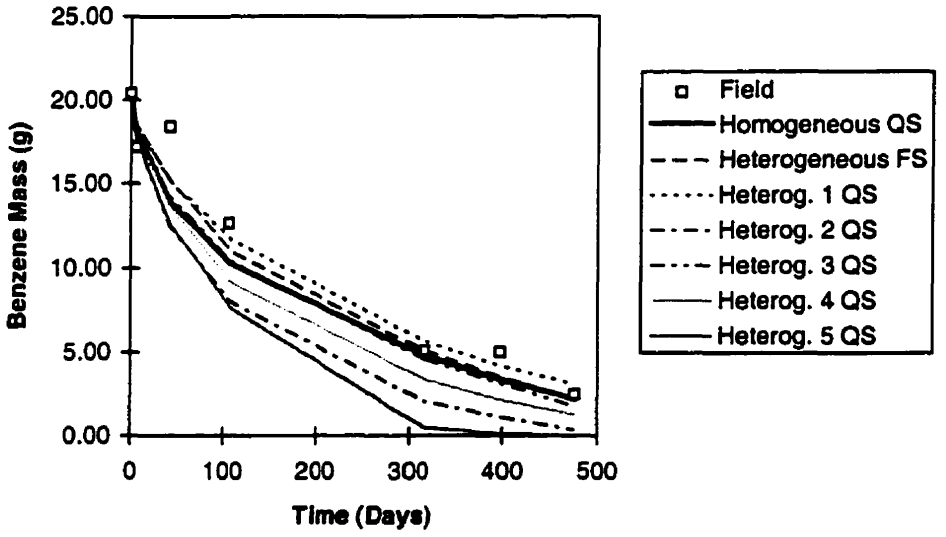

Figure 4.9. Benzene mass loss as measured in the field compared to simulated results using BIO3D by applying base-case parameters to a homogeneous aquifer (QS - quarter source simulated), a heterogeneous aquifer (FS - full source simulated) and five additional heterogeneous aquifers (QS - quarter source simulated). All heterogeneous aquifers were generated using the same statistical parameters.

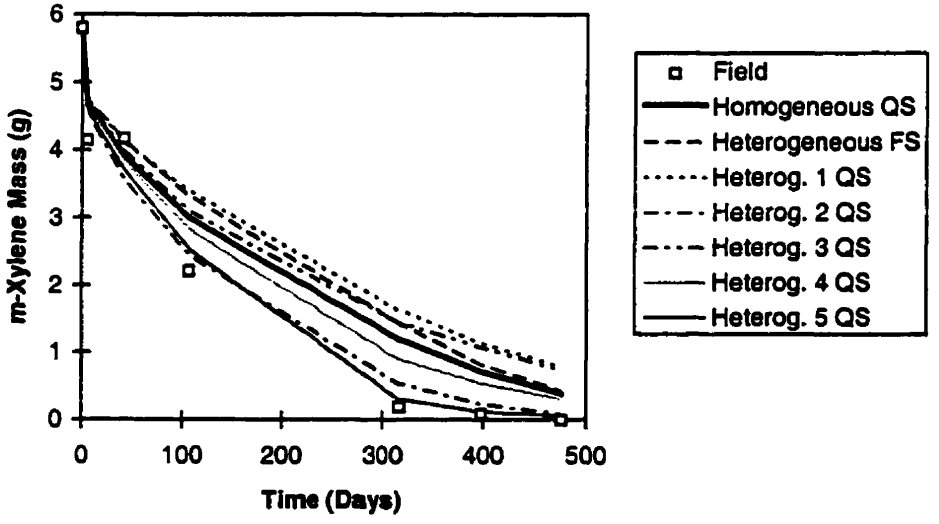

Figure 4.10. M-xylene mass loss as measured in the field compared to simulated results using BIO3D by applying base-case parameters to a homogeneous aquifer (QS - quarter source simulated), a heterogeneous aquifer (FS - full source simulated) and five additional heterogeneous aquifers (QS - quarter source simulated). All heterogeneous aquifers were generated using the same statistical parameters.

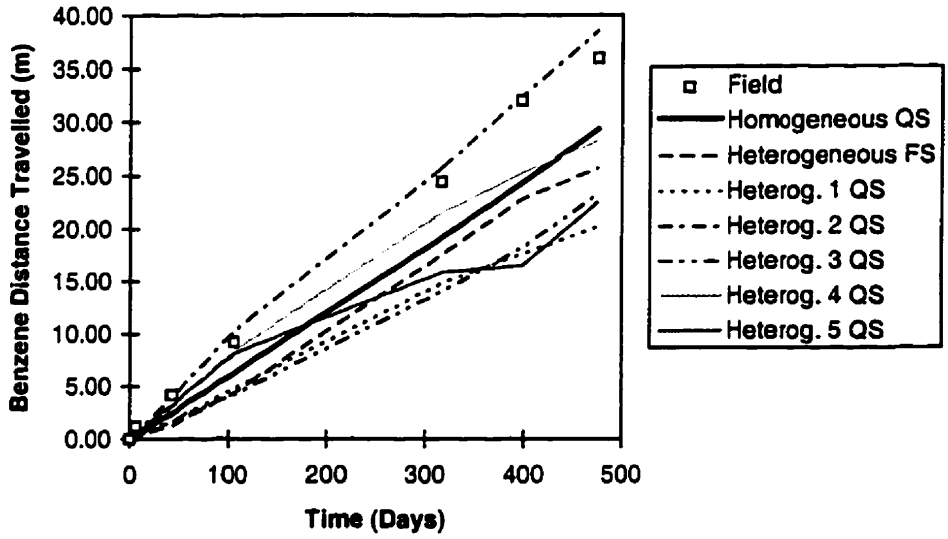

Figure 4.11. Benzene centre of mass as measured in the field compared to simulated results using BIO3D by applying base-case parameters to a homogeneous aquifer (QS - quarter source simulated), a heterogeneous aquifer (FS - full source simulated) and five additional heterogeneous aquifers (QS - quarter source simulated). All heterogeneous aquifers were generated using the same statistical parameters.

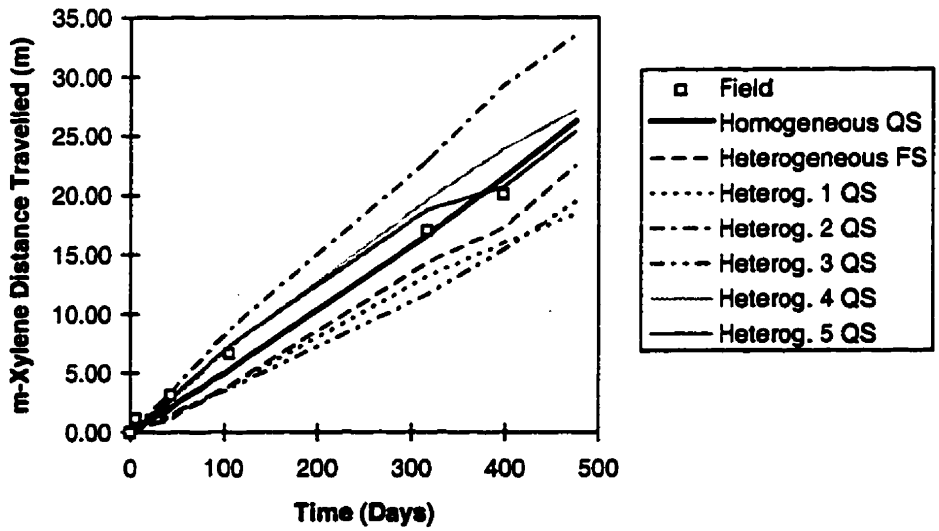

Figure 4.12. M-xylene centre of mass as measured in the field compared to simulated results using BIO3D by applying base-case parameters to a homogeneous aquifer (QS - quarter source simulated), a heterogeneous aquifer (FS - full source simulated) and five additional heterogeneous aquifers (QS - quarter source simulated). All heterogeneous aquifers were generated using the same statistical parameters.

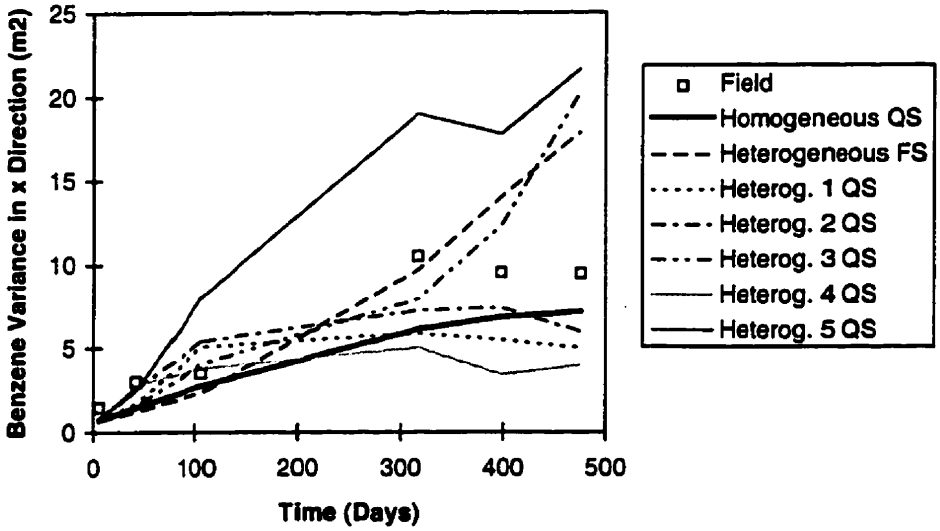

Figure 4.13. Benzene variance of concentration distribution in flow direction as measured in the field compared to simulated results using BIO3D by applying base-case parameters to a homogeneous aquifer (QS - quarter source simulated), a heterogeneous aquifer (FS - full source simulated) and five additional heterogeneous aquifers (QS - quarter source simulated). All heterogeneous aquifers were generated using the same statistical parameters.

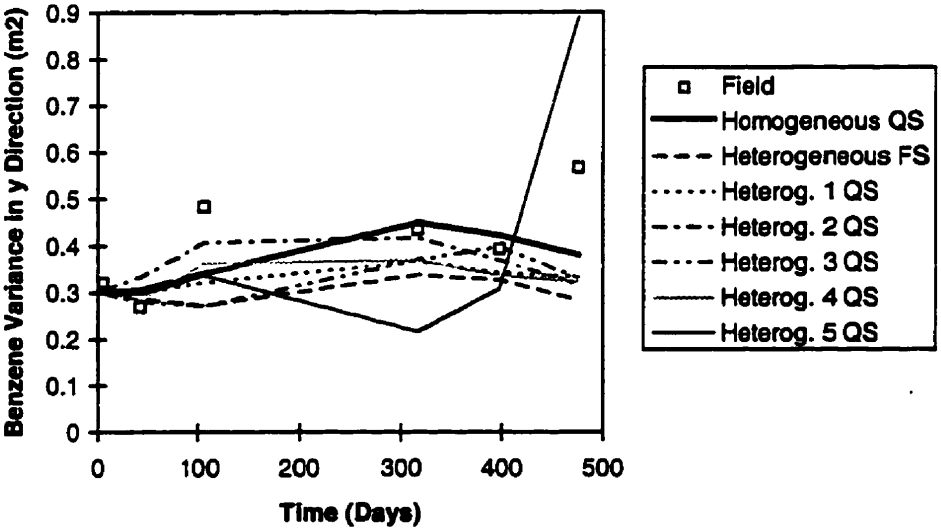

Figure 4.14. Benzene variance of concentration distribution in transverse-horizontal direction to flow as measured in the field compared to simulated results using BIO3D by applying base-case parameters to a homogeneous aquifer (QS - quarter source simulated), a heterogeneous aquifer (FS - full source simulated) and five additional heterogeneous aquifers (QS - quarter source simulated). All heterogeneous aquifers were generated using the same statistical parameters.

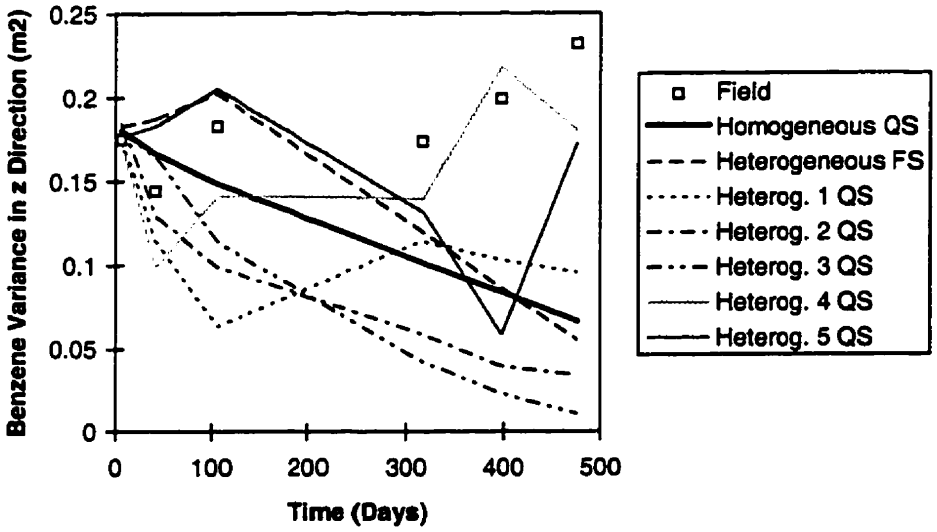

Figure 4.15. Benzene variance of concentration distribution in vertical direction to flow as measured in the field compared to simulated results using BIO3D by applying base-case parameters to a homogeneous aquifer (QS - quarter source simulated), a heterogeneous aquifer (FS - full source simulated) and five additional heterogeneous aquifers (QS - quarter source simulated). All heterogeneous aquifers were generated using the same statistical parameters.

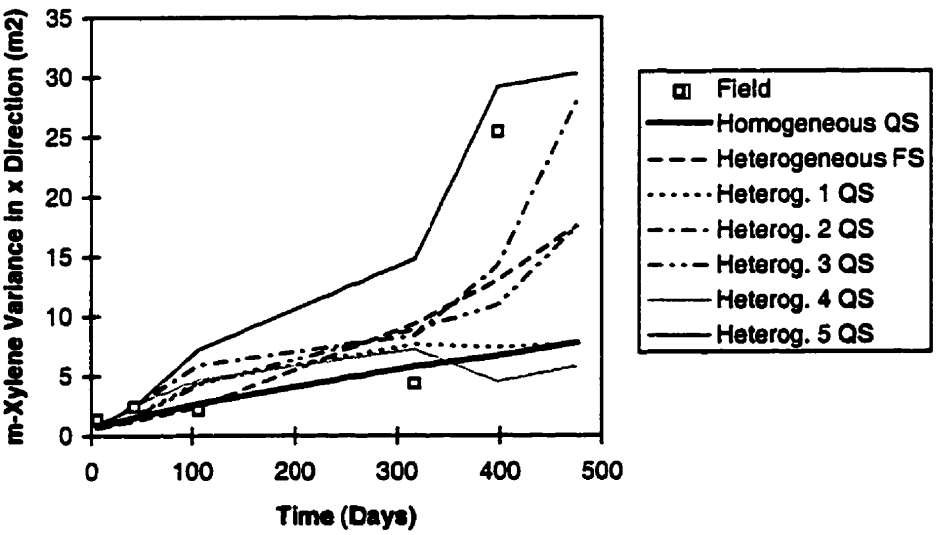

Figure 4.16. M-xylene variance of concentration distribution in flow direction as measured in the field compared to simulated results using BIO3D by applying base-case parameters to a homogeneous aquifer (QS - quarter source simulated), a heterogeneous aquifer (FS - full source simulated) and five additional heterogeneous aquifers (QS - quarter source simulated). All heterogeneous aquifers were generated using the same statistical parameters.

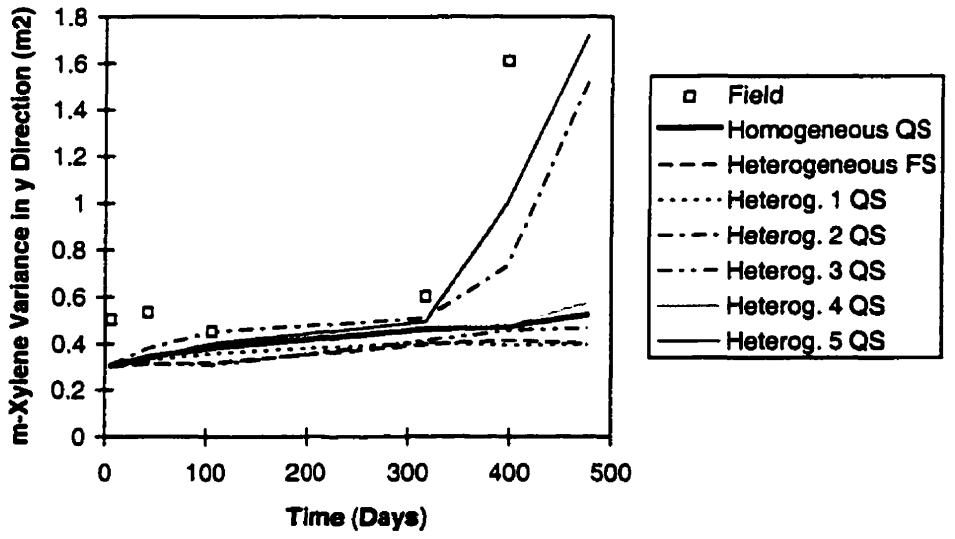

Figure 4.17. M-xylene variance of concentration distribution in transverse-horizontal direction to flow as measured in the field compared to simulated results using BIO3D by applying base-case parameters to a homogeneous aquifer (QS - quarter source simulated), a heterogeneous aquifer (FS - full source simulated) and five additional heterogeneous aquifers (QS - quarter source simulated). All heterogeneous aquifers were generated using the same statistical parameters.

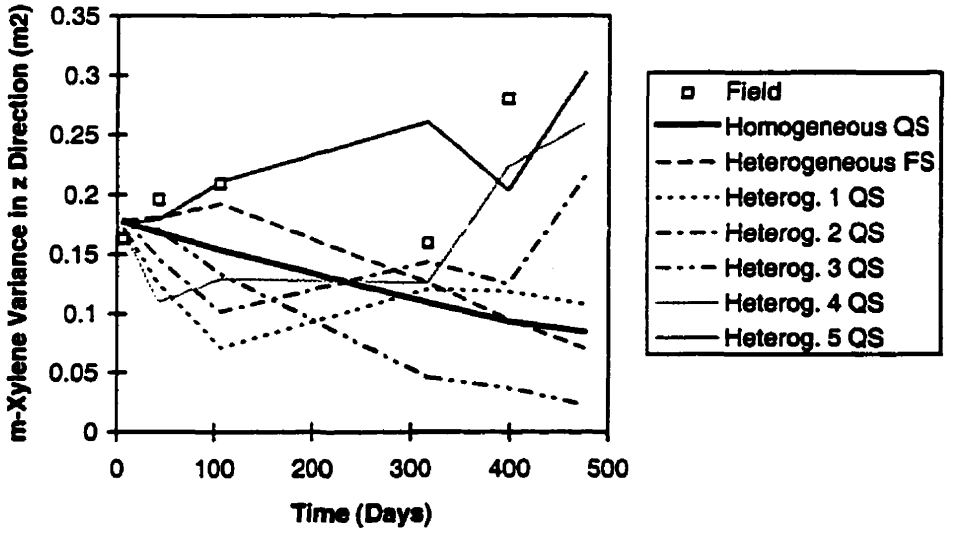

Figure 4.18. M-xylene variance of concentration distribution in vertical direction to flow as measured in the field compared to simulated results using BIO3D by applying base-case parameters to a homogeneous aquifer (QS - quarter source simulated), a heterogeneous aquifer (FS - full source simulated) and five additional heterogeneous aquifers (QS - quarter source simulated). All heterogeneous aquifers were generated using the same statistical parameters.

For all simulations presented in Figures 4.9 to 4.18, the same base-case input parameters were used as described above. Considering that all input parameters were either measured in the field or the laboratory or were derived from literature values and no calibration was attempted, the simulated and experimental results are in good agreement.

The difference in benzene and m-xylene mass decline (Figure 4.9 and 4.10) for the different hydraulic fields used to simulate the degradation process is quite significant, indicating that the flow field has a pronounced influence on the degradation behaviour even in this moderately heterogeneous aquifer. As expected, the majority of the heterogeneous flow fields yield a larger substrate mass loss due to the higher degree of mixing between the substrates and the oxygen introduced by the heterogeneity. However, because the modelling approach using a quarter source for a heterogeneous simulation is not rigorous from the statistical point of view, these simulations are presented for comparison only. Nevertheless, the simulation results indicate that different heterogeneous fields might produce significantly different degradation curves.

The full source heterogeneous run required about 20 days of CPU time on a Pentium II (333 MHz) in comparison to only about 4 days simulation time for the homogeneous run. The results in terms of moments between these two simulations are similar (Figures 4.9 to 4.18) and only the second moments in the longitudinal direction for both substrates show a larger discrepancy (Figures 4.13 and 4.16). It is expected that a different realization of a full source random hydraulic conductivity field would yield slightly different results as is seen from the quarter source heterogeneous runs.

The centres of mass simulated for benzene (Figure 4.11) in general underpredict the advancement of the plume. This is due to the relatively large retardation factor of 1.5 used in the simulations that was calculated from laboratory batch experiments (Hubbard et al., 1994). Hubbard et al. (1994) also point out that a retardation factor of about 1.2, as previously measured in the Borden aquifer by Patrick et al. (1986) and Berry-Spark et al. (1987), is a better representation of the field conditions. However, in order to be consistent in the simulation approach, the same lab derived retardation factors were used throughout the data analysis and numerical simulations. The first moment analysis for m-xylene, on the other hand, shows a good

agreement between the field-measured and simulated results (Figure 4.12), implying that at least for m-xylene equilibrium, laboratory sorption data can adequately describe field retardation behaviour at Borden.

The second moments in the longitudinal and transverse-horizontal directions of flow for benzene and m-xylene compare well with the simulated results (Figures 4.13, 4.14, 4.16 and 4.17). However, the field-measured variances in the vertical direction are somewhat larger than the average of the simulated variances (Figures 4.15 and 4.18). (The very high variance values for m-xylene at Day 398 (Figures 4.16 to 4.18) result from a very small mass remaining that is distributed in two separated slugs). The apparent difference between the measured and simulated variances in vertical direction might be a sampling artifact due to the sample spacing of 20 cm.

It is interesting to note that, with a few exceptions, the calculated and field derived variances in the transverse-horizontal and vertical directions are relatively constant (Figures 4.14, 4.15., 4.17 and 4.18). This implies that the spreading of the plumes due to dispersion is compensated by the shrinking of the plumes due to biodegradation.

Because one full source heterogeneous simulation requires 20 days of CPU time, it is not practical from the computational point of view to perform a sensitivity analysis using this approach. On the other hand, a quarter source heterogeneous run is not a statistically rigorous solution and considering that the homogeneous simulation results fall within the results of the different heterogeneous simulations, it was therefore decided to perform the sensitivity analyses using a homogeneous, isotropic aquifer. For this case, the modelling domain is symmetric about the transverse horizontal and vertical axis of flow and only a quarter of the domain needs to be solved.

4.10.2. Sensitivity Analysis

An extensive analysis was performed to investigate the sensitivity of the most uncertain or, due to lack of information, assumed input parameters and to define the key controlling factors at the field scale. In order to determine the influence of the uncertain Monod kinetic parameters applied to the two lumped compounds "TEX" and "other constituents", a sensitivity analysis was performed by varying the maximum utilization rate k_{max}. Because k_{max} and K_S are highly correlated (Chapter 1), it is not necessary to vary both parameters. In the case of TEX, $k_{max\ 3}$ values of 2.0 and 8.0 day^{-1} were applied in comparison to the base case $k_{max\ 3}$ of 4.0 day^{-1}. For the other constituents, a much larger $k_{max\ 4}$ of 1.0 day^{-1} was applied in comparison to the base case $k_{max\ 4}$ of 0.2 day^{-1}. Each of these three sensitivity analyses showed only a small influence on the mass loss curves of benzene and m-xylene, with a maximum difference of less than 7% with respect to the base case (results not shown). Furthermore, a run was performed introducing Haldane inhibition concentrations for the TEX compounds and the other constituents with $K_{I\ 3}$ = $K_{I\ 4}$ = 93.0 mg/L, an approximate average of the benzene and m-xylene K_I values. Essentially identical degradation curves were observed for benzene and m-xylene with respect to the base-case simulation implying that the K_I values for TEX and the other constituents ($K_{I\ 3}$ and $K_{I\ 4}$) have no significant influence on the modelling results of benzene and m-xylene and can be neglected under the experimental field conditions.

The microbial decay coefficient, b, and the microbial yield of the other constituents, Y_4, are also uncertain input parameters. Three different sensitivity analyses were carried out by increasing b to 0.01 day^{-1} (e.g., Essaid et al., 1995) and applying $Y_4 = 0$ (no microbial growth on the substrate) and $Y_4 = 0.5$, respectively. As for the previous input parameters, no significant difference was observed for the benzene and m-xylene degradation curves with respect to the base case.

The sensitivity analyses presented above aimed to define the influence of the most uncertain input parameters. Within the boundaries of the chosen values, none of those input parameters had a significant influence on the results of benzene and m-xylene. This indicates that the base case parameters are a reasonable representation of the field results and subsequent

sensitivity analyses can be used to identify the key controlling parameters influencing the benzene and m-xylene degradation process.

The flow field was already identified as one of the key controlling factors (Section 4.10.1). It is to be expected that the available oxygen will have an important influence on the degradation process. In the following, the source and background oxygen were changed separately to investigate the effect with respect to the base case benzene and m-xylene mass loss. The source oxygen was set to zero (low source oxygen case) and doubled to 5.1 mg/L (high source oxygen case) compared to the base case of 2.55 mg/L as reported by Hubbard et al. (1994). As can be seen in Figures 4.19 and 4.20, the source oxygen has only a minor influence on the benzene mass decline (Figure 4.19) but influences the m-xylene mass loss quite significantly (Figure 4.20). The reason for the difference between the two compounds is related to the overall mass, which is significantly smaller in the case of m-xylene, and due to the higher degradation rate of m-xylene, which requires a larger percentage of the initially available oxygen. Once oxygen is depleted in the source zone, biodegradation of all compounds relies on mixing of oxygen at the plume edges and therefore, the difference between the three simulated cases decreases.

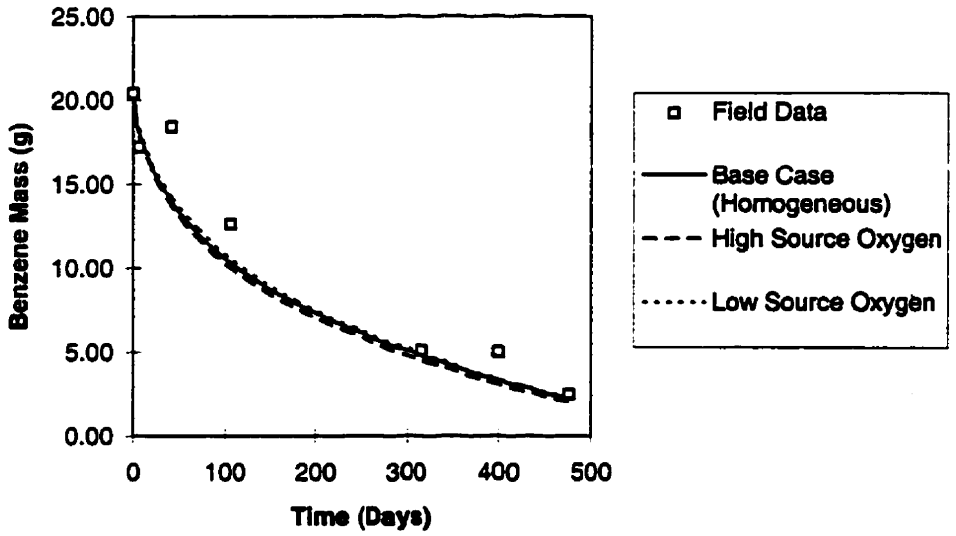

Figure 4.19. Sensitivity of source oxygen content on benzene mass loss. Compared are field mass loss data to simulated base-case results of 2.55 mg/L, a high of 5.1 mg/L and a low of 0.0 mg/L source oxygen.

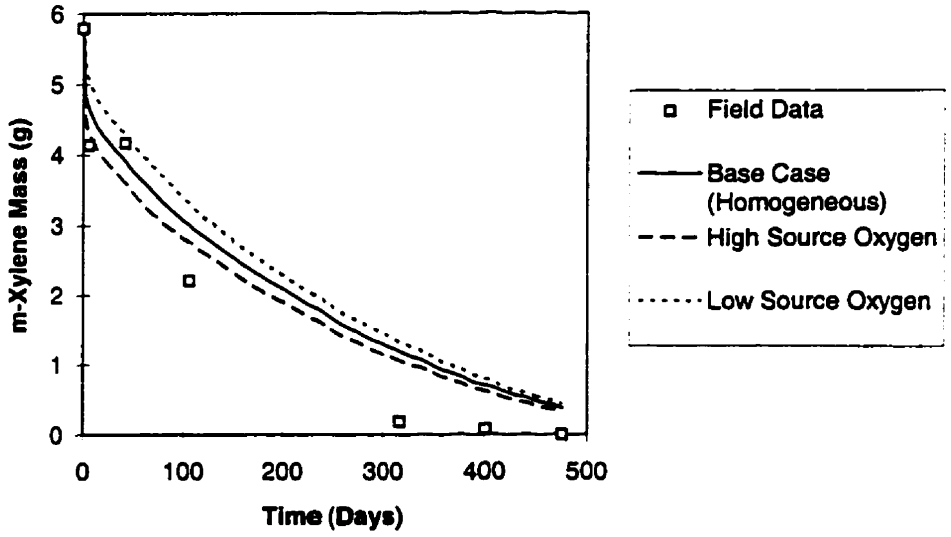

Figure 4.20. Sensitivity of source oxygen content on m-xylene mass loss. Compared are field mass loss data to simulated base-case results of 2.55 mg/L, a high of 5.1 mg/L and a low of 0.0 mg/L source oxygen.

For the base case scenario, an oxygen concentration of 3 mg/L was estimated for the horizontal plane through the centre line of the plumes, with linearly increasing concentrations to 4.5 mg/L oxygen for the horizontal planes 0.5 m below and 0.5 m above the centreline plane. Outside this zone of variable background oxygen, a constant oxygen background concentration of 4.5 mg/L was assumed. To test the influence of the background oxygen, a sensitivity analysis was performed by decreasing the oxygen concentrations by half (1.5 to 2.25 mg/L centre plane to 0.5 m above and below centre plane and 2.25 mg/L elsewhere as low-background-oxygen case) and doubling them (6.0 to 9.0 mg/L centre plane to 0.5 m above and below centre plane and 9.0 mg/L elsewhere as high-oxygen-background case). The difference between the three simulated cases is significant (Figures 4.21 and 4.22) indicating that the available background oxygen has a large influence on the degradation process. This implies that it is crucial to measure oxygen or, in a broader sense, the electron acceptor concentrations and distributions to accurately estimate the biodegradation potential of aquifers.

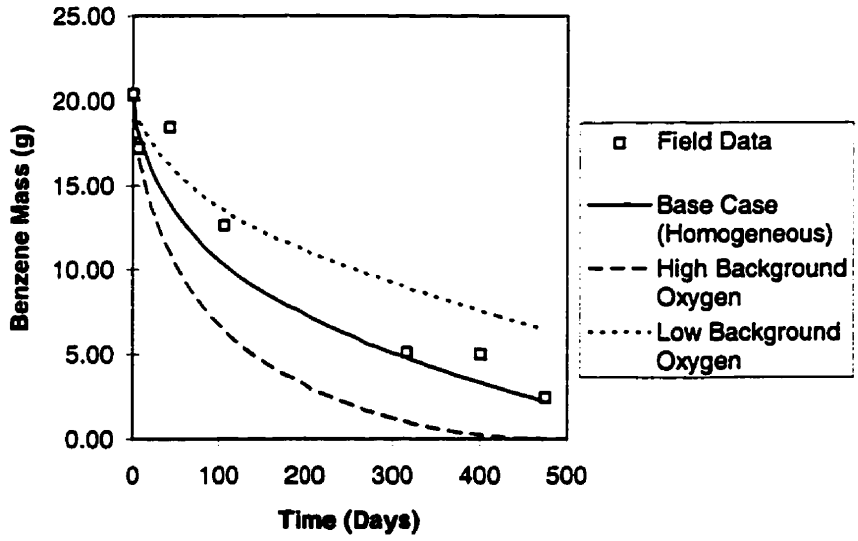

Figure 4.21. Sensitivity of background oxygen content on benzene mass loss. Compared are field mass loss data to simulated base-case results, a high and a low background oxygen content (see text for concentrations used).

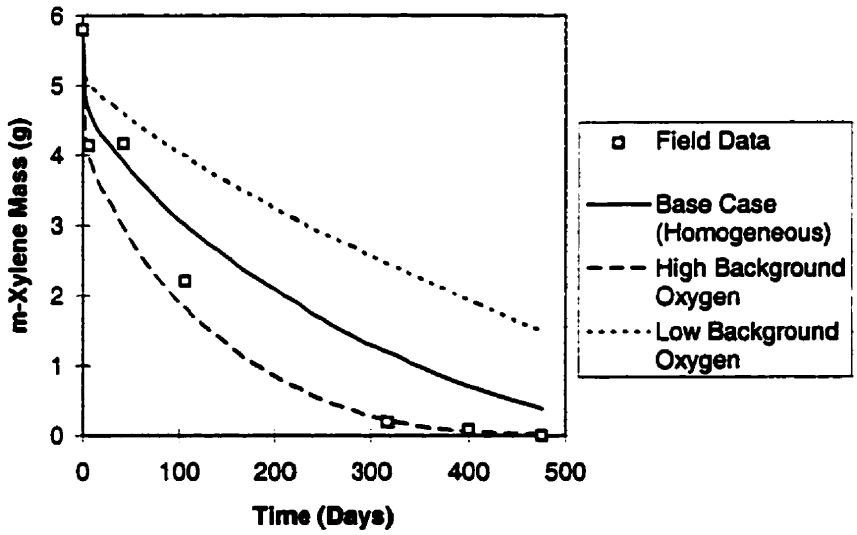

Figure 4.22. Sensitivity of background oxygen content on m-xylene mass loss. Compared are field mass loss data to simulated base-case results, a high and a low background oxygen content (see text for concentrations used).

Let us now investigate the influence of the Monod kinetic parameters on the degradation curves of benzene and m-xylene. As shown in Chapter 1, the Monod parameters are highly

correlated, therefore, it is sufficient to change only one parameter in order to investigate the significance of the overall Monod kinetics. Values of 0.78 and 3.12 day^{-1} for the benzene $k_{max\ 1}$ were applied in comparison to the base case $k_{max\ 1}$ of 1.56 day^{-1}. Although the difference between the three simulated cases is significant for benzene itself (Figure 4.23), it has only a minor influence on the m-xylene degradation behaviour, this influence even decreases with simulation time as the two compounds separate spatially (Figure 4.24).

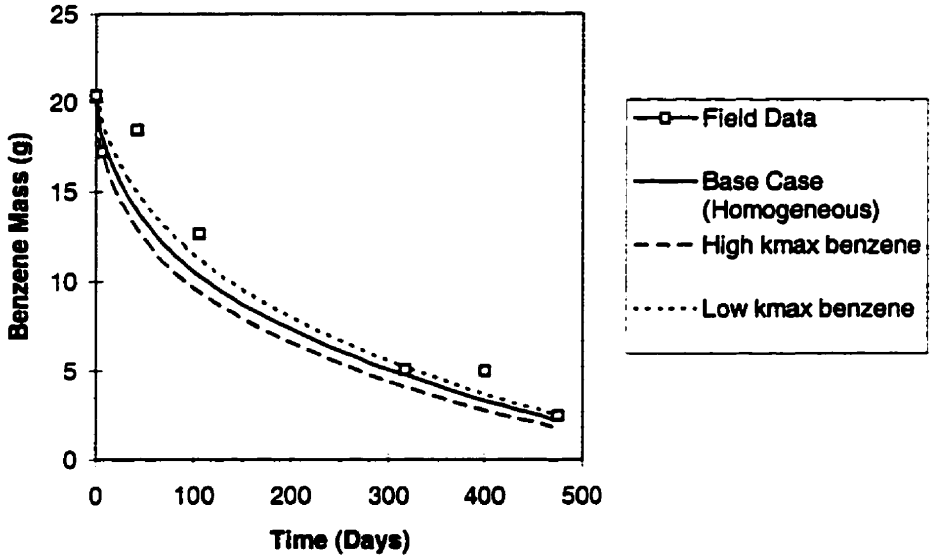

Figure 4.23. Sensitivity of the maximum utilization rate ($k_{max\ 1}$) of benzene on the simulated benzene mass loss. Compared are field mass loss data to simulated base-case results ($k_{max\ 1}$ = 1.56 day^{-1}), a high ($k_{max\ 1}$ = 3.12 day^{-1}) and a low ($k_{max\ 1}$ = 0.78 day^{-1}) maximum utilization rate.

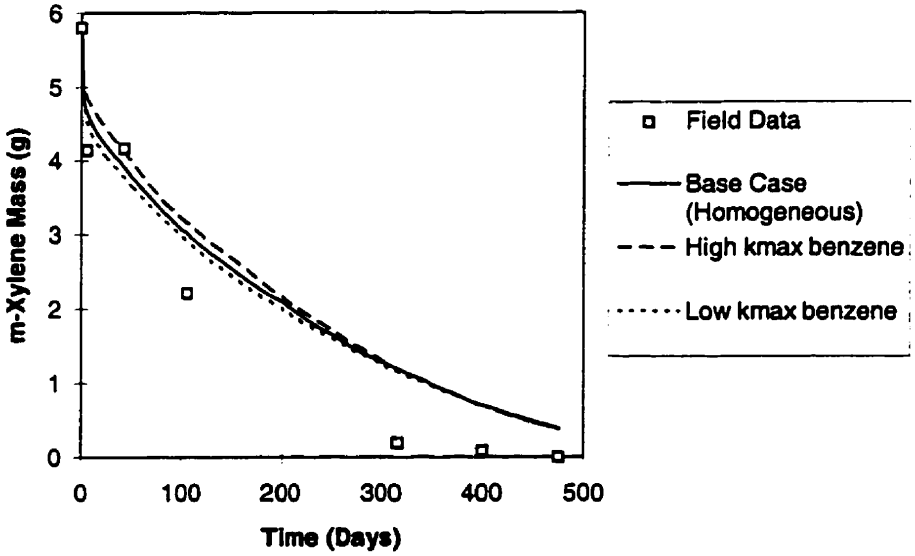

Figure 4.24. Sensitivity of the maximum utilization rate ($k_{max\ 1}$) of benzene on the simulated m-xylene mass loss. Compared are field mass loss data to simulated base-case results ($k_{max\ 1} = 1.56\ day^{-1}$), a high ($k_{max\ 1} = 3.12\ day^{-1}$) and a low ($k_{max\ 1} = 0.78\ day^{-1}$) maximum utilization rate.

Furthermore, values of 2.065 and 8.26 day^{-1} for the m-xylene $k_{max\ 2}$ were applied in comparison to the base case $k_{max\ 2}$ of 4.13 day^{-1}. The difference between the simulated degradation curves of benzene is very small implying that the m-xylene degradation rate has, due to the small m-xylene mass, only a minor influence on the benzene degradation behaviour (Figure 4.25). On the other hand, the difference between the three simulated cases is significant for m-xylene itself (Figure 4.26). The largest difference can be seen at early time when source oxygen is still available. Later on, when the degradation process is controlled by the mixing of oxygen at the edges of the plume, the difference decreases.

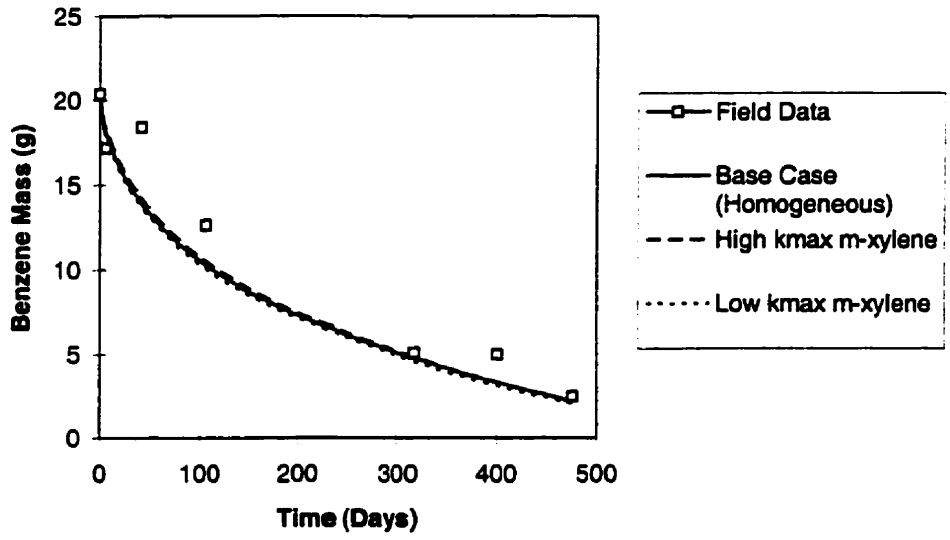

Figure 4.25. Sensitivity of the maximum utilization rate ($k_{max\ 2}$) of m-xylene on the simulated benzene mass loss. Compared are field mass loss data to simulated base-case results ($k_{max\ 2} = 4.13\ day^{-1}$), a high ($k_{max\ 2} = 8.26\ day^{-1}$) and a low ($k_{max\ 2} = 2.065\ day^{-1}$) maximum utilization rate.

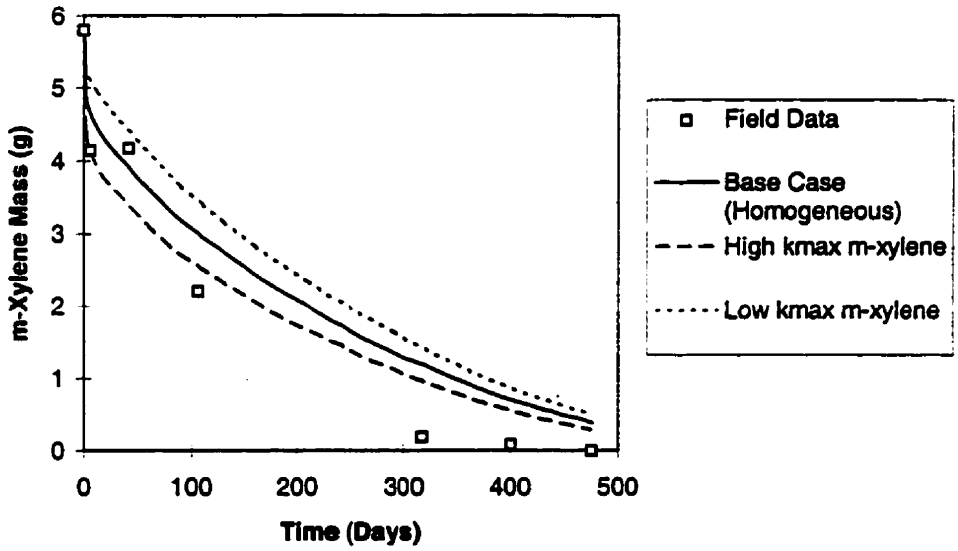

Figure 4.26. Sensitivity of the maximum utilization rate ($k_{max\ 2}$) of m-xylene on the simulated m-xylene mass loss. Compared are field mass loss data to simulated base-case results ($k_{max\ 2} = 4.13\ day^{-1}$), a high ($k_{max\ 2} = 8.26\ day^{-1}$) and a low ($k_{max\ 2} = 2.065\ day^{-1}$) maximum utilization rate.

As presented above, the Monod kinetic parameters from the other two lumped compounds (TEX and other constituents) also do not have a large influence on the benzene and

m-xylene degradation behaviour, therefore, it can be concluded that the kinetic degradation parameters have a smaller overall influence on the field-degradation process than the flow field and the background electron acceptor concentrations.

Additional sensitivity analyses were performed by a) neglecting the lumped compound "other constituents" and b) neglecting the two lumped compounds "TEX" and "other constituents" in the simulations. In case a, where only benzene, m-xylene and TEX were considered, the resulting degradation curves are similar to the base case. This is expected due to the relatively small degradation rate and therefore small oxygen demand of the other constituents. In case b, where only benzene and m-xylene are considered to move through the aquifer, results are obtained that are close to the high-background-oxygen case. This result is expected as well because all the oxygen is available for benzene and m-xylene degradation in this simulation scenario; whereas under the experimental conditions in the field, other substrates were present. This, furthermore, implies that it is important to simulate all potentially degradable compounds present in order not to overpredict the available oxygen.

Finally, a sensitivity analysis was performed on the influence of the initial microbial population. As measured in the laboratory (Chapter 1), the base case microbial concentration in the field was assumed to be 0.003 mg/L. This concentration was changed by an order of magnitude to 0.0003 and 0.03 mg/L to investigate the effect. Except for very early time, no significant difference was obtained for the benzene and m-xylene degradation curves by applying these different initial microbial concentrations.

4.10.3. Comparison of Monod Kinetic Parameters to Zero- and First-order Degradation Rates

It is a common belief that laboratory-derived degradation rates often greatly overpredict mass loss at the field scale because the conditions at the lab scale are usually optimized. Let us now investigate how different rates calculated at the laboratory scale compare to the field scale degradation of benzene as observed by Hubbard et al. (1994). Figure 4.27 shows an example of measured batch data with an initial benzene concentration close to the initial concentration of the field experiment (Hubbard et al., 1994; Table 4.2). The results of this lab experiment were used,

along with four additional initial benzene concentrations, to derive the intrinsic Monod parameters taking microbial growth into account (Appendix A). The resulting parameters are presented in Table 4.2. As described in detail in Appendix A, the apparent lag time of degradation up to about 3 days in the experiment is due to the low initial microbial concentration and can be simulated adequately using the Monod equation by considering microbial growth.

Because it is common practice to calculate zero- and first-order degradation rates from batch experiments, a zero- and a first-order rate were calculated using the lab data presented in Figure 4.27. The best-fit zero-order rate is 3 mg L^{-1} day^{-1}, whereas the best-fit first-order rate is 0.8 day^{-1} assuming a lag time of 3 days during which no degradation occurs.

Applying the calculated laboratory zero- and first-order degradation rates to the field experiment greatly overpredicts the observed field mass loss (Figure 4.28). After 5 and 40 days, respectively, virtually all the benzene is degraded by applying the laboratory zero- and first-order rates to the field scale. On the other hand, the Monod-type degradation rates yield reasonable predictions of the declining benzene mass during the experiment (Figure 4.28).

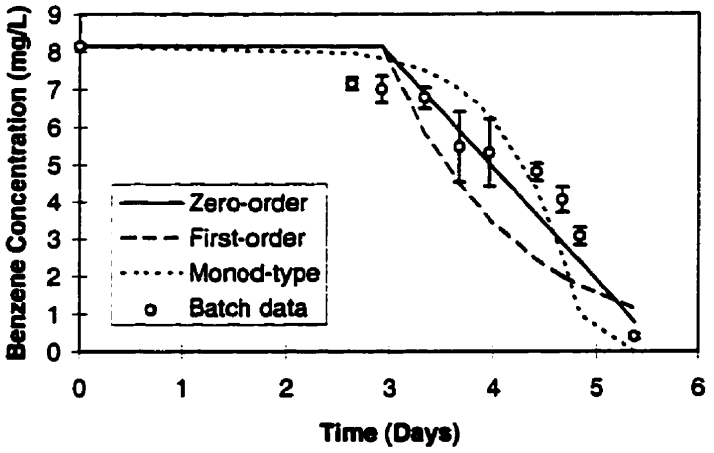

Figure 4.27. Measured benzene biodegradation curve (symbols with error bars of one standard deviation) compared to the best-fit zero-order degradation rate of 3 mg L^{-1} day^{-1}, the best-fit first-order degradation rate of 0.8 day^{-1} and the calibrated Monod parameters k_{max} of 1.56 day^{-1}, K_S of 0.0 mg L^{-1} and K_I of 95.0 mg L^{-1}. A lag time of 3 days is applied to the zero- and first-order degradation rates during which no degradation is occurring.

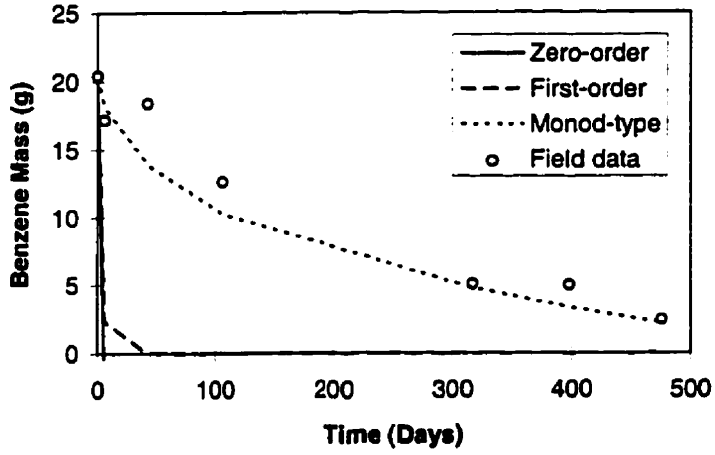

Figure 4.28. Field measurements of benzene mass decline in comparison to calculated mass loss curves using a zero-order degradation rate of 3 mg L^{-1} day^{-1}, a first-order degradation rate of 0.8 day^{-1}, and Monod degradation parameters k_{max} of 1.56 day^{-1}, K_S of 0.0 mg L^{-1} and K_I of 95.0 mg L^{-1}. A lag time of 3 days is applied to the zero- and first-order degradation rates during which no degradation is occurring.

4.11. CONCLUSION

The numerical model BIO3D was applied to simulate biodegradation of multiple organic substrates and use of an electron acceptor by an attached microbial population. The numerical model incorporates groundwater transport and biodegradation interactions in terms of competition for the available electron acceptor (oxygen). The model was used to simulate experimental results at the field scale by using laboratory-derived kinetic degradation parameters. All additional input parameters for the simulations were calculated prior to the simulations using measured lab and field parameters and literature values. An extensive sensitivity analysis was performed for the most uncertain parameters.

It was demonstrated that the laboratory-derived Monod degradation parameters describe the field-measured degradation processes reasonably well. Under the field conditions modelled and the assumptions made for the simulations, it can be concluded that laboratory-derived Monod degradation parameters can describe field-scale degradation processes if all the controlling factors are incorporated in the field-scale modelling that are not observed at the

laboratory scale. In this way, there are no scale relationships to be found that link the laboratory and the field scale; accurately incorporating the additional processes, phenomena and characteristics at the larger scale and applying well defined lab scale parameters should accurately describe field scale processes. On the other hand, if simplified zero- or first-order degradation rates, calculated at the lab scale, are applied to field scale simulations, they might greatly overpredict the remediation potential of the aquifer.

The sensitivity analysis showed that the laboratory-derived Monod kinetic parameters are less sensitive to the simulated mass loss curves than the random heterogeneous flow field chosen and the background oxygen concentrations. It can be concluded that, for the dissolved gasoline experiment simulated, the flow field and the available oxygen are the key controlling factors of the BTEX biodegradation process at the field scale.

4.12. ACKNOWLEDGMENTS

This research was partially funded through a grant of the Natural Science and Engineering Research Council of Canada to J. F. Barker, E. O. Frind and B. J. Butler and the American Petroleum Institute, Health and Environmental Sciences Department. I thank Tina Hubbard for many helpful discussions and for generously providing the field data. Special thanks to John Molson for all his help in further developing the numerical code BIO3D. I thank Jos Beckers for providing the numerical routine to perform the moment analyses for the field data. I also would like to thank Ed Sudicky for many helpful discussions and valuable insights.

4.13. REFERENCES

Acton, D. W. and Barker, J. F. 1992. In situ biodegradation potential of aromatic hydrocarbons in anaerobic groundwaters. Journal of Contaminant Hydrology, 9, 325-352.

Alvarez, P. J. J. and Vogel, T. M. 1991. Substrate interactions of benzene, toluene and para-xylene during microbial degradation by pure cultures and mixed culture aquifer slurries. Appl. Environ. Microbiol., 57(10), 2981-2985.

American Petroleum Institute. 1995. In Geotrans (Ed.), API Biodegradation Modeling Workshop: Comparative Evaluation of Groundwater Biodegradation Models, May 08-09, 1995, Worthington Hotel, Fort Worth, Texas.

Andrews, J. F. 1968. A mathematical model for the continuous culture of microorganisms utilizing inhibitory substrates. Biotechnol. Bioeng., 10, 707-723.

Barker, J. F., Patrick, G. C. and Major, D. 1987. Natural attenuation of aromatic hydrocarbons in shallow sand aquifer. Ground Water Monitoring Review., 7(1), 64-71.

Barker, J. F., Sudicky, E. A., Mayfield, C. I. and Gillham, R. W. 1989. Petroleum hydrocarbon contamination of groundwater: natural fate and in situ remediation - a summary report. Pace Report No. 89-5. Petroleum Association for Conservation of the Canadian Environment.

Baveye, P. and Valocchi, A. 1989. An evaluation of mathematical models of the transport of biologically reacting solutes in saturated soils and aquifers. Water Resources Research, 25(6), 1413-1421.

Bear, J. 1988. Dynamics of fluids in porous media (Reprint ed.). Mineola, NY: Dover Publications, Inc.

Berry-Spark, K. L., Barker, J. F., MacQuarrie, K. T., Major, D., Mayfield, C. I. and Sudicky, E. A. 1987. The behavior of soluble petroleum-derived hydrocarbons in groundwater. Petroleum Association for the Conservation of the Canadian Environment. PACE Phase III Report No. 85-3.

Borden, R. C. and Bedient, P. B. 1986. Transport of dissolved hydrocarbons influenced by oxygen-limited biodegradation - 1. Theoretical development. Water Resources Research, 22(13), 1973-1982.

Borden, R. C., Bedient, P. B., Lee, M. D., Ward, C. H. and Wilson, J. T. 1986. Transport of dissolved hydrocarbons influenced by oxygen-limited biodegradation - 2. Field application. Water Resources Research, 22(13), 1983-1990.

Brookman, G. T., Flanagan, M. and Kebe, J. O. 1985. Laboratory studies on solubilities of petroleum hydrocarbons in groundwater. American Petroleum Institute. API Publication 4395, Washington, D.C.

Burnett, R. D. and Frind, E. O. 1987. Simulation of contaminant transport in three dimensions: 2. Dimensionality effects. Water Resources Research, 23(4), 695-705, 1987.

Butler, B. J., Vandergriendt, M. and Barker, J. F. 1992. Impact of methanol on the biodegradative activity of aquifer microorganims. In SETAC 13th Annual Meeting, November 8-12, 1992. Cincinnati, OH.

Chang, H.-L. and Alvarez-Cohen, L. 1995. Model for the cometabolic biodegradation of chlorinated organics. Environ. Sci. Technol., 29(9), 2357-2367.

Chang, M.-K., Voice, T. C. and Criddle, C. S. 1993. Kinetics of competitive inhibition and cometabolism in the biodegradation of benzene, toluene, and p-xylene by two *Pseudomonas isolates*. Biotechnol. Bioeng., 41, 1057-1065.

Chen, Y.-M., Abriola, L. M., Alvarez, P. J. J., Anid, P. J. and Vogel, T. 1992. Modeling transport and biodegradation of benzene and toluene in sandy aquifer material: comparisons with experimental measurements. Water Resources Research, 28(7), 1833-1847.

Chiang, C. Y., Salanitro, J. P., Chai, E. Y., Colthart, J. D. and Klein, C. L. 1989. Aerobic biodegradation of benzene, toluene, and xylene in a sandy aquifer - data analysis and computer modeling. Ground Water, 27(6), 823-834.

Ely, R. L., Williamson, K. J., Guenther, R. B., Hyman, M. R. and Arp, D. J. 1995. A cometabolic kinetics model incorporating enzyme inhibition, inactivation, and recovery: 1. Model development, analysis, and testing. Biotechnol. Bioeng., 46 (1995), 218-231.

Essaid, H. I., Bekins, B. A., Godsy, E. M., Warren, E., Baedecker, M. J., Cozzarelli, I. M. 1995. Simulation of aerobic and anaerobic biodegradation processes at a crude oil spill site. Water Resources Research, 31(12), 3309-3327.

Freeze, R. E. and Cherry, J. A. 1979. Groundwater. Prentice-Hall, Englewood Cliffs, N.J.

Freyberg, D. L. 1986. A natural gradient experiment on solute transport in a sand aquifer. 2. Spatial moments and the advection and dispersion of nonreactive tracers. Water Resources Research, 22(13), 2031-2046.

Frind, E. O., Sudicky, E. A. and Molson, J. W. 1989. Three-dimensional simulation of organic transport with aerobic biodegradation. In Proc. of the Symposium held during the Third IAHS Scientific Assembly, pp. 89-96. Baltimore, MD: IAHS.

Frind, E. O., Sudicky, E. A. and Schellenberg, S. L. 1987. Micro-scale modelling in the study of plume evolution in heterogeneous media. Stochastic Hydrology and Hydraulics, 1, 263-279.

Fry, V. A. and Istok, J. D. 1994. Effect of rate-limited desorption on the feasibility of in situ bioremediation. Water Resources Research, 30(8), 2413-2422.

Godsy, E. M., Goerlitz, D. F. and Grbic-Galic, D. 1992. Methanogenic degradation kinetics of phenolic compounds in aquifer-derived microcosms. Biodegradation, 2, 211-221.

Haldane, J. B. S. 1930. Enzymes. Longmans, Green and Company, Ltd., UK. Republished by M.I.T. Press, Cambridge, MA, 1965.

Hardison, L. K., Curry, S. S., Ciuffetti, L. M. and Hyman, M. R. 1997. Metabolism of diethyl ether and cometabolism of methyl tert-butyl ether by a filamentous fungus, a *Graphium sp.* Appl. Environ. Microbiology, 63(8), 3059-3067.

Hubbard, C. E., Barker, J. F., O'Hannesin, S. F., Vandegriendt, M. and Gillham, R. W. 1994. Transport and fate of dissolved methanol, methyl-tertiary-butyl-ether, and monoaromatic hydrocarbons in a shallow sand aquifer. Health and Environmental Science Department, API Publication Number 4601, American Petroleum Institute, Washington, DC, 1994.

Holm, P. E., Nielsen, P. H., Albrechtsen, H.-J. and Christensen, T. H. 1992. Importance of unattached bacteria and bacteria attached to sediment in determining potentials for degradation of xenobiotic organic contaminants in an aerobic aquifer. Appl. Environ. Microbiol., 58(9), 3020-3026.

Johnson, W. P., Blue, K. A., Logan, B. E. and Arnold, R. G. 1995. Modeling bacterial detachment during transport through porous media as a residence-time-dependent process. Water Resources Research, 31(11), 2649-2658.

Kindred, J. S. and Celia, M. A. 1989. Contaminant transport and biodegradation, 2. conceptual model and test simulations. Water Resources Research, 25(6), 1149-1159.

Leismann, H. M., and Frind, E. O. 1989. A symmetric-matrix time integration scheme for the efficient solution of advection-dispersion problems. Water Resources Research, 25(6), 1133-1139.

MacIntyre, W. G., Boggs, M., Antworth, C. P. and Stauffer, T. B. 1993. Degradation kinetics of aromatic organic solutes introduced into heterogeneous aquifers. Water Resources Research, 29(12), 4045-4051.

MacQuarrie, K. T. B. 1997. Multicomponent simulation of wastewater-derived nitrogen and carbon in shallow unconfined aquifers. Ph.D. Thesis. University of Waterloo, Department of Earth Sciences, Waterloo, Ontario, Canada.

MacQuarrie, K. T. B., Sudicky, E. A. and Frind, E. O. 1990. Simulation of biodegradable organic contaminants in groundwater - 1. Numerical formulation in principal directions. Water Resources Research, 26(2), 207-222.

Madsen, E. L. 1991. Determining in situ biodegradation - facts and challenges. Environ. Sci. Technol., 25(10), 1663-1673.

Major, D. W., Hodgins, E. W. and Butler, B. J. 1991. Field and laboratory evidence of in situ biotransformation of tetrachloroethene to ethene and ethane at a chemical transfer facility in North Toronto. In Hinchee, R. E. and Olfenbuttel, R. F. (eds). On-site Processes for Xenobiotic and Hydrocarbon Treatment. Butterworth-Heinemann, Boston. pp. 147-171.

Malone, D. R., Kao, C.-M. and Borden, R. C. 1993. Dissolution and biorestoration of nonaqueous phase hydrocarbons: model development and laboratory evaluation. Water Resources Research, 29(7), 2203-2213.

McCaulou, D. R., Bales, R. C. and Arnold, R. G. 1995. Effect of temperature-controlled motility on transport of bacteria and microspheres through saturated sediments. Water Resources Research, 31(2), 271-280.

McNab, W. W. J. and Narasimhan, T. N. 1995. Reactive transport of petroleum hydrocarbon constituents in a shallow aquifer: modeling geochemical interactions between organic and inorganic species. Water Resources Research, 31(8), 2027-2033.

Millette, D., Barker, J. F., Comeau, Y., Butler, B. J., Frind, E. O., Clement, B. and Samson, R. 1995. Substrate interaction during aerobic biodegradation of creosote-related compounds: a factorial batch experiment. Environ. Sci. Technol., 29(8), 1944-1952.

Millette, D., Butler, B. J., Frind, E. O., Comeau, Y. and Samson, R. 1998. Substrate interaction during aerobic biodegradation of creosote-related compounds in columns of sandy aquifer material. Journal of Contaminant Hydrology, 29(2), 165-183.

Molson, J. W., Martin, P. J. and Frind, E. O. 1995. WATFLOW-3D: a 3D numerical flow model for saturated porous media. User Guide, Waterloo Centre for Groundwater Research, University of Waterloo, Waterloo, ON, Canada.

National Research Council. 1990. Ground water models: scientific and regulatory applications. National Academic Press, Washington, D.C., 303 pp.

Oh, Y.-S., Shareefdeen, Z., Baltzis, B. C. and Bartha, R. 1994. Interactions between benzene, toluene, p-xylene (BTX) during their biodegradation. Biotechnol. Bioeng., 44, 533-538.

Patrick, G. C., Barker, J. F., Gillham, R. W., Mayfield, C. I. and Major, D., 1986. The behavior of soluble petroleum-derived hydrocarbons in groundwater. Petroleum Association for the Conservation of the Canadian Environment. PACE Phase II Report No. 86-1.

Robin, M. J. L., Gutjahr, A. L., Sudicky, E. A. and Wilson, J. L., 1993. Cross-correlated random field generation with the direct fourier transform method. Water Resources Research, 29(7), p. 2385-2397, 1993.

Schäfer, W. 1992. Numerische Modellierung mikrobiell beeinflußter Stofftransportvorgänge im Grundwasser. München Wien: R. Oldenbourg Verlag GmbH. (German text).

Schmid, G. and Braess, D. 1988. Comparison of fast equation solvers for groundwater flow problems. In: Groundwater Flow and Quality Modelling. Editors E. Custodio et al., NATO Advanced Science Institute, Series C, Vol. 224, D. Reidel Publishing Company, Dordrecht, Holland.

Semprini, L. and McCarty, P. L. 1992. Comparison between model simulations and field results for in-situ biorestoration of chlorinated aliphatics: Part 2. Cometabolic transformations. Ground Water, 30(1), 37-44.

Stringfellow, W. T. and Aitken, M. D. 1995. Competitive metabolism of naphthalene, methylnaphthalenes, and fluorene by phenanthrene-degrading Pseudomonads. Applied and Environmental Microbiology, 61(1), 357-362.

Sturman, P. J., Stewart, P. S., Cunningham, A. B., Bouwer, E. J. and Wolfram, J. H. 1995. Engineering scale-up of in situ bioremediation processes: a review. Journal of Contaminant Hydrogeology, 19, 171-203.

Sudicky, E. A. , 1985. A collection of analytical solutions for solute transport in porous and fractured porous media. Report, Institute for Groundwater Research, University of Waterloo, Ontario, Canada, 1985.

Sudicky, E. A. 1986. A natural gradient experiment on solute transport in sand aquifer: spacial variability of hydraulic conductivity and its role in the dispersion process. Water Resources Research, 22(13), 2069-2082.

Tan, Y., Wang, Z.-X. and Marshall, K. C. 1996. Modeling substrate inhibition of microbial growth. Biotechnol. Bioeng., 52, 602-608.

Widdowson, M. A., Molz, F. J. and Benefield, L. D. 1988. A numerical transport model for oxygen- and nitrate-based respiration linked to substrate and nutrient availability in porous media. Water Resources Research, 24(9), 1553-1565.

Woodbury, A. D. and Sudicky, E. A. 1991. The geostatistical characteristics of the Borden aquifer. Water Resources Research, 27:533-546.

CONCLUDING REMARKS AND FUTURE DIRECTIONS

The presented work attempts to link biodegradation processes at three different observation scales, the micro-, meso- and macroscale, by means of numerical modelling. Different processes, phenomena and characteristics predominate at each scale. The link between the micro- and mesoscale is performed by using the non-dimensional model BIOBATCH, whereas the three-dimensional transport model BIO3D is used to link the meso- and macroscale. The assumption is made that the small-scale phenomena fully apply at the larger scale, where additional phenomena such as advection, dispersion, spatial and temporal substrate and electron acceptor distributions and spatial heterogeneities play a role as well.

Using laboratory-derived kinetic degradation and sorption parameters along with additional physical, chemical and microbiological information, a dissolved gasoline field experiment at Canadian Forces Base (CFB) Borden was simulated. All additional input parameters were derived from laboratory and field measurements or taken from the literature. The simulated results match the experimental results reasonably well without model calibration.

Based on these results, an extensive sensitivity analysis was performed to estimate the influence of the key controlling factors at the field scale. It is shown that the flow field, the amount of electron acceptor (oxygen) available, and the Monod kinetic parameters have a significant influence on the simulated results. Under the field conditions modelled and the assumptions made for the simulation, it can be concluded that laboratory-derived Monod kinetic parameters can adequately describe field-scale degradation processes. This is an encouraging result indicating that, for this particular field experiment, all key controlling processes, phenomena and characteristics at the three observation scales are fairly well understood. For the presented modelling approach, no scale relationships have to be found to link the laboratory and the field scale. Instead, accurately incorporating the field-scale processes, phenomena and characteristics, such as a) advective and dispersive transport of the contaminants, b) advective and dispersive transport and availability of the electron acceptor, c) mass transfer limitations and d)

spatial heterogeneities, at the larger scale and applying well-defined lab-scale parameters, should accurately describe field-scale processes.

As mentioned in the General Introduction, the simulation of a large-scale heterogeneous aquifer with local-scale dispersivity values and small-scale REVs will eventually yield macrodispersivity values as theory predicts. This study showed that simulating micro- and mesoscale processes within small-scale REVs and applying them to a macroscale aquifer system also yields macroscale degradation phenomena.

However, the system chosen for this study is fairly simple. It remains to be shown whether this conclusion holds for more complicated systems that incorporate dissolution processes, additional electron acceptors and several microbial populations. In addition, the issue of substrate interactions (other than competition for the available oxygen), nutrient supply, the influence of temperature and pH are not addressed in this study. This is a challenge for future work but I am convinced that, if all the key processes are understood and reliable parameters are determined, a numerical model should be able to reproduce field-scale results accurately by applying lab-scale parameters. The understanding of the key processes is crucial for forecasting contaminant behaviour and for making scientifically sound decisions when intervention is necessary in the remediation process.

In terms of the influence of changing flow directions on the biodegradation process (as presented in Chapter 3), future work will attempt to quantify the relationship between flow angle, frequency and dispersivity. This will be attempted by using numerical simulations of slugs with an analysis of spatial moments.

APPENDIX A

IMPLEMENTATION OF A DECREASING MICROBIAL YIELD INTO THE RELATIVE-LEAST-SQUARES TECHNIQUE TO DETERMINE UNIQUE MONOD KINETIC PARAMETERS OF BTEX COMPOUNDS USING BATCH EXPERIMENTS

A.1. ABSTRACT

An analysis of aerobic benzene biodegradation kinetics was performed on the results of laboratory batch microcosms. A modified version of the computer model BIO3D was used to determine the Monod kinetic parameters, k_{max} (maximum utilization rate) and K_S (half-utilization constant), as well as the Haldane inhibition concentration, K_I, for pristine Borden aquifer material. The problem of non-uniqueness of the calculated parameters was overcome by using several different initial substrate concentrations. With the least-square-fit method, unique kinetic degradation parameters were obtained. Calculation of the apparent microbial yield, Y_{app}, based on microbial counts from the beginning and the end of the experiments were crucial for the accurate determination of the kinetic degradation parameters. Assuming a constant microbial yield determined by numerical calibration, rather than using the measured yield values from the batch experiments, would have resulted in erroneous estimates of the kinetic degradation parameters. For the model compound benzene, a decreasing microbial yield (Y_{app}) with increasing initial substrate concentration was observed in this study. This behaviour was modelled using a microbial inhibition term. The kinetic parameters obtained in the present study were found to agree well with values reported in the literature.

A.2. INTRODUCTION

For the case of a constant microbial yield, Y, with different initial substrate concentrations, a method to estimate Monod kinetic parameters is presented in Chapter 1.

However, the microbial yield might decrease with increasing initial substrate concentration as a result of lower carbon conservation for example. Measurements of the microbial yield for a series of benzene degradation experiments using five different initial concentrations showed a consistent decrease in the microbial yield with an increasing initial substrate (benzene) concentration. Because also other workers showed this phenomenon of a decreasing yield (e.g., Goldman et al., 1987; Connolly et al., 1992; Oh et al., 1994), the attempt has been made to incorporate this into the Monod equation using a mathematically appropriate form.

The "Materials and Methods" for the laboratory setup and evaluation of the batch experiments is presented in Chapter 1. Chapter 1 also describes in detail the microbial counts to derive the microbial yield.

The numerical model BIOBATCH along with the assumptions and the governing equations is explained in Chapter 1 as well. The modification of the equations to incorporate the decreasing microbial yield into the Monod equation is described below.

A.3. MODIFIED EQUATIONS IN THE NUMERICAL MODEL BIOBATCH

The numerical model BIOBATCH is a modified version of the advective-dispersive transport model BIO3D (Frind et al., 1989; Schirmer et al., 1995) and described in detail in Chapter 1. The governing equations for substrate and microbes for the special case of a constant microbial yield for different initial substrate concentrations are given by:

$$- dS/dt = k_{max}\, M\, (S / [S + K_S + (S^2/K_I)]\,) / D \qquad (A.1)$$

$$dM/dt = k_{max}\, M\, (S / [S + K_S + (S^2/K_I)]\,)\, Y - bM \qquad (A.2)$$

where S is the organic substrate concentration [mg/L], t is time [days]; k_{max} is the maximum-utilization rate of S [day^{-1}]; M is the microbial concentration [mg/L]; K_S is the half-utilization constant of S [mg/L]; D is the mass distribution coefficient; Y is the microbial yield per unit organic substrate consumed and b is the first-order decay rate of the microbial population [day^{-1}]. To account for substrate toxicity at high concentrations, the Haldane inhibition term [S^2/K_I] (Haldane, 1930; Andrews, 1968) was introduced

where K_I [mg/L] is the Haldane inhibition concentration. The Haldane term yields a slower microbial growth and, therefore, a slower effective substrate utilization rate at higher substrate concentrations. However, because this term is applied to both equations, the microbial yield stays constant. The two governing equations are nonlinear and coupled and, therefore, must be solved iteratively.

The microbial yield, Y, in Equation A.2 represents the ratio of microbes grown to substrate utilized. Another inhibition term has to be introduced to describe a decreased microbial yield with increased initial substrate concentrations (Table A.1). To our knowledge, the inhibition term concept was first introduced by Levenspiel (1980) as $[1-(P/P_{max})]^{\alpha}$ to account for product (P) toxicity. Luong (1987) extended this concept to describe substrate (S) inhibition with a term $[1-(S/S_{max})]^{\alpha}$. We further extend this concept to account for microbial growth inhibition, introducing a term $[1-(M/M_{max})]^{\alpha}$ in the microbial growth equation which mathematically represents the declining microbial yield. M_{max} is the maximum microbial concentration at which the microbial yield approaches zero and the microbial population reaches a steady state. The exponent, α, describes the dependence of the rate of change of inhibition as a function of the microbial concentration. Other workers suggested similar inhibition terms to describe the decrease of microbial yield with higher microbial concentrations (e.g., Kindred and Celia, 1989).

The final equation governing the growth of the microbial population is then given as:

$$dM/dt = k_{max}\, M\, (S / [S + K_S + (S^2/K_I)])\, Y\, [1-(M/M_{max})]^{\alpha} - bM\,. \qquad (A.3)$$

The effective microbial yield, Y_{eff}, can be defined as

$$Y_{eff} = Y\, [1-(M/M_{max})]^{\alpha}\,. \qquad (A.4)$$

Table A.1. Results of the best-fit Monod parameters k_{max} and K_S using BIOBATCH including the Haldane inhibition concentration K_I and the derived apparent microbial yield Y_{app}.

Average Initial Benzene Conc. in mg L^{-1} [a]	Final microbial degrader population in mg L^{-1}	k_{max} in day^{-1}	K_S in mg L^{-1}	K_I in mg L^{-1}	Apparent microbial yield Y_{app} measured	Standard deviation of microbial yield measured	Final microbial yield Y_{app} calculated using BIO-BATCH
2.0	3.2	1.56	0.00	95.0	1.22	0.08	1.17
4.1	6.5	1.56	0.00	95.0	1.21	0.13	1.02
8.2	6.6	1.56	0.00	95.0	0.64	0.05	0.84
19.7	13.9	1.56	0.00	95.0	0.60	0.10	0.52
35.5	16.5	1.56	0.00	95.0	0.39	0.09	0.45

[a] The average aqueous phase benzene concentrations of three replicates are reported in column 1. The microbial yield was calculated based on the microbial degrader mass gained and the product of the substrate mass utilized and the mass distribution coefficient (D).

A.4. DETERMINATION OF THE BEST FIT PARAMETERS

A.4.1. Calculation of the Distribution Coefficient (D)

For our experimental setup, a Henry's Law constant for benzene of 0.113 was measured in separate experiments. The K_d value for benzene for Borden aquifer material was determined using sorption data presented by Patrick et al. (1985). The sorption experiments show linear isotherms with K_d values that include sorption onto both the aquifer material and the glassware surface. A K_d value of 0.31 cm^3/g for benzene was calculated for our experimental conditions. Using these values in Equation 1.6 of Chapter 1 yields a D value of 1.34 for benzene.

A.4.2. Calculation of the Microbial Parameters M_{max}, α and b

For Equations A.1 and A.3, with D defined, there are six unknowns (k_{max}, K_S, K_I, M_{max}, α and b) that describe the system of batch experiments. In the case of a constant microbial yield for all initial substrate concentrations, α can be set to zero and the term

$[1-(M/M_{max})]^{\alpha}$ in Equation A.3 becomes unity. Then, only four unknowns (k_{max}, K_S, K_I and b) remain. The microbial concentrations were measured in the batch experiments, allowing for explicit calculation of the microbial parameters M_{max}, α and b.

Since the experiments were conducted over a relatively short time (less than eight days) and the microbial population was in the exponential or, at most, the early stationary growth phase (Chapelle, 1993), we assumed that the microbial decay constant, b, was small relative to the rate of population increase. This assumption seems reasonable since no convincing evidence of the manifestation of decay in these growth phases is reported in the literature (Gaudy, 1992).

The phenomenon of a decreasing microbial yield with higher initial substrate concentration as we observed for benzene can be described mathematically by an effective microbial yield Y_{eff} as shown above by Equation A.4. Given that we determined the final microbial concentration for each batch experiment, the overall (apparent) yield (Y_{app}) can be determined as:

$$Y_{app} = \Delta M / \Delta S \qquad (A.5)$$

for each initial substrate concentration (Table A.1) where ΔM is the mass of microbes gained and ΔS is the mass of substrate utilized. Rewriting Equation A.5 yields:

$$\Delta S = \Delta M / Y_{app} \qquad (A.6)$$

Using a value Y_{eff} corresponding to the microbial concentration (M) at any given time, the amount of substrate utilized can be calculated as:

$$\Delta S = \int_{M = M_{ini}}^{M_{fin}} \frac{dM}{Y_{eff}} = \int_{M = M_{ini}}^{M_{fin}} \frac{dM}{Y_{max}\left[1-\left(\frac{M}{M_{max}}\right)\right]^{\alpha}} \qquad (A.7)$$

where Y_{max} is the maximum microbial yield and M_{ini} and M_{fin} are the initial and final microbial concentrations [mg/L], respectively. Y_{max} and M_{max} are independent of M. Combining Equations A.6 and A.7 and letting α equal 1, the evaluation of the integral yields:

$$\frac{\Delta M}{Y_{app}} = \frac{-M_{max}\left[\ln\left(1-\frac{M_{fin}}{M_{max}}\right)-\ln\left(1-\frac{M_{ini}}{M_{max}}\right)\right]}{Y_{max}} \qquad (A.8)$$

The resulting equation has two unknowns Y_{max} and M_{max} for any given M. Since this equation must hold for each initial substrate concentration, a set of five equations (five different initial substrate concentrations for the case of benzene) is available to perform the regression analyses to find the best fit values of Y_{max} and M_{max} for this set of five equations. After rearranging Equation A.8 to solve for Y_{app}, MATHLAB™ was used to perform regression analyses and yielded best fit values of $Y_{max} = 1.24$ and $M_{max} = 17.28$ mg/L for α equal 1.

Letting α be a value other than 1 yields another equation by evaluating the integral in Equation A.7. The performed regression analyses, however, did not provide a better fit to the measured yield data, therefore, we simply used $\alpha = 1$ for our benzene data set.

Not accounting for the decreasing microbial yield with increasing substrate concentration (Table A.1) would add another complication in determining unique kinetic parameters. Figure A.1 illustrates that, holding all other parameters constant, different yield factors will give different degradation curves. For the given kinetic parameter combination (which was found to be the unique fit for the entire set of benzene data), the measured microbial yield Y of 0.39 applied as a constant microbial yield for the entire experiment (initial benzene concentration of 35.5 mg/L; Table A.1) does not fit the measured degradation data. However, a larger constant Y of 1.2 fits the degradation curve reasonably well.

Furthermore, Figure A.2 illustrates that different constant microbial yield factors could describe the measured degradation curve when different kinetic parameters (k_{max} and K_S) are used and K_I is kept constant. This finding points out how important it is to measure the microbial yield for all initial substrate concentrations.

A declining microbial yield, as measured for benzene (Table A.1), may be attributed to increased carbon conservation at low substrate concentrations where carbon is the most limiting factor. As substrate concentrations increase, the ratio of carbon to

other limiting factors, such as inorganic nutrients, increases as well which can result in a decreasing microbial yield, and where carbon is not the limiting constituent, a threshold growth yield is reached (Connolly et al., 1992). In our experiments, we provided nutrients in excess to avoid the latter condition. Assuming a constant microbial yield for the entire range of microbial and substrate concentrations may result in an erroneous prediction of the kinetic parameters (Figures A.1 and A.2).

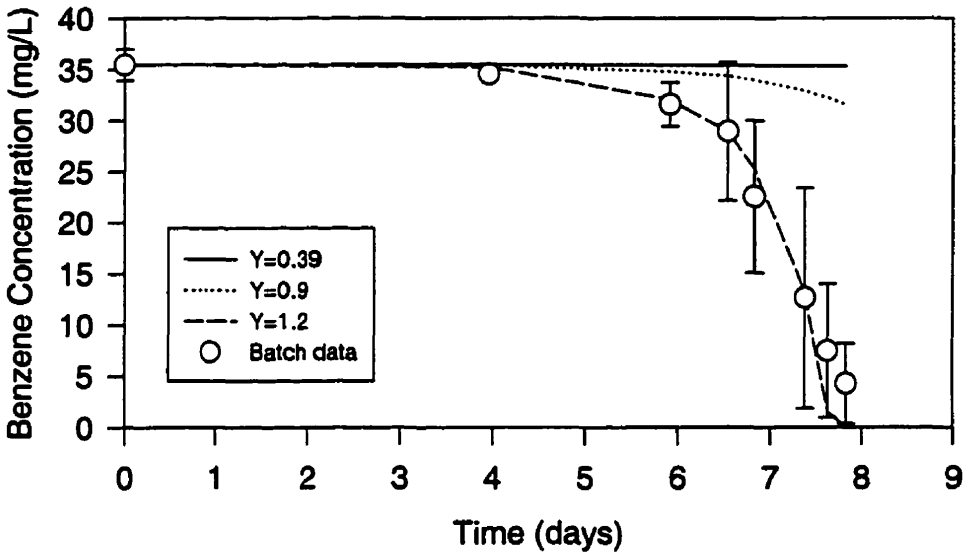

Figure A.1. Calculated benzene degradation curves in comparison to measured data (symbol with error bars of one standard deviation) using constant microbial yields Y of 0.39 (Y_{app} as actually measured in batch experiment), 0.9 and 1.2 and identical kinetic parameters (k_{max} = 1.56 day^{-1}; K_S = 0.0 and K_I = 95.0 mg/L, that were found to be the unique kinetic parameters for the entire set of benzene data).

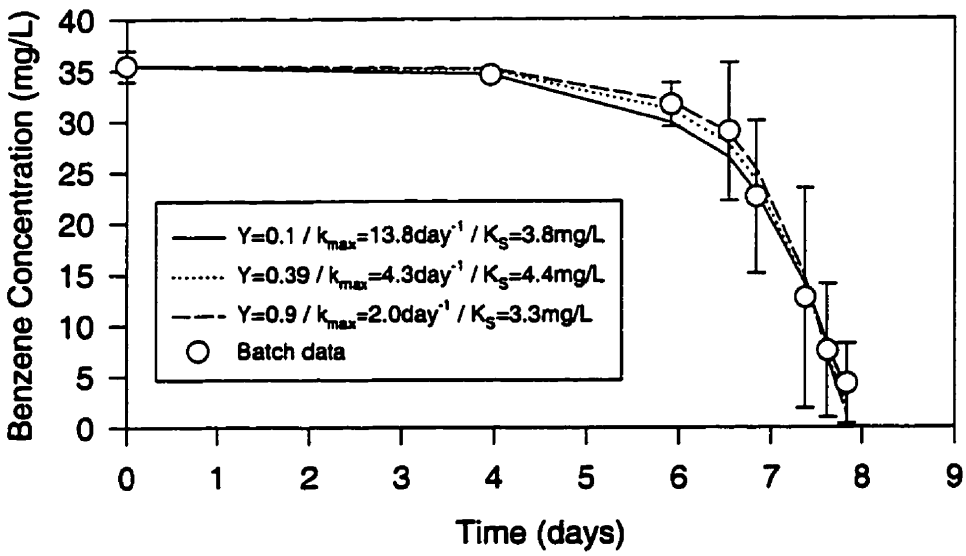

Figure A.2. Best-fit Monod kinetic parameters for benzene degradation in comparison to measured data (symbols with error bars of one standard deviation) using constant microbial yields Y of 0.1, 0.39 (Y_{app} as actually measured in batch experiment), and 0.9 and an identical Haldane inhibition concentration K_I of 95.00 mg/L.

A.4.3. Determination of the Best-fit Kinetic Degradation Parameters k_{max}, K_S and K_I

The three remaining unknowns, k_{max}, K_S and K_I in the Monod kinetic term, must be found. These values have to hold for the degradation curves of each initial substrate concentration. The same initial microbial concentration of 0.003 mg/L was used for each initial concentration as explained in Chapter 1. We can obtain the best fit k_{max}, K_S and K_I parameters by running BIOBATCH for a wide range of different k_{max} / K_S / K_I combinations, typically for $0 \leq k_{max} \leq 20$ day^{-1}, $0 \leq K_S \leq 10$ mg/L and $0 \leq K_I \leq 200$ mg/L. The calculation procedure is described in detail in Chapter 1.

A.5. RESULTS AND DISCUSSION

Aerobic benzene biodegradation experiments were conducted in batch mode for five different initial concentrations. Mean values were used for the degradation curves to determine the RLS (relative least squares; see Chapter 1) that represent the best-fit Monod parameter combination for all benzene degradation curves. This RLS parameter combination represents the global minimum between all measured and calculated degradation curves. The initial total microbial concentration was 1.474 mg/L with an experimentally determined initial degrader population of 0.2 % which yields an estimated initial degrader concentration of 0.003 mg/L (Chapter 1).

Given that the Monod degradation parameters (k_{max} and K_S) together with the Haldane inhibition concentration (K_I) for a compound are, in theory, independent of the initial substrate concentration, we therefore calibrated the best fit k_{max} / K_S / K_I combinations for each initial benzene concentration individually. By summing up the RSE (relative squared error; see Chapter 1) for each Monod parameter combination and each initial concentration, the global RLS for all initial substrate concentrations was found which implies a unique fit of the Monod kinetic parameters for the set of batch experiments.

A k_{max} of 1.56 day^{-1}, a K_S of 0.0 mg/L and a K_I of 95.0 mg/L give a global RLS for all benzene experiments. In addition, the decreasing microbial yield with increasing microbial concentration followed a function described by a Y_{max} of 1.24, an M_{max} of 17.28 mg/L and an α value of 1. If the microbial yield (Y_{app}) had not been measured and a constant yield had been assumed, different kinetic parameters would have been calculated which would not represent the system. In the present study, the microbial decay coefficient, b, was assumed to be small and ignored. For a field application of the parameters it might be necessary to determine b using independent lab studies.

The calculated Monod parameters are summarized in Table A.1 and the results applied to the biodegradation experiments are shown in Figure A.3. There is reasonably good agreement between the calculated and measured values using the same set of k_{max} / K_S / K_I parameters for each experiment. The calculated average microbial yields at the

end of each numerical calibration also agree reasonably well with those measured in the lab.

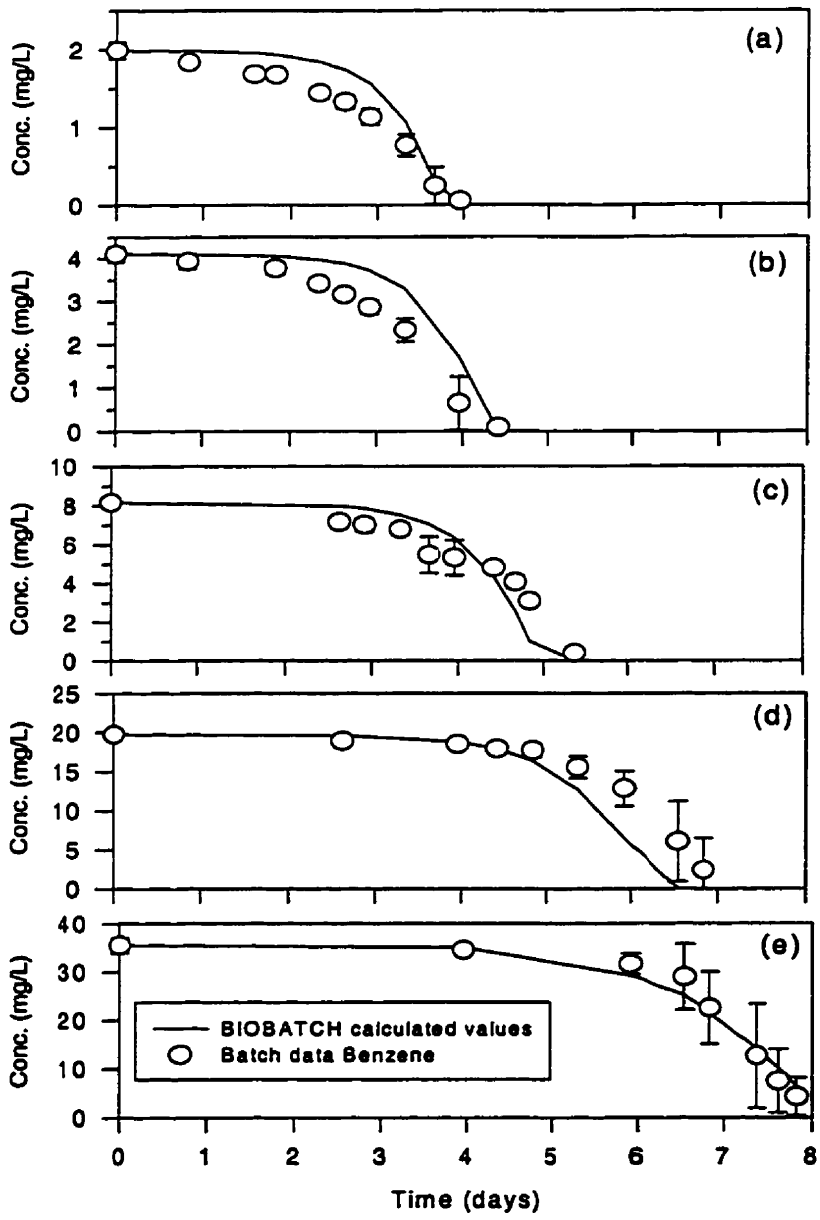

Figure A.3. Measured benzene biodegradation curves (symbols with error bars of one standard deviation) compared to BIOBATCH calibrated best-fit values of $k_{max} = 1.56\ day^{-1}$, $K_S = 0.0$ mg/L and $K_I = 95.0$ mg/L. Initial benzene concentrations are (a) 2.0 mg/L, (b) 4.1 mg/L, (c) 8.2 mg/L, (d) 19.7 mg/L, and (e) 35.5 mg/L.

As noted by Alvarez et al. (1991), estimation of microbial numbers is a major source of variation in determining kinetic parameters in sediments, soils, etc. While direct counts are more reliable than plate counts for determining the total population, viable and nonviable cells are not distinguished, and cells active in degradation cannot be differentiated from non-growing cells, cells growing on metabolites derived from the target compound rather than the target compound itself, or cells growing on other substrates such as dead biomass or humic material present in the environment. Furthermore, microbial counts typical of aquifers are near the lower limit of detection for direct count techniques.

The decreasing microbial yield with higher benzene concentrations was measured in the experiments and therefore, the introduction of the term $[1-M/M_{max}]^{\alpha}$ is justified in order to fit the observations. The decreasing microbial yield is likely a result of better carbon conservation at low substrate concentrations. Carbon would be the most limiting factor in that instance, as Connolly et al. (1992) have noted. As well, because benzene is a potentially toxic substrate its deleterious effects will increase with concentration, and the microorganisms may be forced to direct a greater proportion of their substrate gain to energy production for cell maintenance and repair rather than to carbon for biomass production, at higher benzene concentrations. This will affect the degree of carbon conservation and hence the yield.

The introduction of the Haldane inhibition term into the Monod equation was necessary to account for the slower utilization rate at higher substrate concentrations. This slower utilization rate is caused by an increased substrate toxicity to the microbial population (Peters, 1988). If this term was not introduced, the local RLS for different initial concentrations did not overlap and no global RLS would have been found.

A range of values was obtained from the literature for the parameters k_{max} and K_S pertaining to benzene degradation (Table A.2). The values of k_{max} and K_S obtained within this study using BIOBATCH are comparable, as all the values are within about one order of magnitude. It is important to keep in mind that the above mentioned literature values

are derived from a variety of different sources. Most of them are calculated using laboratory batch and column experiments.

Table A.2. Selected literature values of Monod coefficients for aerobic benzene biodegradation.

k_{max} (day^{-1})	K_S (mg L^{-1})	Remark
3.84	20.0	batch test; gasoline contaminated soil [a]
8.3	12.2	a) batch test; sandy aquifer material [b] b) numerical modelling column experiment [c]
8.05	3.17	batch test; activated carbon fluidized-bed reactor with pure microbial culture [d]
16.32	12.22	batch test; contaminated industrial sludge [e]
10.56	3.36	batch test; contaminated industrial sludge with pure microbial culture [e]
1.176	0.3125	batch test; creosote contaminated soil [f]
0.888-5.256	(negative K_S)	column test; creosote contaminated soil [f]
1.56	0.00	batch test; pristine sandy aquifer material [g]

[a] Goldsmith and Balderson (1988); [b] Alvarez et al. (1991); [c] Chen et al. (1992); [d] Chang et al. (1993); [e] Oh et al. (1994); [f] Kelly et al. (1996); [g] This study

There are many reasons for obtaining different values for kinetic parameters. They will often be site specific, since the microbial populations will vary. Different species of bacteria will differ in their biodegradation ability and possibly the pathway of metabolism. Conditions such as temperature or groundwater geochemistry will also affect the results, especially if limitations of nutrients are involved.

Since batch experiments with natural water samples appear to provide the most ecologically relevant estimates of k_{max} and K_S (Connolly et al. 1992), it is our intention to conduct additional experiments to investigate if the calculated Monod parameters also hold for BTEX mixtures. Then we will simulate a field-scale experiment that has been conducted at CFB Borden (Hubbard et al. 1994). This should give some insight into whether laboratory derived Monod parameters can be applied to the field scale.

A.6. CONCLUSIONS

Unique Monod kinetic parameters can be determined by applying computer modelling to laboratory batch experiments using different initial substrate concentrations. Measurements made for several initial substrate concentrations are crucial to overcome the problem of non-uniqueness of the fitted Monod parameters.

The calculated Monod parameters for the batch degradation experiments were reasonable and comparable to other literature values. The microbial yield is a sensitive parameter. It is very important to have information about the microbial population to accurately examine the Monod kinetic parameters. A failure to account for the microbial concentration at the beginning and the end of the experiment will result in a non-unique or erroneous estimate of the Monod parameters. Applying these erroneous values to simulate field plume behaviour may have serious implications on the predictions.

A.7. REFERENCES

Alvarez, P. J. J., Anid, P. J., Vogel, T. M. 1991. Kinetics of aerobic biodegradation of benzene and toluene in sandy aquifer material. Biodegradation 2, 43-51.

Andrews, J. F. 1968. A mathematical model for the continuous culture of microorganisms utilizing inhibitory substrates. Biotechnol. Bioeng. 10, 707-723.

Chang, M. K., Voice, T. C. and Criddle, C. S. 1993. Kinetics of competitive inhibition and cometabolism in the biodegradation of benzene, toluene, and p-xylene by two *Pseudomonas* isolates. Biotechnol. Bioeng. 41, 1057-1065.

Chapelle, F. H., 1993. Ground-water microbiology and geochemistry. New York, John Wiley and Sons, Inc., pp. 151,152, 322-357.

Chen, Y. M., Abriola, L. M., Alvarez, P. J. J., Anid, P. J. and Vogel, T. M. 1992. Modeling transport and biodegradation of benzene and toluene in sandy aquifer material: comparison with experimental measurements. Water Resources Research 28(7), 1833-1847.

Connolly, J. P., Coffin, R. B. and Landeck, R. E. 1992. Modeling carbon utilization by bacteria in natural water systems. In: Hurst, C. J. (Ed), Modeling the metabolic and physiologic activities of microorganisms. John Wiley and Sons, Inc., New York, pp. 249-276.

Frind, E. O., Sudicky, E. A. and Molson, J. W. 1989. Three-dimensional simulation of organic transport with aerobic biodegradation. In: Abriola, L. M. (Ed), Groundwater Contamination, IAHS Publ. No. 185, pp. 89-96.

Gaudy Jr., A. F., 1992. Introduction to modeling the metabolic and physiologic activities of microorganisms using wastewater treatment as an example. In: Hurst, C. J. (Ed), Modeling the metabolic and physiologic activities of microorganisms. John Wiley and Sons, Inc., New York, pp. 1-30.

Goldman, J. C., Caron, D. A. and Dennett, M. R. 1987. Regulation of gross growth efficiency and ammonium regeneration in bacteria by substrate C : N ratio. Limnology and Oceanography 32(6), 1239-1252.

Goldsmith Jr., C. D. and Balderson, R. K. 1988. Biodegradation and growth kinetics of enrichment isolates on benzene, toluene, and xylene. Water Sci. Technol. 20, 505-507.

Haldane, J. B. S. 1930. Enzymes. Longmans, Green and Company, Ltd., UK. Republished by M.I.T. Press, Cambridge, MA, 1965.

Hubbard, C. E., Barker, J. F., O'Hannesin, S. F., Vandegriendt, M. and Gillham, R. W. 1994. Transport and fate of dissolved methanol, methyl-tertiary-butyl-ether, and monoaromatic hydrocarbons in a shallow sand aquifer. Health and Environmental Science Department, API Publication Number 4601, American Petroleum Institute, Washington, DC.

Kelly, W. R., Hornberger, G. M., Herman, J. S. and Mills, A. L. 1996. Kinetics of BTX biodegradation and mineralization in batch and column systems. Journal of Contaminant Hydrology 23, 113-132.

Levenspiel, O. 1980. The Monod equation: A revisit and a generalization to product inhibition. Biotechnol. Bioeng. 22, 1671-1687

Luong, J. H. T. 1987. Generalization of Monod kinetics for analysis of growth data with substrate inhibition. Biotechnol. Bioeng. 39, 242-248.

Oh, Y. S., Shareefdeen, Z., Baltzis, B. C. and Bartha, R. 1994. Interactions between benzene, toluene, and p-xylene (BTX) during their biodegradation. Biotechnol. Bioeng. 44, 533-538

Patrick, G. C., Ptacek, C. J., Gillham, R. W., Barker, J. F., Cherry, J. A., Major, D., Mayfield, C. I. and Dickhout, R. D. 1985. The behavior of soluble petroleum product derived hydrocarbons in groundwater. Petroleum Association for the Conservation of the Canadian Environment. Phase I, PACE Report No. 85-3.

Peters, R. C. 1988. The toxic effects of mononuclear aromatic hydrocarbons on ground water bacteria. M.Sc. Thesis, Department of Biology, University of Waterloo, Waterloo, ON, Canada, 137 p.

Schirmer, M., Frind, E. O. and Molson, J. W. 1995. Transport and Biodegradation of Hydrocarbons in Shallow Aquifers: 3D Modelling. American Petroleum Institute, Workshop: Comparative Evaluation of Groundwater Biodegradation Models, May 08-09, 1995, Hotel Worthington, Ft Worth, TX.